Hippocampal long-term depression in anaesthetised adult rats: Involvement of glutamate and acetylcholine receptors

A thesis submitted for the degree of Doctor of Philosophy

July 2017

Kenneth Joseph O'Riordan

Department of Pharmacology and Therapeutics

School of Medicine

University of Dublin, Trinity College

Declaration

I declare that this thesis has not been submitted as an exercise for a degree at this or any other university and it is entirely my own work. I agree to deposit this thesis in the University's open access institutional repository or allow the Library to do so on my behalf, subject to Irish Copyright Legislation and Trinity College Library conditions of use and acknowledgement.

_____

Kenneth J. O'Riordan

Abstract

Synaptic long-term depression (LTD) is believed to underlie critical mnemonic processes in the hippocampus. Elucidation of the mechanisms of LTD may provide a means of understanding synaptic plasticity processes that are believed to underlie information storage in learning and memory, as well as memory dysfunction, such as occurs in early Alzheimer's disease (AD). In the work presented here, the mechanisms underlying the induction of synaptic LTD in the adult rat dorsal hippocampus *in vivo,* using different pathways of synaptic activation and pharmacological challenges, were examined.

Induction of LTD in the intact hippocampus of adult animals has proven difficult to achieve; thus, most research on this topic has been performed in hippocampal slices from young animals mainly using electric field stimulation of mixed pathways *en masse*. The recent development of the technique of optogenetics using virally directed expression of a light-activatable trans-membrane ion channel in the hippocampus, promises high temporal precision of synaptic activation, high spatial resolution and a very selective means to study isolated network synaptic plasticity. We compared electrically and optogenetically induced LTD at CA3-to-CA1 apical synapses in urethane anaesthetised rats. We confirmed that the expression of Channelrhodopsin2 (ChR2-eYFP) was specifically, but relatively diffusely, expressed in CA3 pyramidal neurons originating at the site of injection, thereby allowing relatively selective excitation of either Schaffer collaterals or commissural

fibres, avoiding stimulation of *en passant* cholinergic neurons and decreasing the likelihood of peri/extra-synaptic glutamate receptor activation.

LTD induction at apical CA1 synapses has been divided into NMDA receptor (NMDAR) and metabotropic glutamate receptor (mGluR) –dependent forms. Seeing that electrical stimulation is likely to co-activate both perisynaptic mGlu5R and nearby NMDARs, we examined their potential interaction during the induction of LTD by low-frequency stimulation (LFS, 900 pulses of high-intensity at 1 Hz). We found evidence that although LTD induction with electrical LFS of Schaffer collateral/ commissural inputs was primarily dependent on NMDARs, it was also facilitated by endogenously released glutamate-mediated activation of mGlu5Rs. This LTD was only blocked by high local doses of NMDAR antagonists when tested alone and was dependent on GluN2B subunit-containing NMDARs as well as the NMDAR ion channel function. In contrast, LTD induction by optical LFS excitation of CA3 Schaffer collaterals, induced a similar magnitude, input-specific LTD that was also NMDAR-dependent but not modulated by mGlu5R. Whereas selective activation by a highly potent mGlu5R positive allosteric modulator showed no effect on a weak optical stimulation LFS (1Hz, 300 or 600 pulses), it strongly enhanced LTD induction by a weak electrical LFS. Moreover, LTD induction by oLFS was potently blocked by systemic treatment with selective inhibitors of the ion channel and GluN2B subunit of NMDARs.

Previously our laboratory had reported that electrical LFS-induced LTD was muscarinic acetylcholine receptor-dependent. We revisited the involvement of cholinergic transmission, utilising optogenetics to avoid directly activating cholinergic input during LFS. A muscarinic receptor antagonist that abrogated electrically induced LTD did not significantly affect optical induction of LTD. Moreover, pharmacologically boosting endogenous ACh levels lowered the threshold for the induction of LTD by a weak electrical conditioning protocol, yet had no discernible effect on the ability to induce LTD by optical LFS that was either peri-threshold or submaximal.

Finally, we re-examined the role of NMDARs in the ability of synthetic synaptotoxic aggregates of human Aβ1-42 (amyloid-β derived diffusible ligands - ADDLs) to enhance electrically induced LTD and found evidence that it required NMDARs that contain the GluN2B subunit. Furthermore, ADDLs effected a modest facilitation of LTD induced by a weak optical LFS protocol (1Hz, 300 pulses), that appeared to be lateralised: Aβ preferentially facilitated the induction of optically induced LTD at Schaffer collaterals in the left hippocampus.

The present findings provide strong evidence in the living animal that electrical LFS of Schaffer collateral/ commissural fibres triggers an NMDAR-dependent LTD that is strongly modulated by mGlu5R and muscarinic acetylcholine receptor co-activation. In contrast, selective optical LFS of CA3 pyramidal neurons expressing ChR2 induced robust NMDAR-dependent LTD that was relatively independent of mGlu5R and

cholinergic input. The GluN2B subunit and ion channel function mediated the NMDAR-dependence of both forms of LTD. Moreover, both forms of LTD were blocked by a protein synthesis inhibitor, indicating a critical need for new protein synthesis similar to long-term memory consolidation. The data also revealed a role for NMDARs and lateralisation in the facilitation of LTD by Aβ.

Acknowledgements

I would like to take this opportunity to offer my most sincere gratitude to my doctoral supervisor, Prof. Michael Rowan, for his invaluable help and guidance throughout my Ph.D studies.

For unparalleled technical help and guidance, my colleagues: Dr Nengwei Hu, Dr Igor Klyubin, Dr Tomas Ondrejcak, Dr Yingjie Qi and Dr Dainan Zhang.

I would further like to thank Patrick Monahan for assistance in developing the methodology for the optogenetic studies. The plasmid (rAAV/CaMKIIa-hChR2(H134R)-eYFP-WPRE) was kindly provided by Dr Karl Deisseroth (Stanford University). Dr Gavin McManus assisted with fluorescence imaging. Prof. Dominic Walsh and his research fellows, Dr Tiernan O'Malley and Dr Alexader Mably, who supplied synthetic Aβ protein for use in this study. Dr Marian Tsanov for help and advice with the optogenetic technique

Personally, I would like to thank

My wife, Michelle

My parents, Dan and Kathleen

My son, Nate

My brother, Anthony and his family

Abbreviations

Aβ	Amyloid beta
AAV	Adeno-associated virus (serotypes 2 & 5)
ACh	Acetylcholine
AD	Alzheimer's disease
ADDLs	Amyloid-beta derived diffusible ligands
ANOVA	Analysis of variance
CA	Cornu ammonis
CaMKII	$Ca2^{+}$/calmodulin-dependent protein kinase II
ChR2	Channelrhodopsin-2
CNS	Central nervous system
CPP	(R,S)-3-(2-Carboxypiperazin-4-yl)propyl-1-phosphonic acid
D-AP5	D-(-)-2-amino-5-phosphonopentanoic acid
DAG	Diacylglycerol
DG	Dentate gyrus
Donepezil	2,3-Dihydro-5,6-dimethoxy-2-[[1-(phenylmethyl)-4-piperidinyl]methyl]-1H-inden-1-one hydrochloride
DP	Depotentiation
DPX	Distyrene, Plasticizer and Xylene
eLFS	Electrical low-frequency stimulation
EAA	Excitatory amino acid
EEG	Electroencephalogram
E-LTP	Early-phase long-term potentiation

Emetine	(2S,3R,11bS)-2-[[(1R)-6,7-dimethoxy-1,2,3,4-tetrahydroisoquinolin-1-yl]methyl]-3-ethyl-9,10 dimethoxy-2,3,4,6,7,11b-hexahydro-1H benzo[a]quinolizine;hydrate;hydrochloride
EPSP	Excitatory postsynaptic potential
ER	Endoplasmic reticulum
ERK	Extracellular receptor kinase
EYFP	Enhanced yellow fluorescent protein
GPCRs	G-protein coupled receptors
GRIA	Glutamate ionotropic receptor AMPA
gr. DG	Granule cell body layer of the dentate gyrus.
H	Histidine
hChR2 -	Humanised channelrhodopsin-2
HF	Hippocampal fissure
HFS	High-frequency stimulation
i.c.v.	Intracerebroventricular
i.p.	Intraperitoneal
i/o	Input/ output
iGluR	Ionotropic glutamate receptor
IP3	Inositol trisphosphate
L-AP5	L-(+)-2-Amino-5-phosphonopentanoic acid
LFS	Low-frequency stimulation
LTD	Long-term depression
l.mol.	Lacunosum moleculare
LTM	Long-term memory
LTP	Long-term potentiation

L-LTP	Late-phase long-term potentiation
LY 341495	(2S)-2-Amino-2-[(1S,2S)-2-carboxycycloprop-1-yl]-3-(xanth-9-yl) propanoic acid,
MAChR	Muscarinic acetylcholine receptor
MAPK	Mitogen-activated protein kinase
MCI	Mild cognitive impairment
mGluR	Metabotropic glutamate receptor
MK 801	(5S,10R)-(+)-5-Methyl-10,11-dihydro-5H- dibenzo[a,d] cyclohepten-5,10-imine maleate ((+)-maleate/ Dizocilpine)
Mol.	Molecular layer
MTEP	3-((2-Methyl-1,3-thiazol-4-yl)ethynyl)pyridinehydrochloride
mTOR	Mammalian target of rapamycin
NAM	Negative allosteric modulator
NMDA	N-methyl-D-aspartate
oLFS	Optical low-frequency stimulation
P(r)	Probability of transmitter release
PAM	Positive allosteric modulator
PKC	Protein kinase C
PLCβ	Phospholipase C-β
PPF	Paired-pulse facilitation
PS	Picosiemens
PSD	Postsynaptic density
PTP	Post-tetanic potentiation
Ro 25-6981	[R-(R,S)]-α-(4-Hydroxyphenyl)-β-methyl-4-(phenylmethyl)-1-piperidinepropanol hydrochloride hydrate

Scopolamine	(αS)-α-(Hydroxymethyl) benzeneacetic acid (1α,2β,4β,5α,7β)-9-methyl-3-oxa-9azatricyclo[3.3.1.02,4]non-7-yl ester hydrobromide
s.c.	Subcutaneous
SEM	Standard error of the mean
s.o.	Stratum oriens
s.p.	Stratum pyramidale
s.r.	Stratum radiatum
STED	Stimulated emission depletion
STM	Short-term memory
STP	Short-term potentiation
VU0360172	(N-Cyclobutyl-6-[2-(3-fluorophenyl)ethynyl]-3-pyridinecarboxamide hydrochloride)

List of Figures

Fig. 1.2.1 An illustration of the human brain with the hippocampus highlighted in red (adapted from Loonen and Ivanova, 2015).

Fig. 1.2.2 An illustration of the rat brain with the hippocampus also highlighted in red (adapted from Cheung and Cardinal, 2005).

Fig. 1.2.3 An illustration outlining the rat brain hippocampus proper as part of the hippocampal formation (adapted from Mugunthan et al., 2016).

Fig. 1.2.4 A schematic illustrating the direct (III) and indirect trisynaptic (II) pathways within the hippocampus proper (adapted from Deng et al., 2010). Lateral perforant pathway (LPP), medial perforant pathway (MPP).

Fig. 1.2.5 A diagram outlining the monosynaptic (EC to CA1/ CA3) and the trisynaptic (EC to DG to CA3 to CA1) pathways in the hippocampus (adapted from Yau et al., 2015).

Fig. 1.3.1 Representation of seminal Ramón Y Cajal hand drawing of a transverse section of the hippocampus formation (Cajal, 1911).

Fig. 1.6.1 A schematic drawing of the GluA1 subunit (adapted from Lu and Roche 2012).

Fig. 1.7.1 A schematic showing the structure of a typical synaptic NMDAR with the glutamate binding site on GluN2 and glycine binding site on GluN1, along with the magnesium blocked ion channel pore occupied by the M2 subunits (adapted from Benarroch, 2011).

Fig. 1.8.1 A diagram of mGluR activation upon binding glutamate (adapted from Willard and Koochekpour, 2013); amino-terminal domain (ATD), cysteine-rich domain (CRD), transmembrane domain (TMD), cytoplasmic tail domain (CTD).

Fig. 1.8.2 A schematic of the mGluR and the different glutamate binding and activation states (adapted from Niswende and Conn, 2010).

Fig. 1.10.1 Schematic representation of the light activation of Channelrhodopsin-2 (from Prof. Dr Ernst Bamberg).

Fig. 2.2.1 pAAV-CaMKIIa-hChR2(H134R)-EYFP in sequence linearised plasmid map.

Fig. 2.2.2 pAAV-CaMKIIa-hChR2(H134R)-EYFP circular plasmid map.

Fig. 2.3.1 Parasagittal view of dorsal hippocampus and approximate location of virus injection.

Fig. 2.5.1 (a) Photograph of a representative optrode used in this work. (b) Magnified view (converted to black and white for easier viewing) of the tip of the optrode that was implanted into the area CA3 of the rat hippocampus.

Fig. 2.5.2 Stimulation and recording configuration.

Fig. 2.5.3 A topographical schematic of placement of screws, cannula and electrode openings in rat skull for animal recordings when positioned over the left hemisphere; the locations were reversed for electrode placement in the right hemisphere.

Fig. 2.6.1 Representative optical and electrical evoked fEPSPs from a single experiment during which the electrodes were lowered into place.

Fig. 2.6.2 Light microscope (Olympus BX51 upright) images showing a representative location of the (a) stimulating optrode and (b) recording electrode placement. An electrical lesion was created at the wire tip locations.

Fig. 2.7.1 Representative recording of a 4ms optical ‘square-wave’ pulse generated by the 473nm blue light laser unit set to half maximum intensity. The upper (red) trace indicates the signal sent to the laser power unit; the lower (blue) trace indicates the raw trace of the light output recorded with an optical power meter (Thorlabs).

Fig. 2.7.2 Representative recording of an optically evoked fEPSP. The upper (red) trace indicates the signal sent to the laser power unit; the lower (blue) trace shows a typical fEPSP evoked by optical stimulation.

Fig. 2.7.3 Representative recording of an electrically evoked fEPSP.

Fig. 2.7.4 A bar chart showing the recorded latency from stimulus artefact (elec) or beginning of 4 ms optical laser light pulse (opt) to onset of respective fEPSP. Matched recordings from 10 different animals; examples taken from half maximum stimulus recordings during baseline before any experimental perturbation.

Fig. 2.7.5 Representative trace of high-frequency spiking recorded near the tip of the optical fibre in CA3 during a 4ms optical pulse.

Fig. 2.7.6 Representative i/o curves. (a) growth of fEPSP amplitude in response to an increase in optical power; (b) growth of fEPSP amplitude in response to an increase in electrical stimulus current.

Fig. 2.8.1 Confocal image showing representative bilateral expression profile of green ChR2-EYFP and blue DAPI nuclear stain in the dorsal hippocampus.

Fig. 2.8.2 High magnification confocal images showing expression of eYFP and DAPI through layers of area CA1 in the dorsal hippocampus ipsilateral to the side of virus injection. s.o.: stratum oriens; s.p.: stratum pyramidale; s.r.: stratum radiatum; l.mol.: stratum lacunosum moleculare; HF: hippocampal fissure.

Fig. 2.8.3 High magnification of area CA3 pyramidal cell body layer with DAPI (blue) staining nuclear material and eYFP (green) fluorescence. No eYFP expression was detected in saline, as opposed to AAV, injected animals. Calibration bar = 20μm.

Fig. 2.8.4 Regional eYFP fluorescence. (a) Schema of the oval shaped area used to determine relative fluorescence. (b) Bar chart of relative fluorescence measured near the optrode location in the CA3, and the recording electrode location in the CA1 areas ipsilateral and contralateral to the hemisphere of virus injection.

Fig. 2.8.5 Sample image of a transverse hippocampal slice taken with a bright-field microscope illustrating the Nissl stain.

Fig. 2.8.6 Representative confocal images of area CA3 pyramidal cell body layer with DAPI (blue) staining indicating nuclear material and eYFP (green) fluorescence indicating ChR2 expression.

Fig. 2.8.7 Bar chart showing cell count data (number of cell bodies/ mm pyramidal cell body layer) showing that eYFP fluorescence, and hence ChR2 expression, was relatively diffuse compared with total DAPI staining of cell bodies in the CA3 area near the site of virus injection.

Fig. 3.1.1.1 Combined systemic injection of antagonists of NMDA and mGlu5 receptors prevents the induction of hippocampal synaptic LTD by electrical low-frequency conditioning stimulation *in vivo.*

Fig. 3.1.1.2 Group II mGluR antagonism alone or in combination with NMDAR blockade fails to inhibit electrically-induced synaptic LTD *in vivo*.

Fig. 3.1.1.3 GluN2B-subunit-selective antagonist, systemically administered with a mGlu5R antagonist, prevents eLFS induction of LTD.

Fig. 3.1.2. High doses of locally-injected NMDAR antagonists prevent LTD induction by eLFS *in vivo*.

Fig. 3.1.3. Necessity for NMDAR ion channel function in the induction of LTD *in vivo.*

Fig. 3.1.4. Endogenous glutamate release evoked by LFS activates mGlu5Rs to facilitate the induction of LTD *in vivo.*

Fig. 3.2.1.1 The ability to induce LTD of optically evoked synaptic responses was assessed using a variety of low-frequency (1Hz) protocols.

Fig. 3.2.1.2 High-intensity low-frequency stimulation induced robust LTD at CA3-to-CA1 synapses *in vivo.*

Fig. 3.2.1.3 High-intensity low-frequency LTD at CA3-to-CA1 synapses *in vivo* is not lateralised.

Fig. 3.2.1.4 Robust LTD in either the left or right hippocampus, stimulated and recorded in the hemisphere opposite to the site of virus injection.

Fig. 3.2.2.1 Pathway independence of oLFS-induced LTD *in vivo.*

Fig. 3.2.2.2 LTD saturation outlines input selectivity of oLFS-induced LTD *in vivo*.

Fig. 3.2.3.1 Effect of the acetylcholinesterase inhibitor donepezil (1 mg/kg s.c.) on LTD induction in the optical and electrical pathways.

Fig. 3.2.3.2 Cholinergic-independence of oLFS induced LTD *in vivo.*

Fig. 3.2.4. NMDAR-dependence of the induction of synaptic LTD by oLFS *in vivo.*

Fig. 3.2.5. mGlu receptor-independence of optically-induced synaptic LTD *in vivo*.

Fig. 3.2.6. Protein synthesis-dependence of LTD *in vivo.*

Fig. 3.3.1. Alzheimer's disease Aβ enhanced electrically induced LTD is GluN2B dependent but not lateralised.

Fig. 3.3.2. Alzheimer's disease Aβ enhances optically induced LTD preferentially at Schaffer collateral input to CA1 in the left hippocampus.

Table of Contents

		Page
Title		1
Declaration		3
Abstract		5
Acknowledgements		9
Abbreviations		10
List of figures		14
Table of Contents		22
I. Introduction		27
1.1	Preface	28
1.2	Hippocampal anatomy and role in memory	30
1.3	Hippocampal plasticity and memory models	37
1.4	LTP and LTD of excitatory synaptic transmission	39
1.5	The role of glutamate in synaptic plasticity	42
1.6	Amino-3-hydroxy-5-methyl-4-isoxazolepropionic acid (AMPA) receptor subtypes	45
1.7	N-methyl-D-aspartate (NMDA) receptor subtypes	48
1.8	Metabotropic glutamate receptor (mGluR) subtypes	53
1.9	Protein synthesis and synaptic plasticity	59
1.10	Optogenetic activation of glutamatergic transmission and plasticity	60
1.11	Optogenetics in the study of the asymmetric brain and LTD laterality	63
1.12	Cholinergic control of synaptic activity	65

Page

1.13 Synaptic plasticity and Alzheimer's disease Aβ 67

1.14 Objectives 70

II. Materials and Methods 71

2.1 Animals 72

2.2 AAV- Channelrhodopsin vector 72

2.3 Virus injection 75

2.4 Recording apparatus 76

2.5 Animal surgery and electrode implantation 77

2.6 Electrode placement 82

2.7 Recording fEPSPs and input/output (i/o) curves 85

2.8 Imaging and eYFP-ChR2 expression 91

2.9 Compounds 97

2.10 Data analysis 99

III. Results 101

3.1 Physiological activation of mGlu5 receptors supports the ion channel function of NMDA receptors in the induction of hippocampal LTD *in vivo* 103

3.1.1 Role of NMDA and mGlu5 receptors in the induction of hippocampal synaptic LTD by low-frequency conditioning stimulation *in vivo* 103

Page

3.1.2 Absolute requirement for GluN2B-subunit-containing NMDARs during LTD induction by LFS *in vivo* 110

3.1.3 NMDAR ion channel function is required for the induction of LTD *in vivo* 113

3.1.4 LFS-evoked endogenous glutamate release activates mGlu5Rs to facilitate the induction of LTD 115

3.2 Diminished role for cholinergic and mGlu receptor modulation in optogenetically induced hippocampal NMDA receptor-dependent LTD *in vivo* 118

3.2.1 High-intensity optical low-frequency stimulation induced LTD at CA3-to-CA1 synapses *in vivo* 120

3.2.2 Input selectivity of optical low-frequency stimulation induced LTD *in vivo* 128

3.2.3 Role of cholinergic transmission in oLFS induction of LTD *in vivo* 132

3.2.4 NMDAR-dependence of synaptic LTD induced by optical stimulation *in vivo* 137

3.2.5 Role of mGlu receptors in the induction of hippocampal synaptic LTD by optical conditioning stimulation *in vivo* 140

Page

3.2.6 Protein synthesis-dependence of oLFS-induced LTD *in vivo* 143

3.3 GluN2B NMDAR-dependence and lateralisation of Alzheimer's disease Aβ-facilitated LTD 145

3.3.1 Alzheimer's disease Aβ-facilitated LTD induced by electrical LFS is GluN2B dependent, but not lateralised 146

3.3.2 Alzheimer's disease Aβ-facilitated LTD induced by optical LFS is lateralised 149

IV. Discussion 151

4.1 Induction of hippocampal synaptic LTD by optical low-frequency conditioning stimulation *in vivo* 153

4.2 The role of cholinergic transmission in oLFS induction of LTD *in vivo* 156

4.3 The role of NMDA and mGlu5 receptors in the induction of hippocampal synaptic LTD *in vivo* 157

4.4 Absolute requirement for GluN2B-subunit-containing NMDARs and the ion channel function in the induction of LTD *in vivo* 161

4.5 The roles of GluN2B-subunit-containing NMDARs and lateralisation in Alzheimer's disease Aβ-facilitated LTD 162

Page

V. Conclusions 164

VI. Suggestions for future work 165

VI. References 167

VII. Appendix – Drug table 215

I. Introduction

1.1 Preface

1.2 Hippocampal anatomy and role in memory

1.3 Hippocampal plasticity and memory models

1.4 LTP and LTD of excitatory synaptic transmission

1.5 The role of glutamate in synaptic plasticity

1.6 Amino-3-hydroxy-5-methyl-4-isoxazolepropionic acid (AMPA) receptor subtypes

1.7 N-methyl-D-aspartate (NMDA) receptor subtypes

1.8 Metabotropic glutamate receptor (mGluR) subtypes

1.9 Protein synthesis and synaptic plasticity

1.10 Optogenetic activation of glutamatergic transmission and plasticity

1.11 Optogenetics in the study of the asymmetric brain and LTD laterality

1.12 Cholinergic control of synaptic activity

1.13 Synaptic plasticity and Alzheimer's disease Aβ

1.14 Objectives

1.1 Preface

The desire for a fundamental understanding of the molecular process underlying learning and memory has been at the forefront, driving neuroscience research for decades. An elemental understanding of the brain remains as one of the last great challenges to humanity. The most intriguing facet of the human brain is its ability to record contemporaneous daily actions, adapt and commit them to memory for later recall and use. Evolutionarily, particular selection pressures, or adaptive problems, potentially fuelled the development of human memory systems as we know them today (Tooby and Cosmides, 1992). Combined with self-awareness and consciousness, coupled to emotive cues, the ability to learn, store the information as memories, and recall is indispensable to daily human activity. Furthermore, any impingement on any facet of this process can dramatically affect a person's ability to function in modern society; thus, neurological and psychological disease, the processes of ageing and cognitive decline, are becoming increasingly parsed and understood.

From the early musings of artist and scientist Ramon y Cajal (1906) to the ground breaking molecular neuroscience research by more modern Nobel laureates such as Kandel (2000) and MacKinnon (2003) we have been uncovering the veil of mystique the human brain has held humanity under for centuries. The systems involved in learning and memory act as a template for researchers interested in deciphering the molecular machinery that comprise neurophysiological signalling in the nervous system. It stands as a model that can be studied from the sub-

cellular level through to human behaviour and interaction, from neural stem cells to artificial intelligence networks modelling the human brain *in silico*.

A contemporary understanding of learning and memory sees it as persistent molecular and cellular alterations in the structure and strength of synaptic connections (Kandel et al., 2014). Theoretically, altering these connections can lead to changes in the ability to record, code and recall these memories. Currently, the best-supported neurophysiological process that underlies our prevailing model of learning and memory is synaptic plasticity: where increased or decreased neuronal activity results in long-lasting changes in synaptic weights distributed throughout a network (Bliss and Lomo, 1973). A change in the plasticity state can involve presynaptic, postsynaptic or extrinsic factors that modify the synapse; these changes can be short-lived, resulting in a more dynamic synaptic state, or long-term, resulting in a change in synaptic efficacy that can last for several months if not longer, influencing conscious state, altering a behaviour, creating a memory, solidifying a physical task, or indelibly associating an emotional response with a memory (Kandel et al., 2014). There are believed to be many trillions of synaptic connections in the average human brain (Tang et al., 2001), therefore one can understand the importance in elucidating fully the signalling mechanisms involved.

Importantly, synaptic plasticity in the brain is especially vulnerable to disruption by factors that impair cognition in neurological and

psychiatric disease, including Alzheimer's (AD) and related dementias (Kumar et al., 2015). There is a great scientific and medical need to understand the cellular basis of this impairment. Long-term memory (LTM) is believed to share similar mechanisms with those involved in artificially induced persistent synaptic plasticity. Such activity-dependent persistent strengthening of synaptic efficacy is described as synaptic long-term potentiation (LTP), and weakening, long-term depression (LTD), and they are believed to be measurable cellular correlates of learning and memory (Kandel et al., 2014). LTP and LTD involve synaptic remodelling, synaptogenesis, axonal sprouting/ pruning and dendritic remodelling, as well as neurogenesis and recruitment (Ganguly and Poo, 2013). The work presented here examines the cellular and molecular properties of LTD in the dorsal hippocampus in the living rat.

1.2 Hippocampal anatomy and role in memory

The hippocampal structure has captivated neuroanatomists for hundreds of years and was named after its resemblance to the seahorse fish, itself named from the Greek for sea horse ("horse"- hippos, "sea monster"- kampos, Bir et al., 2015). The hippocampus is part of the limbic system and plays a pivotal role in learning and memory in the brain. The hippocampus is integral in the formation and propagation of both long and short-term memory, also known as working memory, which is specifically associated with propositional/ declarative, episodic and spatial memory in a network within the medial temporal lobe (Kandel et al., 2014). In the human brain, it is positioned within the cortical

association regions of the CNS (Fig. 1.2.1). In the rodent brain, the hippocampus takes up a much larger fraction of the cortex (Fig. 1.2.2).

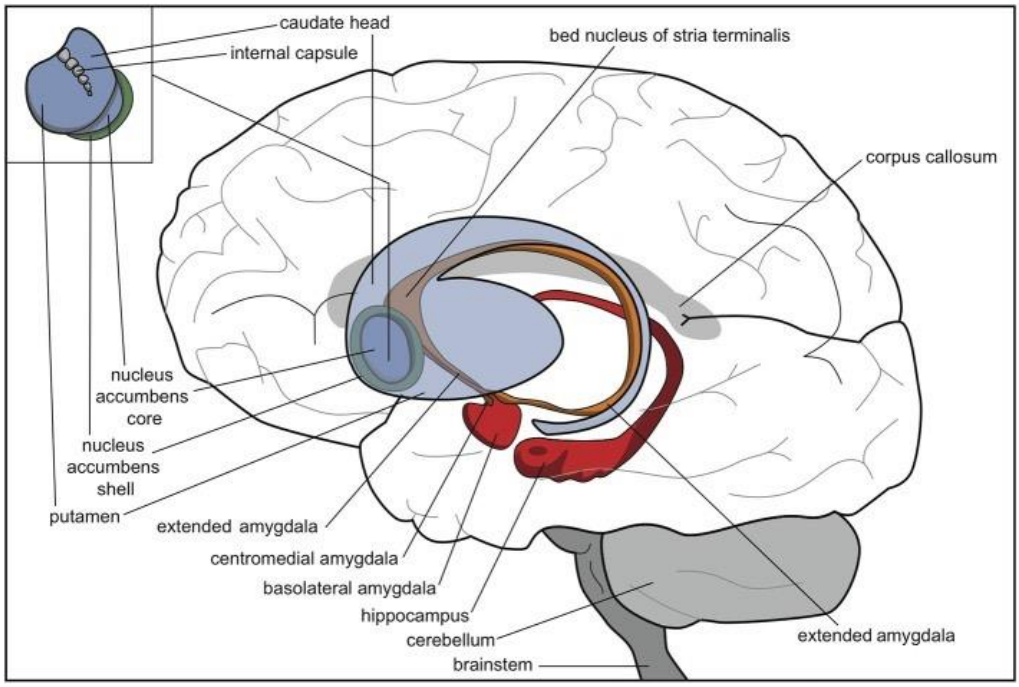

Fig. 1.2.1 An illustration of the human brain with the hippocampus highlighted in red (adapted from Loonen and Ivanova, 2015).

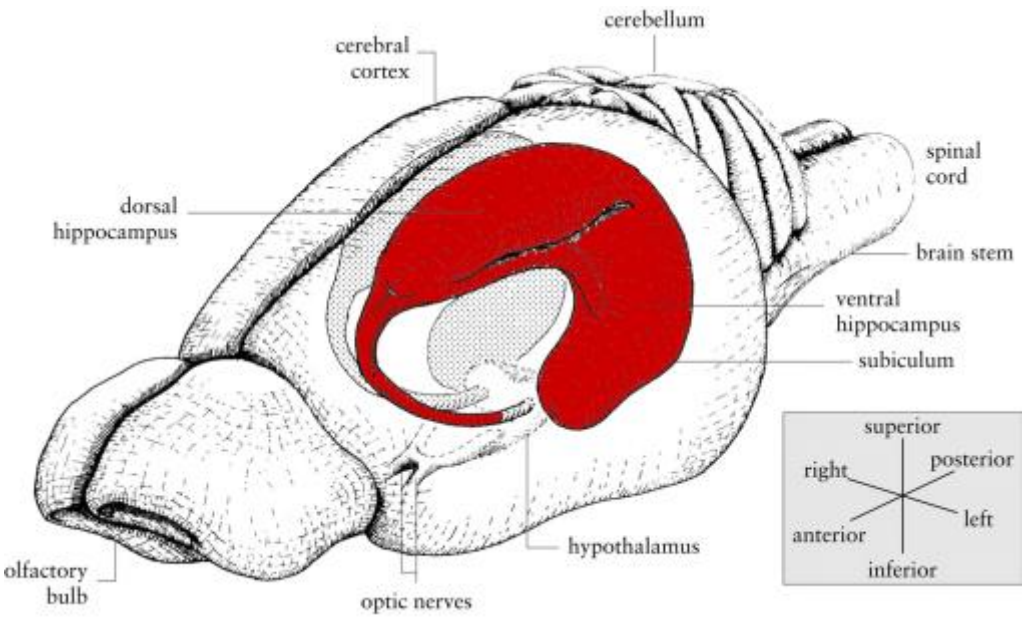

Fig. 1.2.2 An illustration of the rat brain with the hippocampus also highlighted in red (adapted from Cheung and Cardinal, 2005).

The hippocampus proper is part of a larger network termed the hippocampal formation which includes the peri (PC)/ ento-rhinal (EC) cortices, dentate gyrus (DG), subiculum, presubiculum and parasubiculum (Mugunthan et al., 2016). The hippocampus proper is formed with a strict layering of synapses in the dendritic tree, allowing complementary studies both *in vitro* and *in vivo*. The hippocampus proper is compartmentalised into Cornu Ammonis (CA) subdivisions (CA1, CA2, CA3 and CA4) which is further layered across its length, superior through inferior, beginning with the outer layer, the alveus, through to the stratum oriens (s.o.), stratum pyramidale (s.p.), stratum radiatum (s.r.) and stratum lucunosum moleculare (l.mol.). The closely associated DG includes the stratum moleculare (mol.) as well as the granule cell body layer (Fig. 1.2.3).

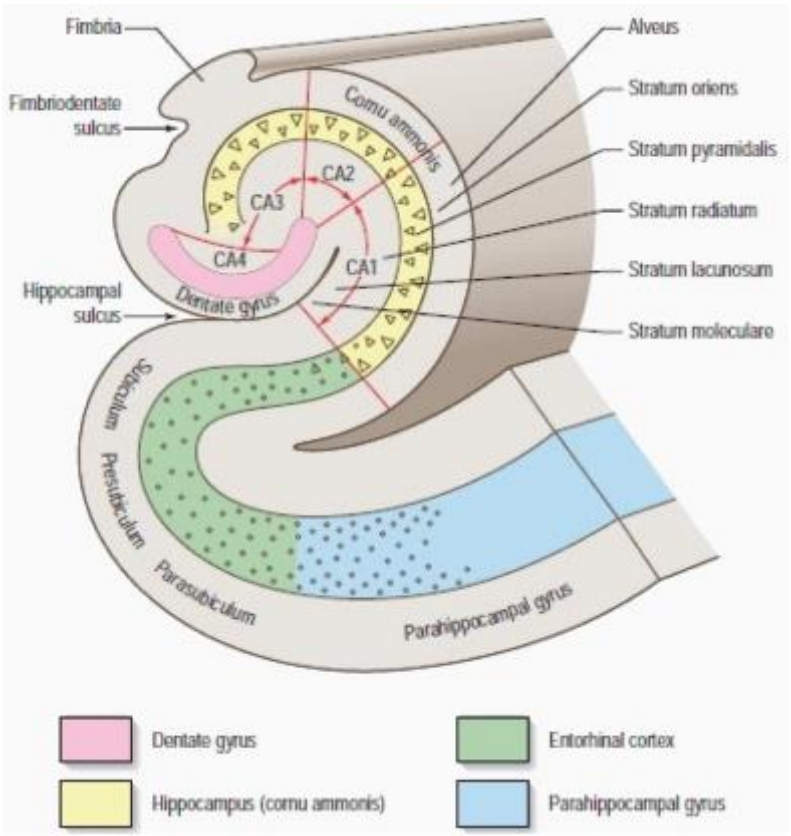

Fig. 1.2.3 An illustration outlining the rat hippocampus proper as part of the hippocampal formation (adapted from Mugunthan et al., 2016).

The principal neuron found within the hippocampus is the pyramidal neuron which is glutamatergic (excitatory), (Graves et al., 2012). These neurons project to both the ipsi- and contralateral entorhinal cortices as well as the contralateral fornix; inter-hemispheric connections utilise neuronal fibres from the ventral hippocampal fissure. In rodents, CA3 pyramidal neurons travel via the commissural pathway to the contralateral CA3 and CA1. Further, efferents project to the ventral striatum and mammillary bodies via subicular neurons from the CA1 (Vann and Nelson, 2015). All principal pyramidal cell bodies in the hippocampus arrange into a single layer with synaptic inputs delineated into well-defined dendritic lamina. This laminar structure has allowed for easy characterisation and definition of principles of unidirectional excitatory neurotransmission (Slomianka et al., 2011). This has allowed for straightforward and quantifiable study of the actions and mechanisms of various types of excitatory and inhibitory amino acid neurotransmitters as well as the transmitter uptake mechanisms, activity-dependent synaptic plasticity and ensuing effects of similar pharmacological agents in the search for treatment and cures of human neurological disease and disorders.

Information arrives at the hippocampus from a variety of cortical sensory areas via the EC and PC which are located near the rhinal fissure in the temporal lobe, as well as being functionally connected to the prefrontal cortex. From there, afferents project into the hippocampal formation along the perforant pathway, thusly named as it perforates the subiculum and hippocampal fissure on its way to the DG. There are two

types of input, an indirect pathway and a direct pathway. The latter relays information coming from layer III of the EC; these neurons form synapses on the distal apical dendrites of CA1 pyramidal neurons. From studies by Larry Squire and David Amaral on patient R.B., we know the importance CA1 pyramidal cells play in working memory and LTM consolidation (Rempel-Clower et al., 1996).

Along the indirect pathway, signals from layer II of the EC travel to the granule cells of the DG (Yau et al., 2015). From the DG, glutamatergic mossy fibres transmit the signal along the mossy fibre pathway into the CA3 pyramidal cells and sequentially from there along the Schaffer collateral pathway which terminates on dendrites of the CA1 pyramidal neurons. This is also known as the trisynaptic pathway given its use of three separate pathways: the perforant pathway leading to the mossy fibre pathway and on to the Schaffer collateral pathway. Sensory information usually arrives via the direct pathway and is considered important in episodic memory consolidation (Figs. 1.2.4. and 1.2.5.). From the hippocampus, signalling from the subiculum mainly projects to the subcortex, whereas the EC projects to the neocortex.

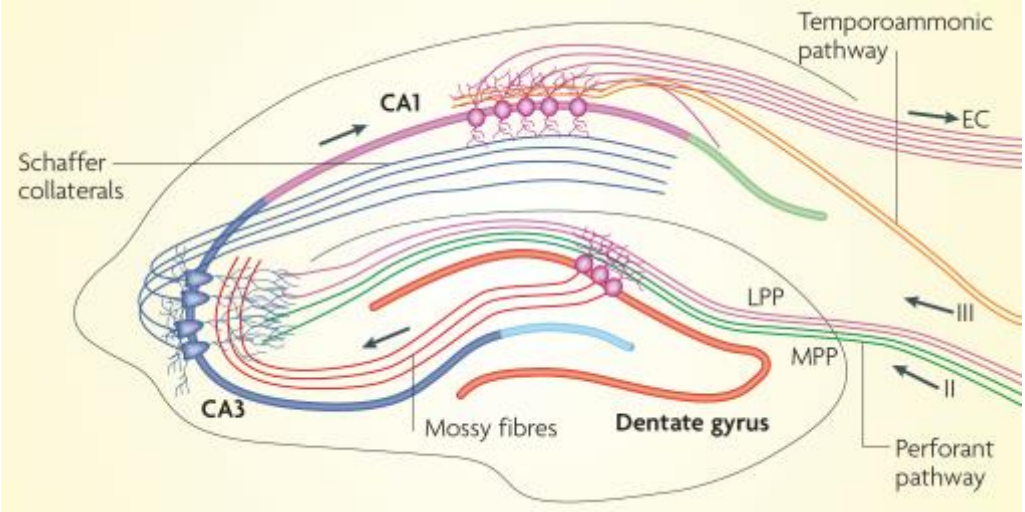

Fig. 1.2.4 A schematic illustrating the direct (III) and indirect trisynaptic (II) pathways within the hippocampus proper (adapted from Deng et al., 2010). Lateral perforant pathway (LPP), medial perforant pathway (MPP).

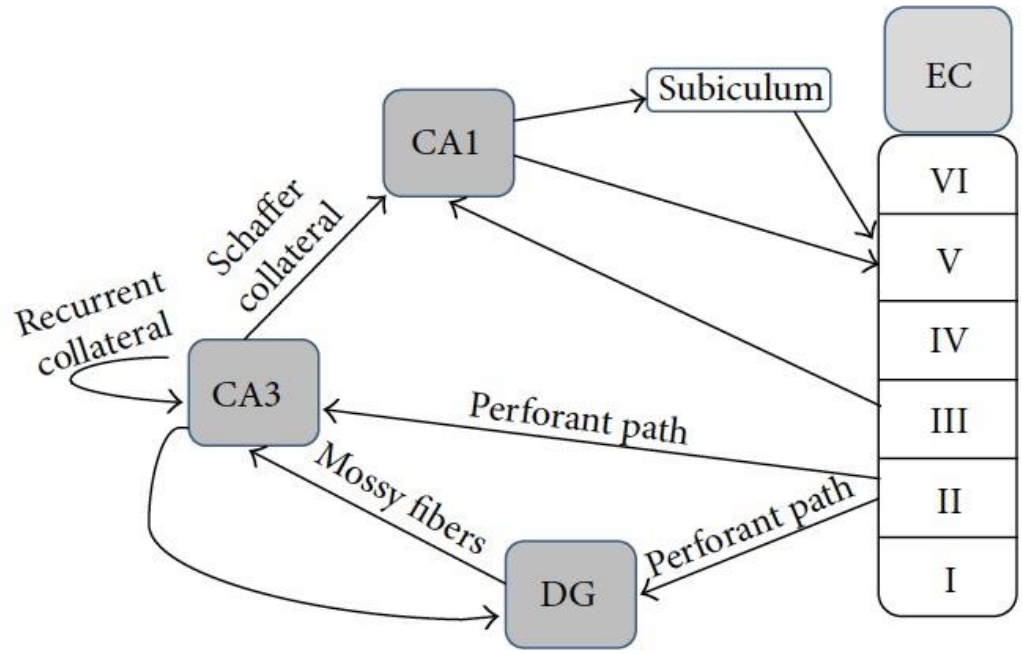

Fig. 1.2.5 A diagram outlining the monosynaptic (EC to CA1/ CA3) and the trisynaptic (EC to DG to CA3 to CA1) pathways in the hippocampus (adapted from Yau et al., 2015).

Current understanding of the compartmentalisation of areas CA1, CA2 and CA3 in the rat hippocampus proper defines that CA2 and CA3 pyramidal cells are larger than those found in area CA1, and mossy fibre projections from the DG mainly innervate area CA3, terminating in a narrow blade just above the CA3 pyramidal cell layer called the stratum lucidum (s.l.). This essentially defines the thin blade of CA2 separating area CA3 from CA1; CA2 is composed of larger pyramidal cell bodies than CA1. The s.l. is easily recognisable in histology due to the translucent unmyelinated mossy fibre terminals. DG mossy fibres terminate on CA3 pyramidal cells in one of three bundles: infrapyramidal, intrapyramidal and suprapyramidal, the latter of which occupies the s.l. It is here where mossy fibres form synapses with branched dendritic spines (thorny excrescences) of CA3 pyramidal cells; the presynaptic mossy fibre terminals form very complex, highly irregular, unusually large *en passant* synaptic varicosities. The thorny excrescences are so distinctive they also further help demarcate the division between areas CA3 and CA2. The suprapyramidal and infrapyramidal regions of area CA3 is where the CA3 associational recurrent collaterals are found along with CA3 to CA1 Schaffer collaterals (Jonas and Lisman, 2015).

The point where the Schaffer collateral CA3 to CA1 innervation ends defines the border between the CA3 and subicular complex (a term sometimes used for the grouping of the presubiculum, subiculum and parasubiculum). Even though a large proportion of hippocampal electrophysiological studies have focused on recording Schaffer collateral signals in the apical dendrites of the stratum radiatum in the

CA1, the basal dendrites of the stratum oriens are just as heavily innervated by axons from the CA3, all in a highly ordered and networked topographical manner.

1.3 Hippocampal plasticity and memory models

Over a century ago, Ramón Y Cajal (Cajal, 1894) proposed a theory that long-term memories are expressed in the brain, in part, by changes in synaptic connectivity (Fig. 1.3.1). This theory was further developed by Donald Hebb in 1949 outlined in his book “The Organization of Behavior” whereby the repeated or persistent activity of cell A firing locally upon cell B results in a metabolic change in either or both cells that increases the efficiency of cell A acting upon cell B. A modern interpretation of synaptic plasticity states that “activity-dependent synaptic plasticity is induced at appropriate synapses during memory formation and is both necessary and sufficient for the encoding and trace storage of the type of memory mediated by the brain area in which it is observed” (Martin et al., 2000).

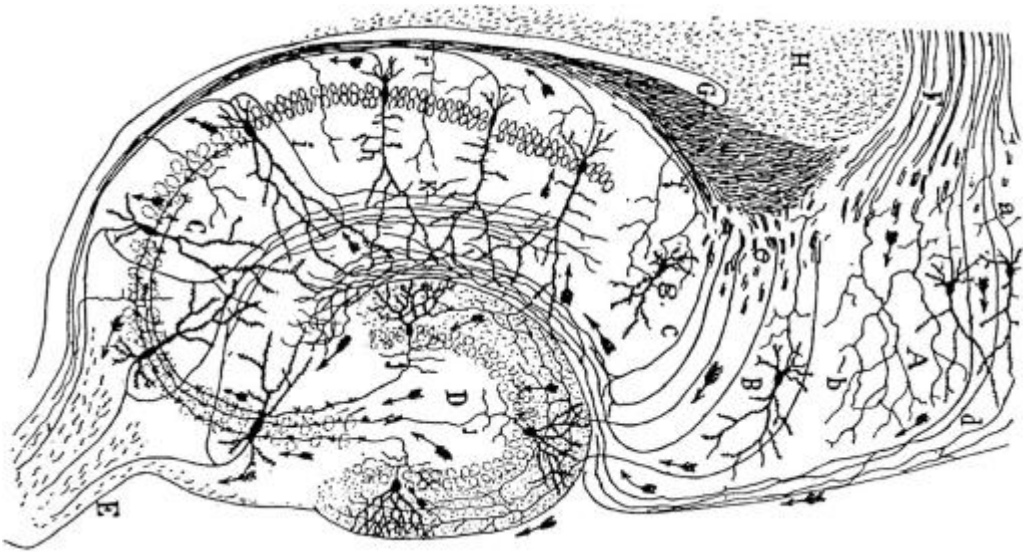

Fig. 1.3.1 Representation of seminal Ramón Y Cajal hand drawing of a transverse section of the hippocampus formation (Cajal, 1911).

In the hippocampus, short-term memory may be represented as a short-term change in the amplitude of excitatory transmission known as short-term plasticity (STP) where the change in synaptic efficacy returns to pre-tetanised amplitudes within minutes of a conditioning stimulation (Fioravante and Regehr, 2013). Hippocampal spatial working memory is believed to traffic transient and current representations of goal-oriented knowledge (Kandel et al., 2014). In humans, it is further believed to be divided into verbal and visuo-spatial information which are both controlled by the executive control processes which allocate attentional resources to monitor, manipulate and update stored representations such as speech-based conscious awareness (Kandel et al., 2014). In rodents, hippocampal lesion studies have linked hippocampal memory to spatial representation and object recognition (Broadbent et al., 2004), which can be short-term or long-lasting.

LTP of excitatory transmission in the hippocampus is understood as an activity-dependent, long-lasting increase in synaptic efficacy and is believed to be a part of the cellular correlate for the expression of LTM (Lamprecht and LeDoux, 2004). Studies by Brenda Milner and her former student Suzanne Corkin on patient H.M. (Henry Molaison), (Scoville and Milner, 1957; Penfield and Milner, 1958; Milner et al.,1968; Corkin, 2002;) demonstrated that not all LTM was dependent on the hippocampus as illustrated by Mr Molaison's ability to demonstrate implicit memory function via motor unconscious and automatic skill learning, habituation, sensitisation as well as priming (Squire, 2009; Wixted and Squire, 2011). In rodents, implicit memory has been linked to both associative and non-associative learning; however, explicit (declarative) and semantic memory requires the hippocampus, at least in part (Mayford et al., 2012). Patient studies in humans (Simons and Spiers, 2003) and lesion studies in rodents have shown that the encoding of long-term storage of explicit memories integrally involves the medial temporal lobe and specifically begins in the hippocampus (Cohen S. et al., 2013).

1.4 LTP and LTD of excitatory synaptic transmission

In learning and memory studies over the last few decades, LTP has been one of the most tested models of synaptic plasticity, a process believed to be integral in memory function and a property of most excitatory synapses in the brain. LTP has been studied extensively since its initial description as a Hebbian-like response in the dentate gyrus by Bliss and Lømo (1973), (for review: Bliss and Collingridge, 1993; Malenka and

Nicoll, 1999); their work developed from experiments initially performed by Per Andersen and Terje Lømo (Andersen, 1960). It is relatively input-specific and can be associative, in that enhanced synaptic efficacy at one set of synapses can influence a nearby set of synapses, believed to be the mechanism underlying associative conditioning in behavioural neuroscience.

LTP was initially termed long-lasting potentiation but was renamed to long-term potentiation by Douglas and Goddard, in 1975. LTP can last for many hours in slices (Capron et al. 2006) and up to a year *in vivo* (Abraham, 2003). LTP can be induced by brief high-frequency tetanic electrical stimulation applied to a select group of afferent cells, where physical structural alterations in the shape, size, number and proximity of the synapses are triggered (Kandel et al., 2014). For example, a 100Hz conditioning stimulus delivered to CA3 pyramidal neurons in the hippocampus can trigger a persistent potentiated state at synapses with CA1 pyramidal neurons. LTP in this particular pathway was first described by Schwartzkroin and Wester in 1975.

Conversely, LTD can be induced by a low-frequency conditioning stimulation paradigm (1-5Hz) to the same cells in the CA3 area to trigger a persistent reduction in the efficacy of the transmission to CA1 pyramidal neurons that can last from hours to days (Collingridge et al., 2010). Our current knowledge of LTD evoked by electrical low-frequency stimulation (LFS) in the adult animal is relatively poor. Inducing LTD *in vivo* in the intact hippocampus of adult animals is known to be very difficult (Xu et

al., 1997, Staubli and Scafidi, 1997). Thus, most research on this topic has been performed in hippocampal slices from young animals. Utilising transverse hippocampal slices, Timothy Bliss and Terje Lømo (1973) described the phenomenon of synaptic plasticity first, studying glutamatergic inputs into the rabbit DG by characterising the long-lasting change in the amplitude of EPSPs in response to tetanising the perforant pathway (PP) from Layer II of the entorhinal cortex (EC) with a high-frequency of electrical stimulation (Bliss and Lømo, 1973). The first reported induction of LTD by LFS *in vitro* was reported by Dunwiddie and Lynch (1978)**.** However, they only used 100 pulses at 1Hz, and it was not until Dudek and Bear (1992) reported that 900 pulses at 1Hz was capable of reliably producing LTD in hippocampal slices. It has since been reported that LTD can persist for days in chronically implanted animals (Abraham et al., 1994; Doyère et al., 1996) and is considered to be as critical a process as LTP in the hippocampus by preventing network saturation and being involved in preserving an overall homeostatic level of excitability in the network (Connor and Wang, 2016).

A similar protocol that can persistently reverse previously induced LTP, but should not be confused with LTD, is depotentiation (DP). It is a form of synaptic plasticity that is believed to be a natural attenuator of synaptic potentiation, and together with LTD increases synaptic flexibility and storage capacity of neuronal circuits as well as limiting potentiation saturation (Huang et al., 2001; Latif-Hernandez et al., 2016; Dayan and Willshaw, 1991). This allows for a bi-directional model of synaptic plasticity; LTD is activity driven rather than a passive process and results

in a long-lasting reduction in synaptic efficacy. DP and LTD utilise different phosphatases during depression induction (Lee et al., 2000), and there is a limited time window after LTP induction during which DP can return the potentiation back to baseline levels (Staubli and Lynch, 1990), whereas LTD can be induced at any time in naive synapses.

The types of LTP and LTD expressed in all pathways in the hippocampus are not singular; there is a family of processes that can strengthen or weaken synaptic transmission at different synapses in different pathways. Indeed, multiple types of LTP/ LTD can be induced by different patterns of synaptic activity (Latif-Hernandez et al., 2016). In a similar way that some neurons have different complements of ion channels that dictate their firing properties, neurons can vary their expression of LTP or LTD based on, but not limited to, what time in development the test subject is examined, which specific synapses are being tested and recorded from as well as the composition of the pre- and post-synapse neurotransmitter receptors.

1.5 The role of glutamate in synaptic plasticity

The neurotransmitter at all major excitatory synapses is glutamate, including at the mossy fibre synapses in the CA3 area (Watkins and Jane, 2006). Glutamate and structurally similar amino acids, also known as excitatory amino acids (EAAs) mediate excitatory activity via interaction with glutamate receptors, such as the NMDAR, at the postsynaptic membrane. From its initial observation by Hayashi (1952, 1954) to the

first description of its activity by Curtis, Watkins and Phillis (Curtis and Watkins, 1960; 1965; Curtis et al., 1960; 1961) in the isolated frog spinal cord as well as in the cat spinal cord *in vivo*, glutamate has been established as a synaptic neurotransmitter in the brain. After many years of examination, glutamate eventually satisfied the four main criteria for classification as a neurotransmitter as outlined by Fonnum 1984: (1) it is localised pre-synaptically; (2) it is specifically released by physiological stimuli in concentrations high enough to elicit a postsynaptic response; (3) it demonstrates identity of action with the naturally occurring transmitter, including response to antagonists; (4) and mechanisms exist that will terminate transmitter action rapidly (Fonnum, 1984).

Specifically, glutamate filled vesicles are released from the active zone of the presynaptic membrane exocytotically, and rapidly diffuse to the postsynaptic membrane, where glutamate generates a brief synaptic EPSP upon binding to the ligand-gated ionotropic membrane receptors. In glutamatergic synapses in the central nervous system, this postsynaptic structure is called the postsynaptic density (PSD) and it is composed of both membranous and cytoplasmic proteins localised at the postsynaptic plasma membrane. There is a heterogeneous mix of membranous postsynaptic ionotropic glutamate receptors (iGluR), which include 1.5 Amino-3-hydroxy-5-methyl-4-isoxazolepropionic acid (AMPA), N-methyl-D-aspartate (NMDA) and kainate receptors. Non-ionotropic G-protein coupled metabotropic glutamate (mGlu) receptors are also present.

AMPARs are considered to be the workhorse of glutamatergic transmission driving large and rapid neurotransmission of the evoked synaptic response, whereas NMDARs are considered to be classical learning and memory receptors (Henley and Wilkinson, 2013). LTP at many synapses is believed to be dependent on calcium influx through the NMDA receptor (Dudek and Bear, 1992; Mulkey and Malenka, 1992), where signalling involves calcium entering the postsynaptic dendritic spine receptors, triggering a postsynaptic calcium signal that is required to induce changes in synaptic plasticity. The NMDAR ion channel pore is blocked by magnesium ions at resting membrane potentials (Nowak et al., 1984). Either binding of glutamate or release of the magnesium block is insufficient alone for channel activation. Therefore, the coincidence of strong depolarising current along with glutamate binding, results in the magnesium block being removed, allowing for transmembrane calcium transportation; in this regard, NMDARs function as coincidence detectors at the postsynaptic membrane (Seeburg et al., 1995). Even though calcium entry through the postsynaptic NMDAR can result in either LTP or LTD, it has been proposed that different levels of calcium influx can couple to different intracellular signalling mechanisms resulting in one synapse modification over another (Lisman, 1989). Moreover, differences in spike timing can lead to differences in the calcium signal that can modulate calcium dynamics and bidirectional plasticity via the NMDAR (Shouval et al., 2002).

CA3-to-CA1 synaptic hippocampal LTD has been divided into NMDA receptor (NMDAR) and metabotropic glutamate receptor (mGluR)

–dependent forms. NMDARs activate much slower than AMPARs generating peak conductance long after the AMPAR and remain open, conducting cationic transmission for much longer (He et al., 2014). For LTP or LTD to be induced, it is believed that a differentiated level of activation of the NMDARs may be integral; a strong and rapid NMDAR activation pattern, increasing intracellular calcium, can trigger LTP (Bear and Malenka, 1994) and induce LTD (Cummings et al., 1996), whereas NMDAR inhibition blocks homosynaptic LTD (Ahmed et al., 2011; Dudek and Bear, 1992). It is understood that there is a lot of crosstalk between the many glutamate receptors in the PSD; for example, mGluRs are believed to modulate the NMDAR mediated activity (Rosenbrock et al., 2010).

1.6 Amino-3-hydroxy-5-methyl-4-isoxazolepropionic acid (AMPA) receptor subtypes

Today it is generally accepted that synaptic alterations take place after a tetanising signal to excitatory synapses which results in persistent changes in AMPAR membrane surface expression and trafficking at the PSD (Lüscher et al., 1999) as well as changes in presynaptic neurotransmitter release. AMPARs are ligand-gated heterotetrameric ion channels comprising different subunit proteins, GluA1-GluA4. GluA1 GluA2 are the most common subunits in area CA1, believed to comprise over 80% of synaptic AMPARs in hippocampal neurons (Lu et al., 2009); GluA3 is believed to be present at about 10% the levels of GluA1 and A2 (Sans et al., 2003). GluA4 is tightly developmentally regulated and

sparsely expressed at glutamatergic synapses in the adult brain (Zhu et al., 2000). However, GluA4 containing AMPARs are rapid-gating, high-conductance receptors and play a key role in AMPAR-mediated transmission in inhibitory interneurons (Pelkey et al., 2015). Further, the synaptic expression of GluA4 containing AMPARs is driven by protein kinase A (PKA) activation, which in turn recruits GluA4 containing AMPARs to immature synapses, effectively unsilencing them (Luchkina et al., 2014). Moreover, GluA4 is believed to play a role in addiction, where alcoholics showed an up-regulation of the GluA4 encoding gene glutamate ionotropic receptor AMPA type subunit 4 (GRIA4), (Enoch et al., 2014) which may result in increased membrane depolarization and an up-regulation of glutamate ionotropic receptor NMDA subunits 2B and 2D.

AMPARs respond very quickly to glutamate binding and desensitise rapidly allowing a quick turnaround. AMPARs being a subtype of the ionotropic glutamate receptors (iGluRs) are cation permeable (Henley and Wilkinson, 2013). Each subunit has an identical membrane topology and core structure made up of about 900 amino acids with a molecular weight of 105 kDa; the amino terminus is extracellular, and carboxy‑terminal intracellular; AMPARs all have three membrane-spanning domains with one re-entrant loop domain (Fig. 1.6.1). The preferred configuration in hippocampal pyramidal cells is a four-subunit channel made up of two identical heterodimers of either GluA1/A2 or GluA2/A3 (Mansour et al., 2001; Wenthold et al., 1996). The principal difference between GluA receptors involves the length of their

carboxy-terminal tail with GluA1 and GluA4 having slightly longer tails than GluA2 or GluA3 (e.g. GluA1 has a 23 amino acid longer c-tail than GluA2); this is a highly variable region that provides a platform for both the protein interactions and the post-translational modifications which regulate subunit-dependent trafficking and regulation (Henley and Wilkinson, 2013). It has long been understood that AMPAR trafficking is a function of the intracellular C-terminal domain, with GluA1 and GluA4 dictating the trafficking properties; however, much about this process is unknown and recent research has brought into question the roles of specific AMPAR subunits in activity-dependent trafficking and synaptic plasticity (Granger et al., 2013, Granger and Nicoll, 2014).

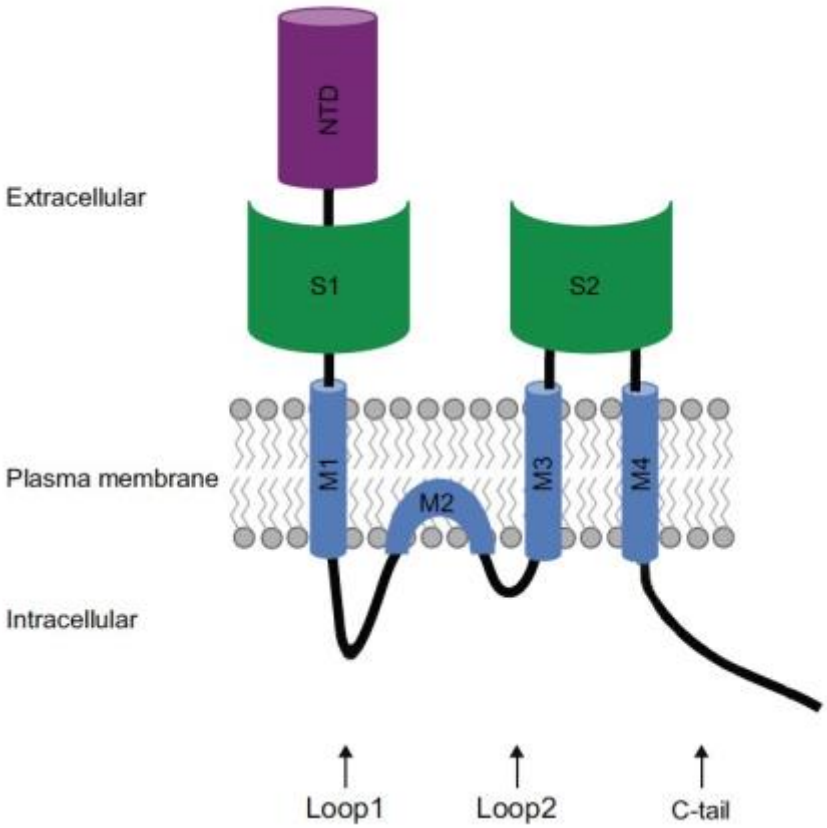

Fig. 1.6.1 A schematic drawing of the GluA1 subunit (adapted from Lu and Roche, 2012.)

However, the currently accepted mechanism controlling postsynaptic expression of either LTP or LTD involves the insertion or removal of AMPARs (Bredt and Nicoll, 2003; Malinow and Malenka, 2002), which is believed to take place perisynaptically (Henley and Wilkinson, 2013) and involves the SNAP (Soluble NSF Attachment Protein) REceptor (SNARE) protein-mediated exocytosis (Kennedy and Ehlers, 2011) and dynamin-dependent mediated endocytosis (Carroll et al., 2001). An important interactor involved in AMPAR folding and export from the endoplasmic reticulum (ER) directing correct postsynaptic membrane insertion are the transmembrane AMPAR regulatory proteins (TARPs), (Tomita et al., 2005). Activity-dependent addition of GluA1-containing AMPARs to synapses results in synaptic strengthening, and hence LTP; activity-dependent endocytosis of AMPARs from synapses results in synaptic weakening, and thus LTD. GluA1 containing AMPARs have not only been implicated in alterations of LTP and LTD *in vitro* but in learning and memory studies *in vivo* (Whitlock et al., 2006; Matsuo et al., 2008).

1.7 N-methyl-D-aspartate (NMDA) receptor subtypes

The NMDAR is far more structurally complex than the AMPAR comprising a much slower channel conductance (Traynelis et al., 2010). NMDARs can be found on both the pre- and postsynaptic membranes, and it is believed that different populations of NMDAR subunit composition may give rise to different plasticity mechanisms (Shipton and Paulsen, 2014). NMDARs in the hippocampus can be found perisynaptically and extrasynaptically as well as within the synapse

(Petralia, 2012). Differential expression and recruitment of these three populations of postsynaptic NMDARs are believed to play distinct functional roles in the modulation of synaptic strength. The functional composition of hippocampal NMDARs is significant in its influence on kinetics, desensitisation and molecular interactions of receptors.

Hippocampal NMDAR-mediated signalling involves synaptic NMDARs that are heterotetramers and consist of four subunits; two of these subunits are always GluN1, and the remaining two are either GluN2 or GluN3 (Fig. 1.7.1). The GluN2 subunit comes in four subtypes: GluN2A, GluN2B, GluN2C and GluN2D (Iacobucci and Popescu, 2017). In the adult rodent hippocampus, the predominant GluN2 subunit is either GluN2A or GluN2B, where GluN2C and GluN2D are primarily expressed during early development. Thus, many hippocampal synaptic NMDARs are either diheteromeric consisting of two subunits of GluN1 in combination with two subunits of GluN2A or GluN2B, or are triheteromeric consisting of two subunits of GluN1 and one GluN2A and one GluN2B. Frank et al. 2015 reported brain region-specific differences in the molar ratio of GluN2A:GluN2B subunit expression which they believe raises the possibility that the NMDAR forms supercomplexes with AMPARs of different GluA1 and GluA2 receptor composition, which are allocated into neuroanatomically distinct synapses. The ratio of synaptic triheteromeric NMDARs is believed to be high but has not yet been confirmed (Tovar et al., 2013). GluN1/ GluN2B heteromers are believed to be the main type of extrasynaptic NMDAR (Petralia 2012).

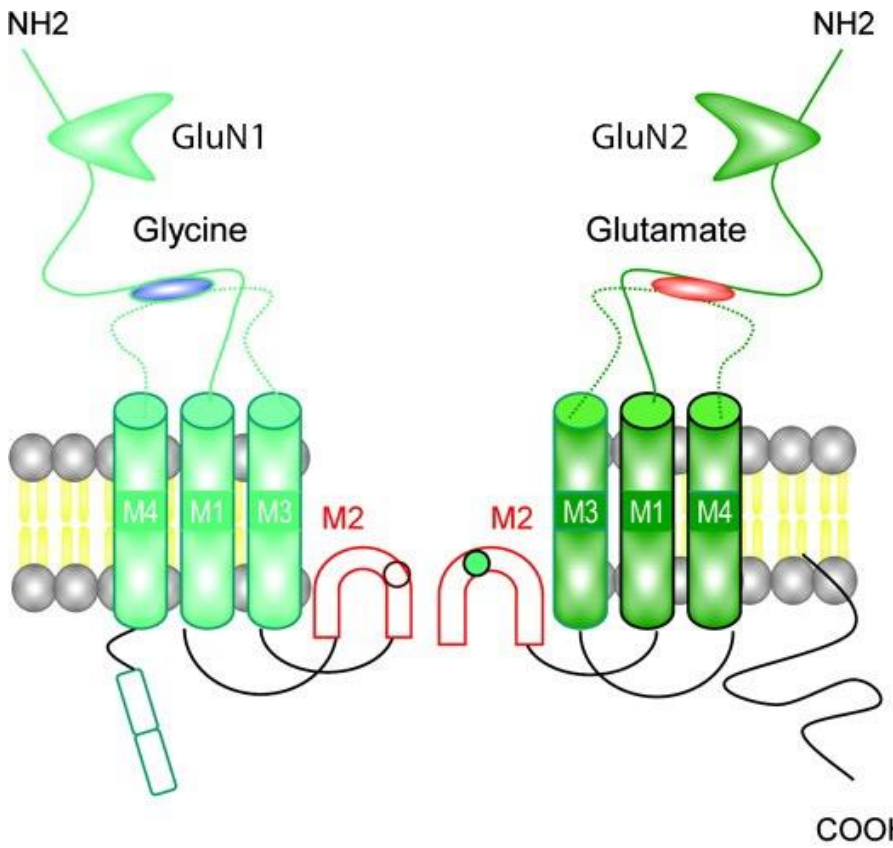

Fig. 1.7.1 A schematic showing the structure of a typical synaptic NMDAR with the glutamate binding site on GluN2 and glycine binding site on GluN1, along with the magnesium blocked ion channel pore occupied by the M2 subunits (adapted from Benarroch, 2011).

The ratio of diheteromers (GluN1/GluN2A: GluN1/GluN2B) at the postsynapse can result in differences in NMDAR channel currents and postsynaptic electrophysiological responses which can influence the type of plasticity expressed at that particular synapse (Vicini et al., 1998; Gray et al., 2011). GluN1/GluN2A containing NMDARs have a higher probability of opening in response to glutamate than GluN1/GluN2B or triheteromeric NMDARs (Erreger et al., 2005; Vicini et al., 1998). In a single active channel patch recording setup, charge transfer through GluN1/GluN2B subunits was greater than through GluN1/GluN2A

subunits**,** and the GluN1/GluN2B channels were able to support twice as much charge transfer relative to GluN1/GluN2A channels due to the slower deactivation rate of the GluN1/GluN2B channels (Erreger et al., 2005) indicating the importance of GluN1/GluN2B channels in LFS induced hippocampal synaptic LTD.

Different charge transfer abilities of different populations of diheteromers and triheteromers may be important in triggering different forms of synaptic plasticity, that require different levels of calcium postsynaptically to modulate downstream signal transduction mechanisms. For example, activation of calcineurin leads to the activation of protein phosphatase 1 (PP1) via disinhibition, allowing CaMKII to be dephosphorylated, promoting the expression of LTD (Lisman, 1989; Carroll et al., 2001). Thus, a greater ratio of GluN2B containing NMDAR channels will generate a higher calcium influx which could have a greater influence on hippocampal synaptic plasticity. Further, the number and location of NMDARs could alter the basal active state of a dendritic spine.

Some recent research reports have challenged the traditional role of ionotropic NMDAR calcium signalling in synaptic plasticity, presenting a non-canonical, metabotropic role of the NMDAR in mediating CA3-to-CA1 synaptic hippocampal LTD (Babiec et al., 2014; Gray et al., 2016; Nabavi et al., 2013). For example, Nabavi et al., (2013) found that LTD was inducible in the presence of an NMDAR uncompetitive antagonist (MK-801) which blocks the NMDAR ion channel function, and the

absence of intracellular calcium rise. Interestingly, this suggests that LTD involves a metabotropic form of NMDAR signalling where conformational changes in NMDARs activated by glutamate binding can trigger downstream signalling pathways at these synapses, similar to that believed to be involved in mGluR signalling. Another potentially MK-801 insensitive function of metabotropic NMDAR signalling involves Aβ-induced synaptic dysfunction in AD; Kessels et al., (2013) found that elevated oligomeric Aβ requires the metabotropic function of GluN2B-containing NMDARs to produce synaptic depression. It is clear that the metabotropic function of the NMDAR in hippocampal LTD needs to be examined more closely.

The first NMDAR antagonist to be used in research with sub-μMolar potency was D-(-)-2-Amino-5-phosphonopentanoic acid (D-AP5), (Davies et al., 1981) and it has proven an invaluable experimental tool in establishing a role for NMDARs involvement in seizures and excitotoxity, as well as synaptic plasticity. Systemic treatment with a broad acting competitive NMDA receptor antagonist CPP has been shown to impair short-term working memory in rats *in vivo* (Cole et al., 1993). A more specific and activity-dependent GluN2B selective NMDAR antagonist (αR,βS)-α-(4-Hydroxyphenyl)-β-methyl-4-(phenylmethyl)-1-piperidinepropanol maleate (Ro 25-6981) has been reported (Fischer et al., 1997) to aid in the determination of function of NMDARs comprising the GluN2B subunit over GluN2A (Jiménez-Sánchez et al., 2014). This compound is important as it has shown antidepressant-like effects in pre-clinical trials (Li et al., 2010) indicating the necessity to target NMDAR

subtypes specifically. D-AP5 binds at the orthosteric site of the NMDAR, similar to CPP, antagonising the metabotropic function of the receptor.

1.8 Metabotropic glutamate receptor (mGluR) subtypes

It has been shown that NMDAR- and mGluR-dependent forms of LTD coexist as two mechanistically distinct forms of LTD in the Schaffer collateral pathway in the rat hippocampus (Nicoll et al., 1998; Oliet et al., 1997; Palmer et al., 1997). Neither form of LTD was able to occlude the other, indicating an independence of the associated expression mechanisms (Kemp et al., 2000). Indeed, it is possible to selectively inhibit either mGluR or NMDAR LTD without affecting expression of the other, using specific mGluR or NMDAR antagonists (Yang et al., 1994). Certain mini EPSC quantal size and frequency differences pointed to a possible presynaptic basis for mGluR-dependent LTD versus a postsynaptic basis for NMDAR-dependent (Bolshakov and Siegelbaum, 1994; Oliet et al., 1997).

mGluRs are class-C G-protein coupled receptors (GPCRs) that are found throughout the CNS and are intricately involved in synaptic plasticity (Niswender and Conn, 2010). Due to their abundance, they are very attractive pharmacological therapeutic targets. There are currently eight known mGluRs which can be subdivided into three groups: group I (mGlu1 and mGlu5), group II (mGlu2 and mGlu3) and group III (mGlu4, mGlu6, mGlu7, and mGlu8). It has been demonstrated that mGluRs can support bidirectional changes in synaptic strength, similar to, but also independent of, NMDARs. mGluRs are activated by the binding of

glutamate to the large extracellular N-terminal domain which comprises a Venus Flytrap Domain (VFD), (Niswender and Conn, 2010). mGluRs have been demonstrated to be important in associative learning and memory (Balschun et al., 2006), specifically at CA3-CA1 synapses (Gil-Sanz et al., 2008).

The G proteins that mGluRs are coupled to are comprised of three different subunits: α, β, and γ, which form the G protein heterotrimer complex (Niswender and Conn, 2010). Inactivated heterotrimers are bound to guanosine 5/ - diphosphate (GDP) and become active via the exchange of a phosphate group onto GDP forming guanosine 5/ - triphosphate (GTP) on the α subunit. Group I mGluRs are intracellularly linked at the postsynapse to these heterotrimers at G-$\alpha_{q/11}$. mGluR stimulation via binding of glutamate at the VFD further activates intracellular signal transduction mechanisms at the PSD via the phospholipase Cβ1 (PLC)-associated pathway. Hydrolysation of GTP back to GDP inactivates the G-$\alpha_{q/11}$ subunit and reassembly of the heterotrimer at the cytoplasmic side of the postsynaptic membrane (Fig. 1.8.1).

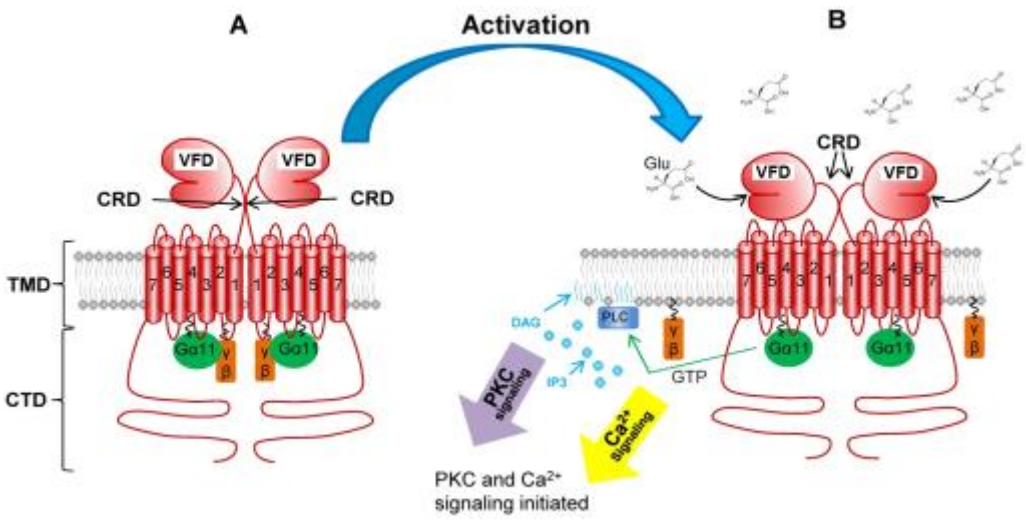

Fig. 1.8.1 A diagram of mGluR activation upon binding glutamate (adapted from Willard and Koochekpour, 2013); amino-terminal domain (ATD), cysteine-rich domain (CRD), transmembrane domain (TMD), cytoplasmic tail domain (CTD).

It is more common to find mGlu5R both extrasynaptically and perisynaptically (Kuwajima et al., 2004) in the dendritic fields of the stratum radiatum of the hippocampus. Group II mGluRs are more commonly found presynaptically where they inhibit the release of neurotransmitter from the presynaptic terminal (Niswender and Conn, 2010). Activation of mGluRs results in the inhibition of predominantly N-type voltage-gated calcium currents in the hippocampal CA regions. The localisation of mGluRs allows for quick and selective regulation and redistribution of neighbouring NMDA and AMPA receptors allowing for modulation of synaptic plasticity (Anwyl, 1999). Activation of mGlu5R enhances neuronal excitability and NMDAR currents; therefore, there is a good chance that a mGlu5R antagonist may reduce the enhancement in neuronal excitability, particularly in brain regions involved in anxiety.

Lüscher and Huber, 2010, have reviewed the evidence that simple activation of group I mGluRs, such as application of the selective orthosteric agonist 3,5-dihydroxyphenylglycine (DHPG) to hippocampal slices, can itself induce an NMDAR-independent form of LTD via the endocytosis of AMPARs.

Group I mGluRs are predominantly coupled to the activation of phospholipase Cβ (PLCβ) generating inositol trisphosphate (IP3) and diacylglycerol (DAG), (Niswender and Conn, 2010). IP3 activation stimulates the release of calcium from intracellular stores via protein kinase C (PKC), including further downstream effectors such as components of the mitogen-activated protein kinase/extracellular receptor kinase (MAPK/ERK) pathway, and the mammalian target of rapamycin (mTOR)/p70 S6 kinase pathway, thought to be imperatively involved in the expression of hippocampal synaptic plasticity (Traynelis et al., 2010). However, this process is not thought to be involved in mGluR-LTD generation in the hippocampus when using the agonist DHPG (Collingridge et al., 2010). On the C-terminal side of group 1 mGluRs, there is an important interaction between the adaptor protein Homer1c and mGlu5R that is critical for the conversion of hippocampal CA1 STP into LTP which involves both mTOR and ERK (O'Riordan et al., 2014). Homer proteins are necessary for mGluR activity, participating in the assembly of protein complexes at the C-terminal tails and as a result, mediate downstream functional responses.

Ultimately, activation of the synaptic group I mGluRs can trigger endocytosis of local ionotropic AMPARs (GluA1/A2 and GluA2/A3) as well as reducing the quantity of available PSD cell surface AMPARs (Moult et al., 2006), as they diffuse laterally to extrasynaptic sites. The role of the endoplasmic reticulum (ER) in CA1 pyramidal dendritic spines is also believed to be important seeing that ER containing spines are more likely to express mGluR-LTD over those that do not (Holbro et al., 2009); ER containing spines produced larger synaptic currents than those without, upon activation of mGluRs. Further, this form of LTD requires rapid protein synthesis (Huber et al., 2000) which is believed to be necessary for the synthesis of AMPARs and other proteins regulating AMPAR trafficking at the PSD.

The VFD is very important for studies utilising pharmacologic agonist/ antagonist compounds to parse out the function of the mGluR in health and disease. There are two lobes of glutamate binding capability in the N-terminal domain of the mGluRs that capture and bind glutamate comprising the VFD. It is believed *in situ* there are two VFDs that bind glutamate resulting in a conformational change which is propagated structurally through the mGluR via cysteine-rich domains (CRDs) to the heptahelical domain (HD) which is found on the C-terminal tail (Rondard et al., 2006). The two VFDs can be found in three different confirmations: open-open, open-closed and closed-closed. These are directly influenced by activating or inhibiting drugs; open-open is the inactive confirmation which is stabilised by antagonists. Agonists bind in the open-closed or closed-closed confirmation (Niswende and Conn, 2010).

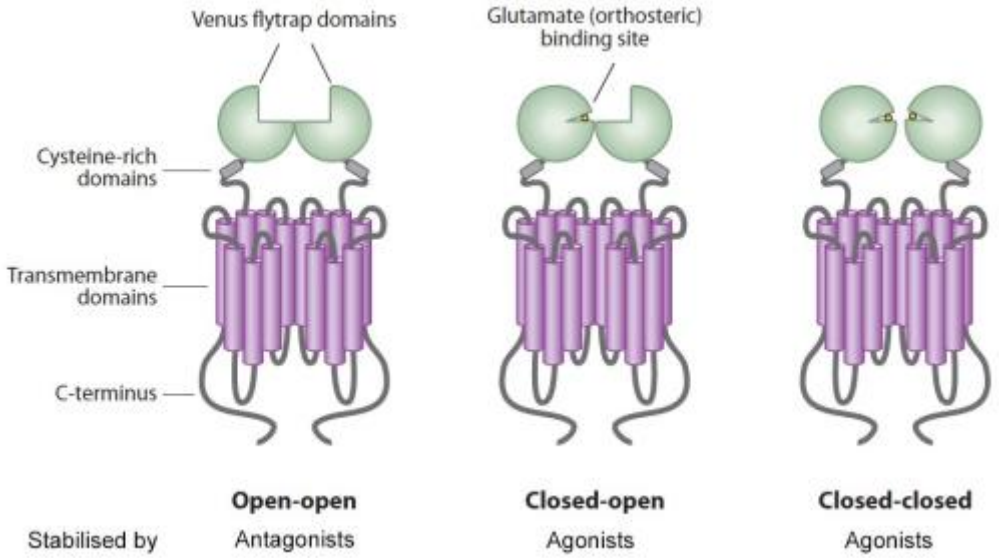

Fig. 1.8.2 A schematic of the mGluR and the different glutamate binding and activation states (adapted from Niswende and Conn, 2010).

There is a variety of selective orthosteric antagonists of group I mGluRs such as LY367385, which is selective for mGlu1R over mGlu5R as well as LY341495, which is highly selective for group II mGluRs over group I. MTEP, which is highly selective for the mGlu5R, is a very potent negative allosteric modulator (NAM), and easily penetrates the blood-brain barrier, which makes it very useful for *in vivo* studies. There are many mGlu5R NAMs undergoing clinical trials in humans (Porter et al., 2005, Jacquemont et al., 2011). A very potent and highly selective positive allosteric modulator (PAM) VU 0360172 was developed to activate the mGlu5R by binding the HD, effectively enhancing the response to glutamate. PAMs are also currently being studied for their potential therapeutic use, such as in the treatment of schizophrenia (Conn et al., 2008).

1.9 Protein synthesis and synaptic plasticity

Protein translation is required in animal brains to convert short-term labile memories into consolidated long-term stable memories for future access and function (Kandel, 2001; McGaugh, 2000, Richter and Klann, 2009). The cellular and molecular changes that take place after a memory forming event usually occur within hours, and the translational machinery required for sustained activity at the synapse does not have the capacity for maintenance without further transcription and translation, processed by the cell body, as well as locally in the dendrites.

Synaptic facilitation/ short-term potentiation (STP) or depression can occur on a timescale of hundreds of milliseconds to seconds, and augmentation or post-tetanic potentiation (PTP) can last for tens of seconds to minutes (Fioravante and Regehr, 2013). STP and PTP are believed to be mediated by different physiological mechanisms. STP can also be observed as an initial decremental potentiation as a result of a high-frequency tetanus that usually decays over a period of tens of minutes (Park et al., 2013; e.g. E-LTP) and can be expressed without local translational activity. Longer lasting change, known as late phase synaptic plasticity (e.g. L-LTP) is mechanistically distinct from E-LTP, lasts on a time scale of hours (and longer: Abraham, 2003), and is protein synthesis-dependent. Further, there is an interim time-period between the early and late phases of LTP, with a variable requirement for protein synthesis (Winder et al., 1998; Raymond et al., 2000). A common interpretation distinguishing STP from LTP states that STP is expressed

as an alteration in the probability of transmitter release, P(r), whereas LTP is expressed by a postsynaptic modification (Park et al., 2013). The overall net plasticity expressed at synapses will reflect consolidated expression of multiple forms of locally expressed, temporally overlapping, synaptic plasticity (Fioravante and Regehr, 2013).

Similarly, protein synthesis-dependent (Manahan-Vaughan et al., 2000; Xu et al., 1998; Huber. et al., 2001; Kauderer and Kandel, 2000) and independent (Pöschel and Manahan-Vaughan, 2007; Xiong et al., 2006) forms of LTD have been reported. Defects in the translational machinery involved in synaptic plasticity maintenance may lead to neurological disease; hence, there is a concerted research effort to target dysregulated translational control in cognitive disorders and synaptic dysfunction.

1.10 Optogenetic activation of glutamatergic transmission and plasticity

The technique of optogenetics is relatively young having been first described in hippocampal neurons by Boyden et al., in 2005. It is a combination of the genetic targeting and expression in mammalian nerve tissue of a light-activatable microbial opsin, e.g. channelrhodopsin, which is a light-gated ion channel protein originating from retinal photoreceptor cells of *Chlamydomonas reinhardtii*. Adeno associated virus (AAV) can be used to package multiple proteins for expression including a promoter targeted to well-defined areas and types of neural tissue (e.g. excitatory) to produce sufficiently strong and specific opsin expression, activation of

which directly elicits electrical current across the expressing nerve extracellular membrane in response to a specific wavelength of light (Fig. 1.8.1). The channelrhodopsin used in this study allows monovalent and divalent cations (H^+, Na^+, K^+ and Ca^{2+}) to flow freely through the opsin pore upon absorption of a photon of light. In microbiota, channelrhodopsin is used as a fast sensor for phototaxis in visible light, and as a result, expression in glutamatergic neurons elicits an excitatory depolarising current similar to that evoked by electrical stimulation (Lin, 2011). The humanised channelrhodopsin 2 (hChR2) is maximally activatable by blue light at a wavelength of 473nm.

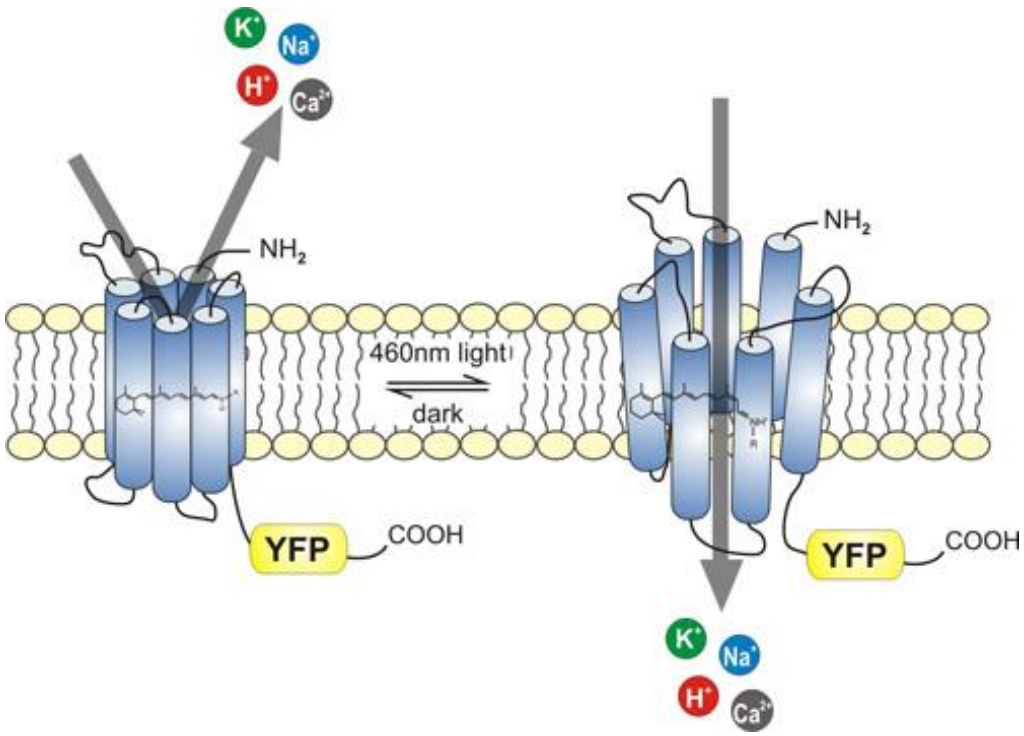

Fig. 1.10.1 Schematic representation of the light activation of Channelrhodopsin-2 (from Prof. Dr Ernst Bamberg, http://www.biophys.mpg.de/uploads/tx_templavoila/bamberg2_02.jpg).

The channel conductance of a single ChR2 is believed to be well below 1 picosiemen (Lin et al., 2009) which is less than most

physiologically common membrane ion channels. Thus, it is believed that about half a million ChRs need to be activated at the same time to depolarise the membrane 15mV when the resistance is 50MΩ, and assuming 100 femtosiemens single-channel conductance, a reversal potential of 0 mV, and a membrane potential −60 mV (Lin, 2011). An important balance for conductance with channelrhodopsin is quick open/ close turnover but with as little sacrifice for sensitivity to the light source. Another consideration is that it can take 5-fold more functional channelrhodopsins to reach a consecutive depolarisation after an initial stimulation due to desensitisation (Nagel et al., 2003), known as the time it takes for the ChR2 conductance to move enough current to lift the membrane potential to firing threshold. Recovery from desensitisation is modulated by intracellular/ extracellular H+ concentration: a higher extracellular H+ coupled with the negative membrane potential will accelerate desensitisation recovery, whereas higher intracellular H+ slows it down (Nagel et al., 2003).

Our aim in the present research is to selectively stimulate glutamatergic responses relatively independently of *en passant* cholinergic fibres. In fact, optogenetics has already been used to induce long-term changes in synaptic efficacy in cultured hippocampal cells (Zhang and Oertner, 2007).

1.11 Optogenetics in the study of the asymmetric brain and LTD laterality

The presence of asymmetry in the animal brain is not unusual and is, in fact, a canonical facet of neural biology (Rogers, 2014). In many mammalian brains, the two hemispheres function differently and display different anatomical structures and features, believed to have developed over time with evolutionary bias (Vallortigara et al., 2010). It is well accepted that the anatomical and functional layouts of the brain are organised asymmetrically, with some specialisations heavily lateralised such as with language and motor functions (Mårtensson F., 2007, Mutha et al., 2012). Even though the 2 hippocampi in humans are anatomically and connectively comparable, there is a potential that task-related activity may be localised to one hemisphere (Squire et al., 1992), such as that seen when left hippocampal dominance was observed with semantic information being most task-relevant, and right hippocampal dominance when spatial information was important (Motley and Kirwan, 2012). The behavioural importance of this lateralisation of function in the human hippocampus was recently highlighted by Iglói K, et al., 2010, who demonstrated that the right hippocampus can predict the use of an allocentric spatial representation, whereas the activation of the left hippocampus predicts the use of a sequential egocentric representation in a navigational memory task. From a structural perspective, mouse brain asymmetry has demonstrated functional differences in postsynaptic spine morphology and receptor distribution in CA1 pyramidal neurons dependent on laterality of originating CA3 input (Shinohara et al., 2008;

Kawakami et al., 2003). Fundamentally, apical CA1 postsynaptic spines, receiving inputs from the left CA3, are thinner and comprise more GluN2B subunit-containing NMDARs than right apical CA1 spines, which tend also to be mushroom-shaped.

Our current employment of optogenetics in this work opens up the opportunity to address the possibility that LTD, like LTP (Kohl, 2011; Shipton, 2014), is lateralised. The induction of LTP was found to be asymmetric by selective stimulation of left and right CA3 inputs to CA1 in the stratum radiatum of adult mice *in vitro*; conditioned stimulation of Schaffer collateral or associational/ commissural inputs from left, compared with right hippocampal CA3 pyramidal neurons, preferentially triggered LTP at apical dendrites on CA1 pyramidal neurons (Kohl, 2011; Shipton, 2014). Intriguingly, LTD is preferentially induced in slices from adult mice that congenitally symmetrically express the type of apical synapse that right CA3 neurons form with CA1 (Kawahara, 2013), raising the prospect that, in wild-type animals, LTD may be preferentially induced at CA1 synapses formed by right CA3 pyramidal neurons.

1.12 Cholinergic control of synaptic activity

It is well accepted that cholinergic signalling is intricately involved in memory acquisition and storage, however, the precise role remains elusive (LeDoux, 2012). Innervating septo-hippocampal cholinergic afferents are sparsely distributed and extensively arborised and interweave with many other projections containing different synaptic phenotypes (Wu et al., 2014). It has been demonstrated with LTP that activation of hippocampal muscarinic receptors can result in a G protein-mediated block of a number of potassium channels, including enhancing NMDAR function, probably mediated by high-affinity postsynaptic muscarinic M2 receptors (Segal and Auerbach, 1997). Recently Leung and Doralp demonstrated *in vivo* that an anticholinesterase drug can enhance LTP in the area CA1, and basal-dendritic LTP can be facilitated in the behaving rat, while it is generating cholinergically driven theta activity as it moves around its environment, which was probably modulated by muscarinic M1 receptors (Leung et al., 2003; Doralp and Leung, 2008). Interestingly, ACh applied directly to the CA1 in acute slices can promote synaptic plasticity (Buchanan et al., 2010), thought to be a result of presynaptic AChRs enhancing glutamate or GABA release. Previous reports have demonstrated an LTD that is at least in part inhibited by muscarinic acetylcholine receptor (mAChR) antagonists *in vitro* (Volk et al., 2007). Further, Hu et al., 2014 have shown that mAChR dependent LTD lasting over 5 h can be induced that requires endogenously released ACh providing significant evidence of the crucial role ACh plays in synaptic information storage.

Moreover, presynaptic cholinergic hypofunction is a hallmark of AD which is believed to at least partly result from degeneration of septo-hippocampal cholinergic neurons, leading to lower choline acetyltransferase levels and choline uptake, as well as reduced acetylcholine synthesis (Blennow et al., 2006). G protein-coupled mAChRs in the hippocampus play a major role in cognition (Reis et al., 2009), and learning and memory, and are a prime target for understanding the molecular mechanisms involved (Wess et al., 2007).

This has led to the “cholinergic hypothesis” in AD treatment; the central deficits play a major role in the progressive cognitive dysfunction and some behavioural impairment associated with AD. Therefore, hypothetically, restoring cholinergic function at these synapses via activation and upregulation of the cholinergic system may help alleviate some of the related symptoms (Fisher, 2008). In the current work, application of the acetylcholinesterase inhibitor donepezil was examined, on the grounds that donepezil is highly selective with good pharmacokinetic properties, as well as being currently used in human therapeutic clinical trials (Sabbagh et al., 2016; Homma et al., 2016). Furthermore, donepezil has been shown to lower the threshold for LTD induction *in vivo* (Hu et al., 2014) and antagonize the suppressive action of Aβ1-42 on LTP *in vitro* (Kapai et al., 2010; Solntseva et al., 2014; but see Kroker et al., 2013). Current symptomatic treatments of AD are limited to acetylcholinesterase inhibitors (AChE-I) and N-methyl-D-aspartate receptor (NMDAR) antagonists, and mostly only provide incremental and transient benefits (Kim et al., 2017).

1.13 Synaptic plasticity and Alzheimer's disease Aβ

Although AD is the most common neurodegenerative disorder, the specific molecular mechanisms behind the development of the progressive cognitive and memory impairment remain unknown (Nestor et al., 2004). Since its initial description over a century ago by Emil Kraepelin and Alois Alzheimer in 1909 (Alzheimer A., 1915), it is well accepted that the hippocampal formation is a major target for pathological changes of neuroanatomy in patients suffering from AD (Jack et al., 1998; Convit et al., 1997). It has since been discovered that the initial burden of AD begins in the entorhinal cortex and hippocampus (Pennanen et al., 2004) before invading, and causing widespread destruction of, the cerebral cortex (Braak and Braak, 1991). The etiological course of symptoms begin with impairment of episodic memory as the accumulation of amyloid plaques and neurofibrillary tangles take hold, leading to progressive dysfunction of other cognitive abilities as well as limb apraxias, and eventually to severe global impairment of cognitive function including amnesia, aphasia and agnosia (Kumar et al., 2015). Extensive research has identified that an accumulation of amyloid-β protein (Aβ) is an early and essential aetiological factor in AD (McLean et al., 1999); moreover, the accumulation of Aβ into the amyloid plaque is a characteristic hallmark of the disease.

There is evidence that proposes a glutamatergic role in the generation of some of the symptoms of AD (Hynd et al.,2004) as well as

illustrating that Aβ promotes glutamatergic excitotoxicity (Haass and Selkoe, 2007). Soluble Aβ oligomers have been shown to rapidly and potently disrupt glutamatergic synapses and plasticity mechanisms, including LTP (Shankar et al., 2008). Interestingly, a deficit in synaptic transmission can be detected before the formation of insoluble Aβ deposits (Hsia et al., 1999), and NMDAR-dependent LTP has been shown to be impaired by Aβ (Wang et al., 2004), and indeed Aβ is synaptotoxic in the absence of plaques (Mucke et al., 2000). More recently, the GluN2B subunit-containing NMDARs have been implicated in regulating the actions and localisation of Aβ oligomers (Li et al., 2009) and preventing Aβ-mediated synaptic plasticity disruption *in vivo* (Hu et al., 2009). The current research examined *in vivo* mechanisms of disruption of synaptic plasticity by a synthetic form of Aβ, amyloid-β derived diffusible ligands (ADDLs) and tested its dependence on NMDAR activity.

There has been a considerable effort to map and image the temporal changes in the human brain from early mild cognitive impairment (MCI) through to late/ end-stage AD, with a particular emphasis on measuring the changes witnessed in hippocampal volume over time, with the intent to track the AD progression and understand the pathogenesis (Wang et al., 2003). Where many studies have reported bilateral changes in hippocampal volume (Pennanen et al., 2004; Jessen et al., 2006) a few have reported on distinctive lateralisation of alterations in morphologic lesions and hippocampal volume associated with AD (Moossy et al., 1989; Wolf et al., 2001; Zhang et al., 2007). Even though

there appears to be a left-less-than-right asymmetry (Thompson et al., 2003) in controls, MCI and AD patients across multiple studies, Shi et al., 2009, among others, believe that this may adjust dynamically over the course of the disease progression, although Long et al., 2011, believe that hemispheric asymmetry alterations may be helpful for monitoring AD progression and thereby improve the management of these neurodegenerative disorders.

1.14 Objectives

Considering the importance of fundamentally understanding the critical processes that are believed to underlie information storage processes in learning and memory, as well as in memory dysfunction, the work presented in this thesis aims to:

- Determine if specific expression of ChR2 by AAV transduction in excitatory CA3 pyramidal neurons elicited functional synaptic responses at apical dendrites in the *stratum radiatum* of area CA1 in the living rat.

- Compare canonical LTD induced by electrical LFS of Schaffer collateral/ commissural pathways with LTD induced in the Schaffer collateral pathway by selective optical LFS; determine the requirement for *de novo* protein translation, and if LTD induction and expression in the electrical and optical pathways are independent.

- Assess the role of NMDA and mGlu5 receptors in hippocampal synaptic LTD induced electrically and optically.

- Evaluate the requirement for activation of cholinergic transmission in optogenetically and electrically driven LTD.

- Probe the involvement of NMDARs and lateralisation in Alzheimer's disease Aβ-facilitated LTD.

II. Methods

2.1 Animals

2.2 AAV-Channelrhodopsin vector

2.3 Virus injection

2.4 Recording apparatus

2.5 Animal surgery and electrode implantation

2.6 Electrode placement

2.7 Recording fEPSPs and input/ output (i/o) curves

2.8 Imaging and eYFP-ChR2 expression

2.9 Compounds

2.10 Data analysis

2.1 Animals

All work was carried out in accordance with guidelines under license from the Health Products Regulatory Authority, Ireland. Adult male Wistar and Lister hooded rats, supplied in-house by Trinity College Comparative Medicine and Harlan laboratories, were housed in a monitored 12-h light-dark cycle (8 am – 8 pm), at room temperature (19–22 °C) and humidity (55-70%), all controlled electronically. All animals (10-36 weeks old/ 300-500g) underwent the same electrode implantation procedure under non-recovery (urethane) anaesthesia. For optogenetic studies animals (10-12 weeks/ 300-330g) were pre-injected with the virus under recovery anaesthesia and underwent non-recovery anaesthesia ~8-28 weeks later for electrode implantation.

2.2 AAV-Channelrhodopsin vector

Optogenetic stimulation was carried out in those animals transduced with channelrhodopsin 2 (ChR2) DNA using viral vectors AAV2 or AAV5, which are two different serotypes of the 11 currently identified serotypes of AAV. They are helper-dependent members of the *Dependovirus* genus of the Parvoviridae family; they have no known pathology, and there are no symptoms nor association with allergic or toxic effects, and thus there is no known risk to human health, animals or plants. This is an important safety issue for the operators and laboratory. The recombinant AAV that is produced by cells is recombinant deficient and can only replicate in the presence of helper adenovirus genes. If exposed to the environment it is unlikely to survive for extended periods. Further, the resultant vector is

not capable of altering the pathogenicity, survivability or fitness of the recipient organism.

The AAV directs the expression of a humanised channelrhodopsin (hChR2-H134R - histidine to arginine conservative mutation at position 134), fused to an enhanced yellow fluorescent protein (EYFP) allowing post-hoc visualisation of expression and localisation. In-frame fusion to EYFP via a *NotI* site makes visualisation of ChR2-expressing cells easier. Expression is driven by a calcium/ calmodulin-dependent protein kinase II (CaMKII) promoter in the vector sequence. A woodchuck hepatitis virus posttranscriptional regulatory element (WPRE) was also used as it can substantially increase the expression of the hChR2. ChR2 is one of the best characterised and most widely used actuators in optogenetics; its activation requires a control signal and a source of energy, both of which were provided in this laboratory as computer directed blue laser light. Optogenetics is believed to be very precise and safe for long-term expression and study (Ivanova and Pan, 2009).

The rAAV/CaMKIIa-hChR2(H134R)-EYFP-WPRE plasmid used in this study was provided by Dr Karl Deisseroth (Stanford University). The virus solution (5.1-8.5 x 10^{12} vg/ml) was prepared by the University of North Carolina (UNC) vector core at Chapel Hill, North Carolina, where it was grown in human embryonic kidney cells (HEK293). Upon arrival, the sample was separated on ice into 3µL aliquots and stored at -80°C. Unless otherwise stated the sample was not diluted for injection. The linear (Fig. 2.2.1) and circular plasmid diagrams (Fig. 2.2.2) indicate the arrangement of exons in sequence.

Fig. 2.2.1 pAAV-CaMKIIa-hChR2(H134R)-EYFP in sequence linearised plasmid map.

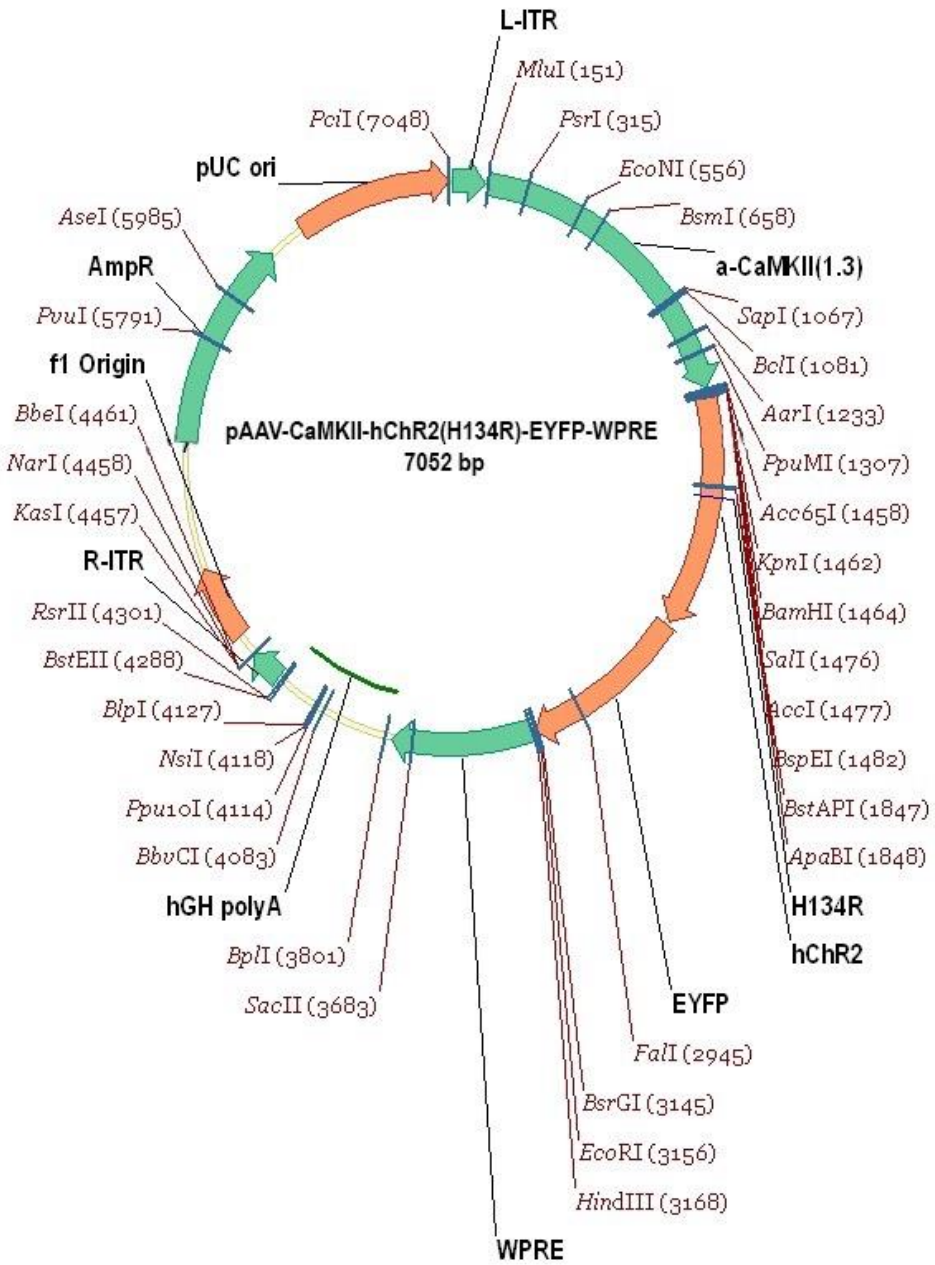

Fig. 2.2.2 pAAV-CaMKIIa-hChR2(H134R)-EYFP circular plasmid map.

2.3 Virus injection

For virus injection, the animals were anaesthetised with ketamine (80mg/kg) and xylazine (8mg/kg), both i.p., under biosafety Level 2 conditions. After local application of betadine to the pericranial scalp, a subcutaneous injection of lignocaine (20mg/ml) was administered. A small hole was drilled into the skull at coordinates -3.8mm posterior to the coronal suture, and -3.8mm lateral to the sagittal suture, measured from bregma (Fig. 2.3.1). A 10µl Hamilton syringe containing 2.5 ± 0.25µl virus preparation was lowered 3.8mm from the surface of the skull into either the right or left dorsal hippocampus area CA3; one hemisphere, either right or left, was transduced in equivalent numbers of animals. 1.0 ± 0.1µl of the stock virus was injected continually over a period of 10 min at 100nl/min; the syringe was left in place for a further 10 min. A 1:5 and a 1:10 dilution (in saline) of the stock virus was tested; however, the ChR2 expression was not sufficient two months' post-surgery to trigger a reliable optical fEPSP for study. Therefore, it was decided to inject stock, undiluted virus. After withdrawal of the syringe, the opening was sealed with glue, the scalp incision sutured with stainless steel wound clips (Reflex 7 skin closure system, World Precision Instruments, Inc. Sarasota Fl. USA) and further glued with cyanoacrylate tissue adhesive (Vetbond, 3M). The animals were monitored until fully conscious and housed singly for one week or until wound healing had completed, after which they were housed in pairs with continuous access to food and water *ad libitum*. Animals were monitored twice daily for the first 3 days' post-op, and daily thereafter.

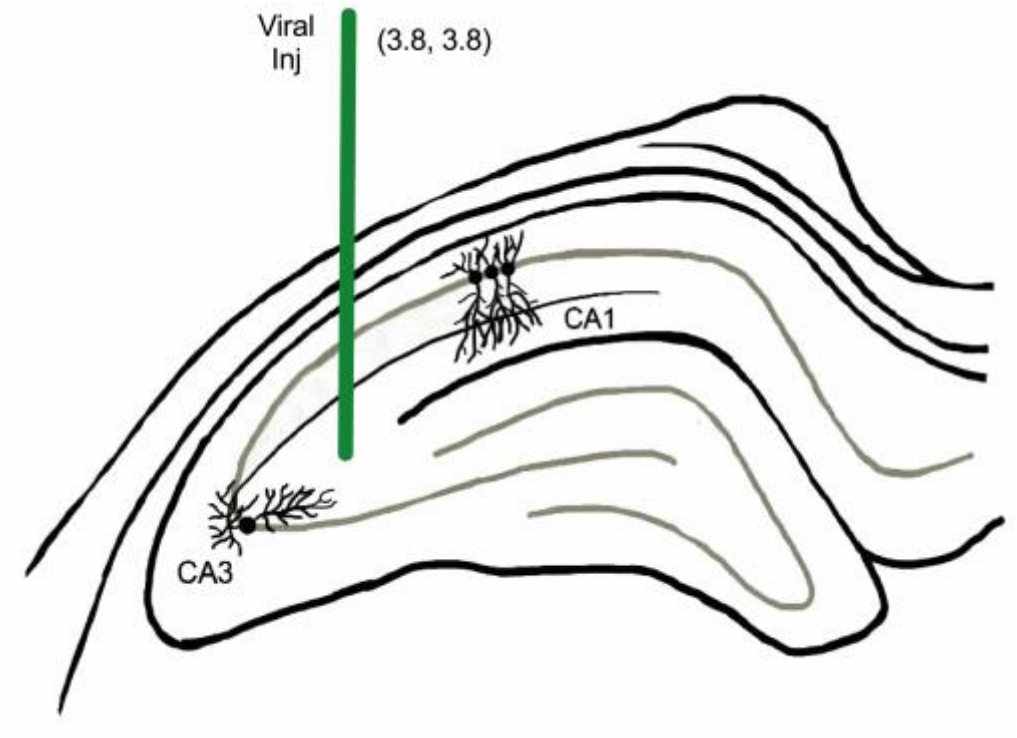

Fig. 2.3.1 Parasagittal view of dorsal hippocampus and approximate intended location of virus injection.

2.4 Recording apparatus

All experimental recording procedures took place in a Faraday cage to remove background and environmental electrical interference. All equipment, including the cage itself, were grounded to a central node eliminating electrical interference. The constant current isolation unit (Grass Instrument Co.) was coupled to the stimulating output of the recording unit. The evoked field potential responses were sent via a pre-amplifier, with the gain set to 11, to an analogue-to-digital converter (Powerlab 2/26, AD Instruments) controlled by the software program LabChart.

2.5 Animal surgery and electrode implantation

Animals were anaesthetised with urethane (1.5 -1.6 g/kg, i.p.) and core body temperature was maintained at 37°C while the animal was secured in a stereotaxic apparatus for the duration of the experiment. A twisted bipolar Teflon-coated tungsten wire (inner core diameter 50µm, external diameter 75µm) was used as the electrical stimulating electrode. In the case of virally transduced animals, a 200 µm optical fibre was attached to the twisted bipolar Teflon-coated tungsten wire to form an optrode assembly (Fig. 2.5.1), where the tips of the electrical twisted pair wire were within ~100µm of the tip of the optical fibre. The optrode coordinates were -4.2 mm posterior to the coronal suture, and -3.8mm lateral to the sagittal suture, measured from bregma. A monopolar Teflon-coated tungsten wire (inner core diameter 75µm, external diameter 112µm) recording electrode was lowered into the hippocampus area CA1 at coordinates -3.5 mm posterior to the coronal suture, and -2.5mm lateral to the sagittal suture, measured from bregma (Fig. 2.5.2). Screw electrodes located over the contralateral cortex were used for reference and earth.

a **b**

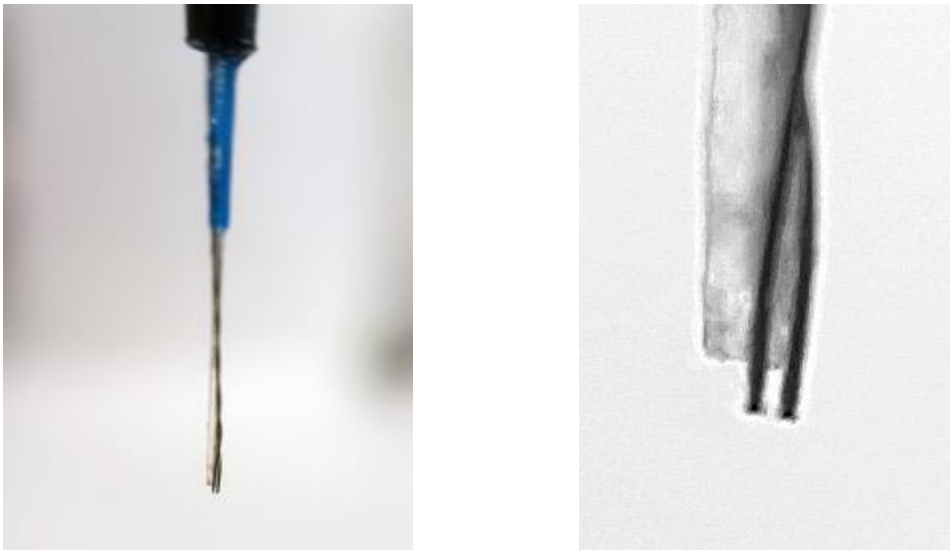

Fig. 2.5.1 (a) Photograph of a representative optrode used in this work. (b) Magnified view (converted to black and white for easier viewing) of the tip of the optrode that was implanted into the area CA3 of the rat hippocampus.

a

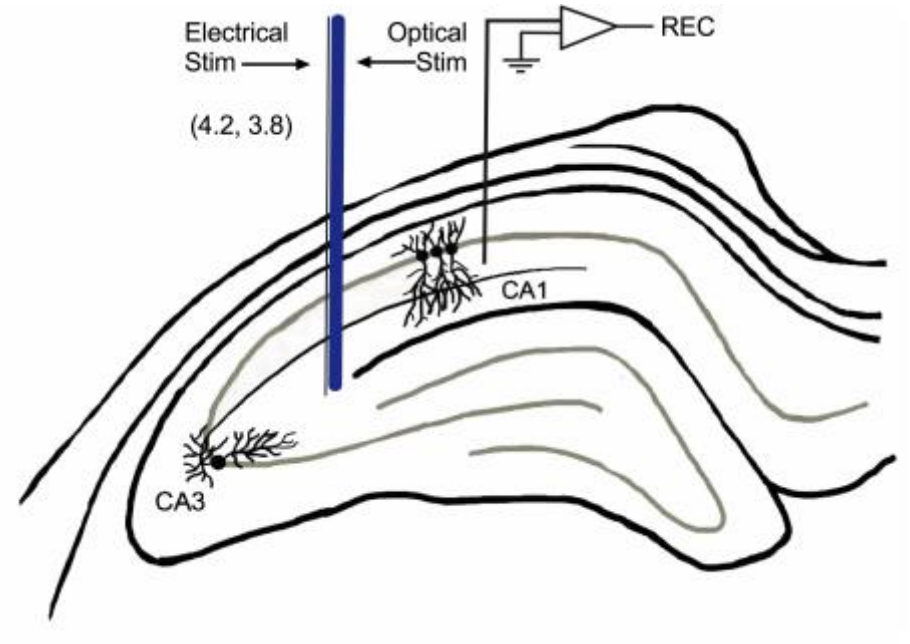

b

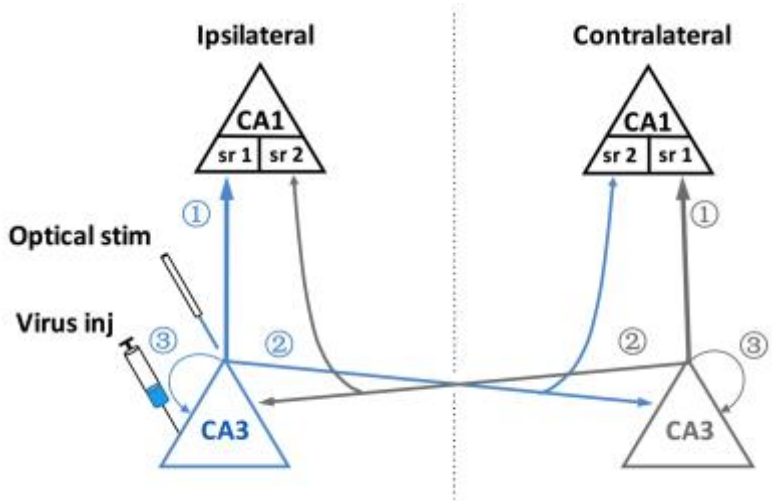

Fig. 2.5.2 Stimulation and recording configuration. (a) Parasagittal view of dorsal hippocampus and intended location of stimulating optrode and recording electrode. (b) Schema of the pathways activated by optical stimulation (stim) after virus injection (inj). CA3 neurons expressing ChR2 (blue) send (1) Schaffer collaterals to ipsilateral CA1, (2) commissural fibres to contralateral CA3 and CA1, and (3) recurrent collaterals within the ipsilateral CA3. With the optrode in the ipsilateral CA3 area, optical stimulation, in contrast to electrical stimulation, selectively activates Schaffer collaterals in the ipsilateral CA1 area.

Unless otherwise stated, the stimulation and recording electrodes were placed in the same hemisphere together, ipsilateral to the side of virus injection (Fig. 2.5.2). The optical fibre was located such that the emitted light was directed towards the dendrites and cell bodies of CA3 pyramidal neurons. In a small number of experiments designed to photo-activate commissural fibres (Results section 3.2.1) we used the same electrode coordinates but contralateral to the side of virus injection. In pilot studies (n=4) we placed the optrode close (3.8 mm posterior to the coronal suture, and -2.8 mm lateral to the sagittal suture) to the recording electrode in the CA1 area in order to locally stimulate the Schaffer collateral fibres and terminal boutons. Similar, but markedly smaller magnitude fEPSPs and LTD were elicited when the optical fibre was located in CA1 area adjacent to the recording electrode. Hence we did not carry out further experiments with this configuration.

Where necessary, a stainless-steel cannula (22 gauge, 0.7 mm outer diameter) was implanted above the ipsilateral-to-stimulation ventricle during the electrode implantation procedure (500µm posterior to the coronal suture, and 1 mm lateral to the sagittal suture, lowered 4.2 mm from the surface of the skull) and secured in place with dental cement (Fig. 2.5.3). The i.c.v. application of drug/ vehicle was facilitated through an internal cannula (28 gauge, 0.36 mm outer diameter). All solutions were injected no quicker than 1 µl per min. Verification of the placement of the cannula was performed post-mortem with the injection of 1 µl bromophenol blue solution to stain the ventricles.

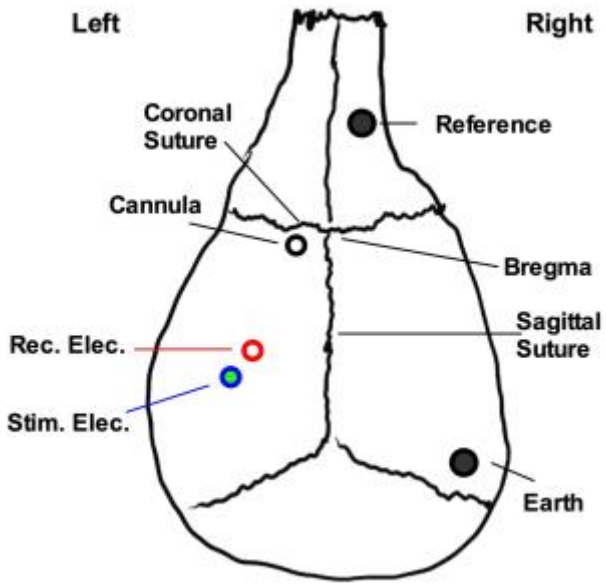

Fig. 2.5.3 A topographical schematic of placement of screws, cannula and electrode openings in rat skull for animal recordings when positioned over the left hemisphere; the locations were reversed for electrode placement in the right hemisphere.

2.6 Electrode placement

Responses to electrical stimulation were used to guide the localisation of the electrodes. In transduced rats alternating 473nm 4ms optical (average half maximum was 0.5-1.0 mW dependent on individual rat, expression level, age, with a maximum intensity of 9 mW), (Shanghai Laser and Optics Century Co., Ltd., China) and electrical test pulses were delivered to the Schaffer-collateral/ commissural pathway every 10 sec, at a frequency of 0.1Hz, to evoke field excitatory postsynaptic potentials (fEPSPs) at a low-intensity, monitoring the evoked responses as the electrodes were slowly positioned. Both stimulating and recording electrodes were initially lowered 1.0mm from the surface of the brain (Figs. 2.6.1 a). The stimulating electrode was lowered further until an upward deflection in the fEPSP was noted for both optical and electrical stimulation (Figs. 2.6.1 b,c). Once the wire tip of the optrode passed through the cell body layer, the recording electrode was then lowered until it too passed through the stratum pyramidale into the stratum radiatum in area CA1 (Figs. 2.6.1 d). After a period of 30 to 60 min to allow for electrode settlement in their respective locations, the positioning was further fine-tuned for optimal fEPSP size and shape. Direct current (44mA for 3s) was delivered to create a lesion at the wire tip locations (with a Grass S88 stimulator). The final placement of electrodes was confirmed via post-mortem analysis (Fig. 2.6.2).

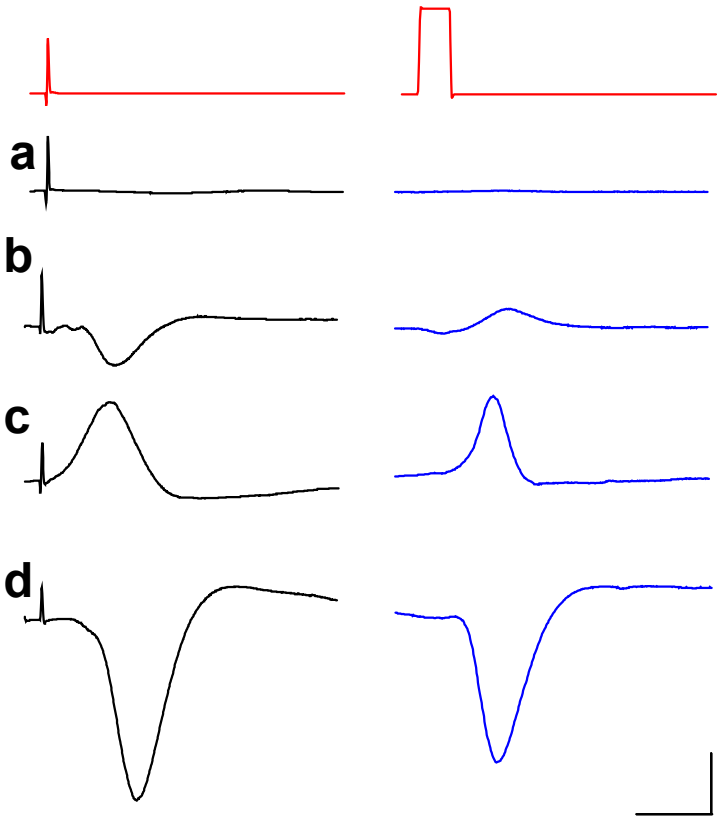

Fig. 2.6.1 Representative optical and electrical evoked fEPSPs from a single experiment during which the electrodes were lowered into place. (a) Both the stimulating optrode and the recording electrode were 1mm deep from the surface of the brain (left red line denotes the electrical stimulus and the right red line the optical excitation of a 4ms pulse); (b) the stimulating optrode was moved deeper giving this characteristic shape when it was in the stratum oriens; (c) the stimulating electrode was moved deeper, through the stratum pyramidale and into the stratum radiatum in area CA3, confirmed by the electrical fEPSP polarity; (d) the recording electrode was then positioned in the stratum radiatum of area CA1 and fine-tuned for optimal EPSP size and shape. Calibration bars: vertical, 1mV; horizontal, 10ms.

a **Stimulating optrode**

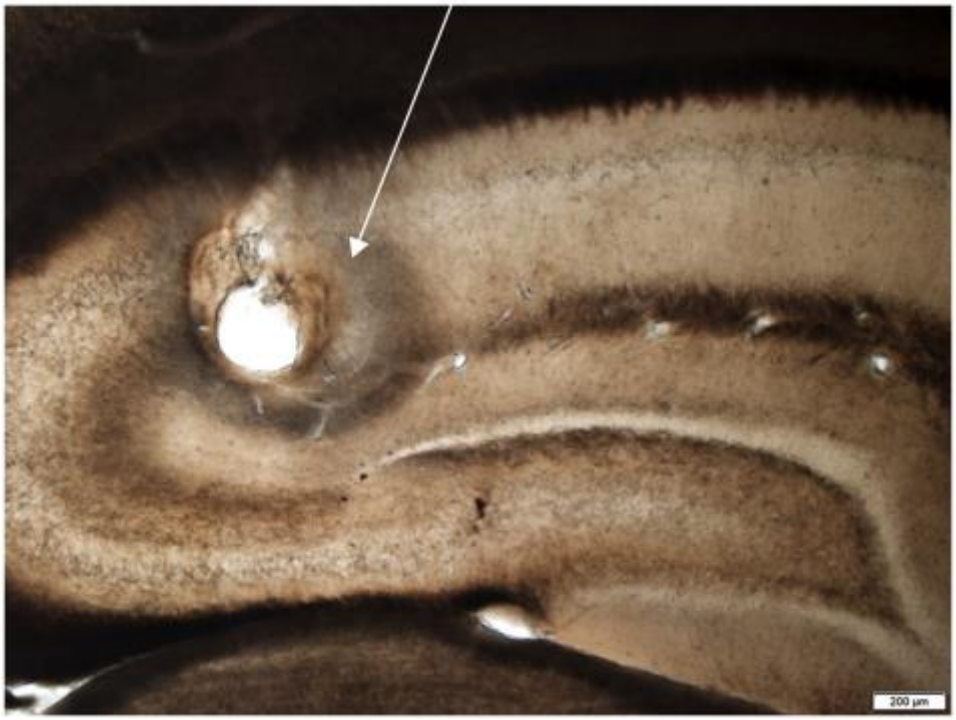

b **Recording electrode**

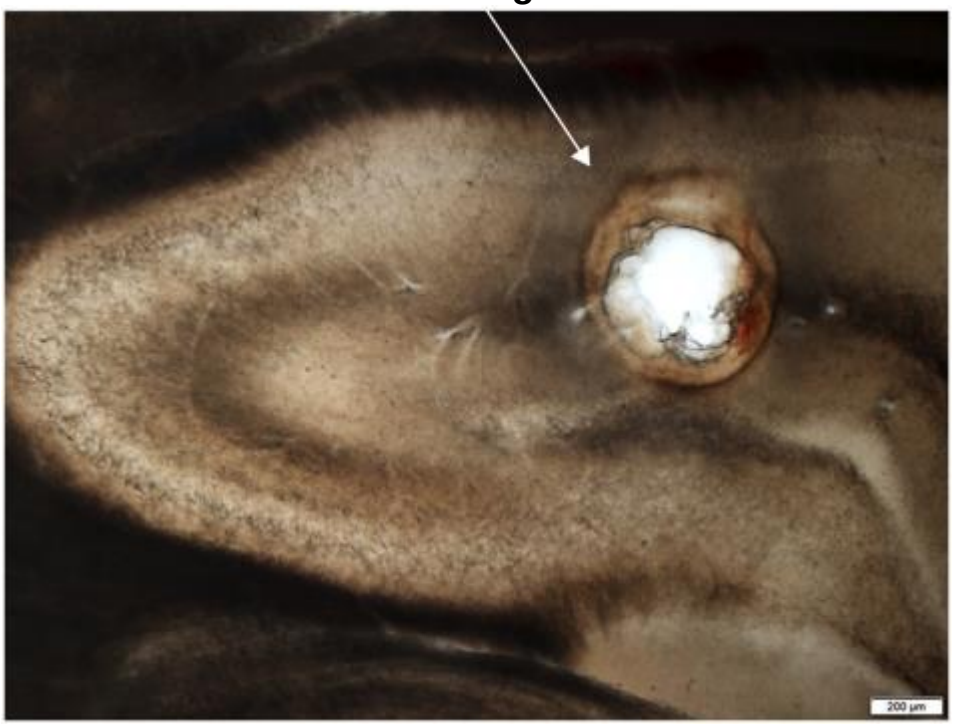

Fig. 2.6.2 Light microscope (Olympus BX51 upright) images showing a representative location of the (a) stimulating optrode and (b) recording electrode placement. An electrical lesion was created at the wire tip locations.

2.7 Recording fEPSPs and input/ output (i/o) curves

The optical fibre was attached to the laser unit, which in turn was connected to the power unit, which was controlled by Macintosh (Mac) software Scope, version 4.0.1, which directed a data acquisition unit (Powerlab 2/25, AD Instruments); the electrical stimulation wires were controlled by personal computer (PC) software PowerLab version 7.3.8, also attached to a Powerlab 2/25. The laser unit utilised an experimenter-controlled analogue knob to regulate output power. When the output of the optical fibre to the 4 ms optical square wave pulse was tested using an optical power meter (Thorlabs), the output was noisy and not as flat as anticipated (Fig. 2.7.1). Nonetheless, the optical pulse was capable of evoking an optical fEPSP (Fig. 2.7.2) that had a similar shape and amplitude to an electrically evoked fEPSP (Fig. 2.7.3).

The latency of onset of fEPSP measured from the beginning of the 4 ms optical laser light pulse was recorded as 7.0 ± 0.3 ms, whereas the latency from the stimulus artefact to onset of electrical fEPSP was recorded as 4.25 ± 0.5 ms, where n = 10 different animals, and matched recordings were taken from the same experimental animal during the baseline before any experimental perturbation (Fig. 2.7.4). This difference could be accounted for by the variable onset of the optical stimulus initial synchronous discharge of CA3 pyramidal cells, recorded as a spike (Fig. 2.7.5).

In pilot studies, we tested an LED source which evoked similar fEPSPs, but the maximum output was insufficient to evoke large responses. Optical test pulses were run at a frequency of 0.017 Hz and an intensity that evoked half maximum fEPSPs. Interleaved test fEPSPs were evoked by electrical square wave pulses of 200μs duration and adjusted to evoke half maximum fEPSP amplitude, also at a frequency of 0.017 Hz.

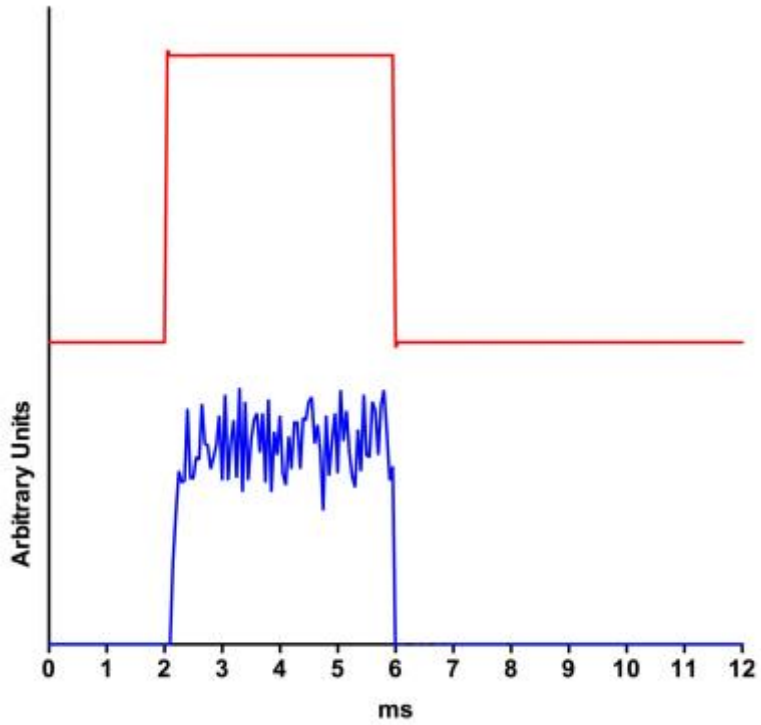

Fig.2.7.1 Representative recording of a 4ms optical ‘square-wave’ pulse generated by the 473nm blue light laser unit set to half maximum intensity. The upper (red) trace indicates the signal sent to the laser power unit; the lower (blue) trace indicates the raw trace of the light output recorded with an optical power meter (Thorlabs).

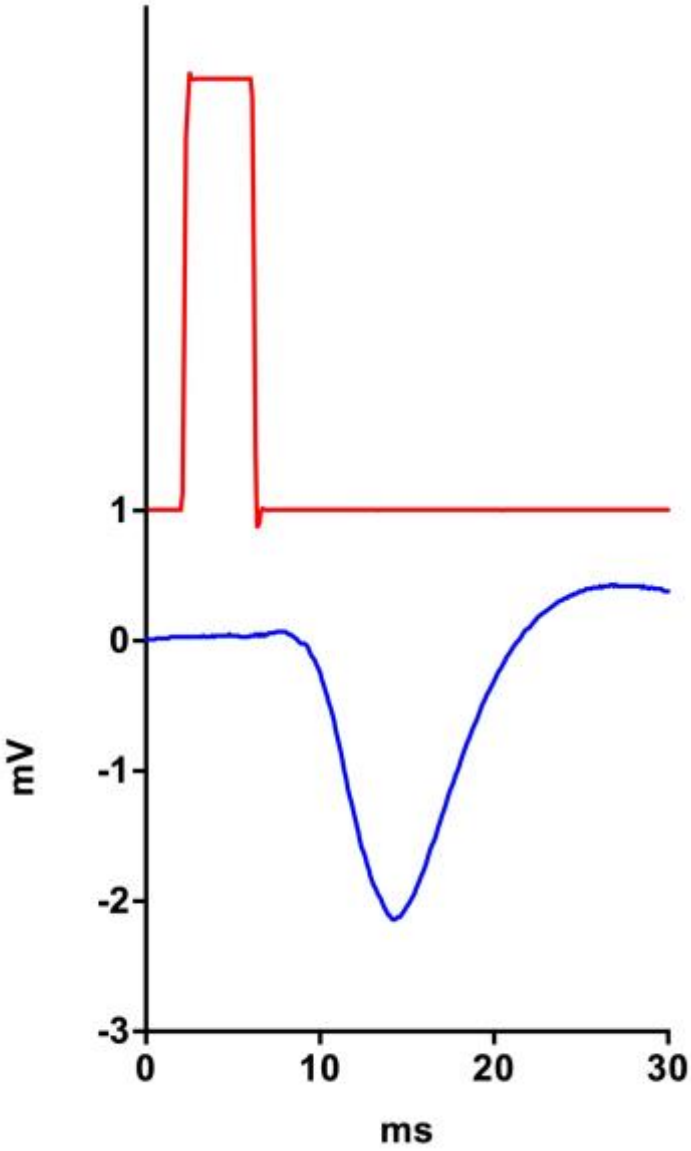

Fig.2.7.2 Representative recording of an optically evoked fEPSP. The upper (red) trace indicates the signal sent to the laser power unit; the lower (blue) trace shows a typical fEPSP evoked by optical stimulation.

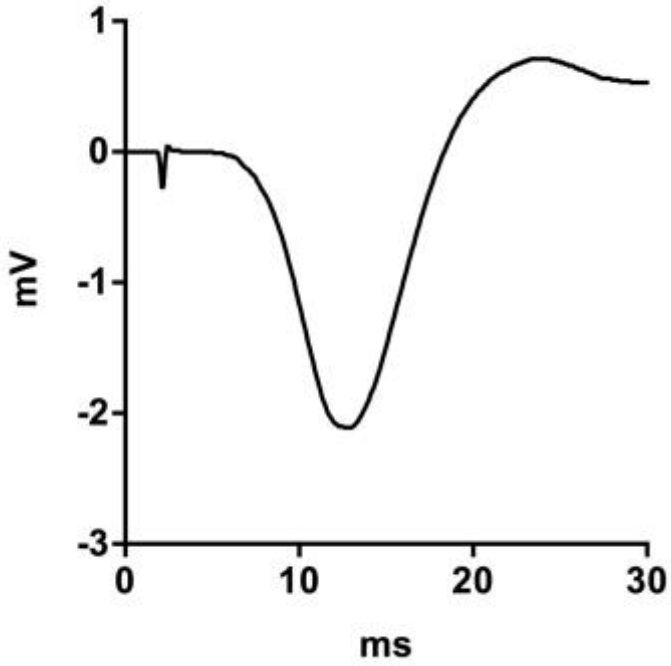

Fig.2.7.3 Representative recording of an electrically evoked fEPSP.

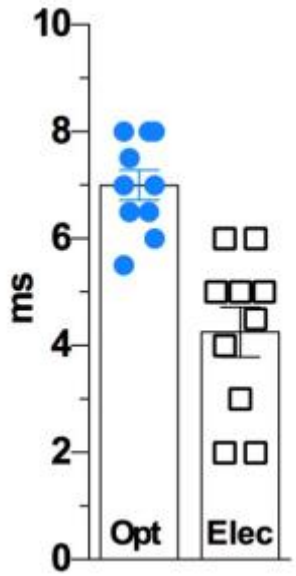

Fig.2.7.4 A bar chart showing the recorded latency from stimulus artefact (elec) or beginning of 4 ms optical laser light pulse (opt) to onset of respective fEPSP. Matched recordings from 10 different animals; examples taken from half maximum stimulus recordings during baseline before any experimental perturbation.

In order to measure the evoked synchronous discharge of CA3 pyramidal cells in the virally transduced rats by the 4ms optical pulse, the electrical stimulating bipolar electrode in the optrode was repurposed as a recording electrode. With the optical fibre located such that the emitted light was directed towards the dendrites and cell bodies of CA3 pyramidal neurons, and the test pulse set at an intensity that evoked a half maximum fEPSP in the CA1 area, multiple spikes were recorded adjacent to the optical fibre in CA3 (Fig. 2.7.5). In order to record the spikes, separate from any local CA3 fEPSP, a 300 Hz high pass filter and 1.5 kHz low pass filter was applied, utilising the LabChart software.

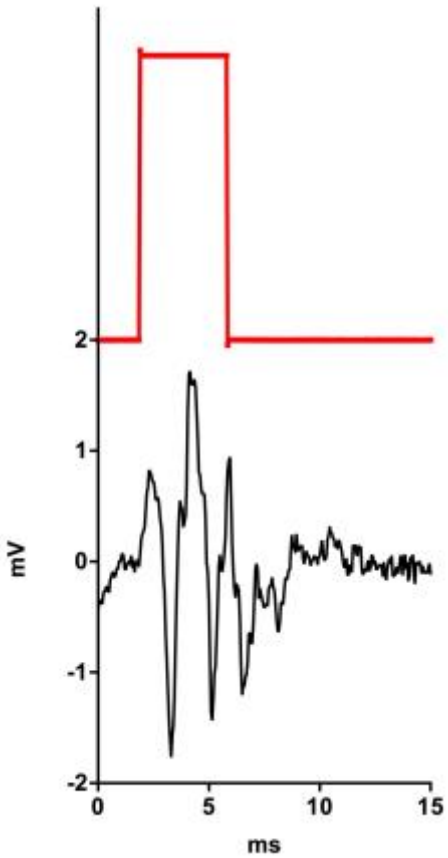

Fig.2.7.5 Representative trace of high-frequency spiking recorded near the tip of the optical fibre in CA3 during a 4ms optical pulse.

Once the fEPSP size and shape stabilised, usually ~30-60 min after final electrode positioning, optical and electrical i/o curves were generated for each rat separately to ascertain half maximum stimulation optical power (mW) and electrical (mA) intensities (Fig. 2.7.6). The electrical and optical i/o curves were run independent of one another and in triplicate with a 10min break between each modality. For the electrical i/o curve, 0.2ms pulses were applied from 4.5 to 15mA at a frequency of 0.05Hz and increasing in 0.75mA increments, sequentially. For the optical i/o curve, 4ms pulses were applied from 0mW to 9mW. Where possible, at the end of each experiment, i/o curves were recorded to monitor any change in the synaptic responses.

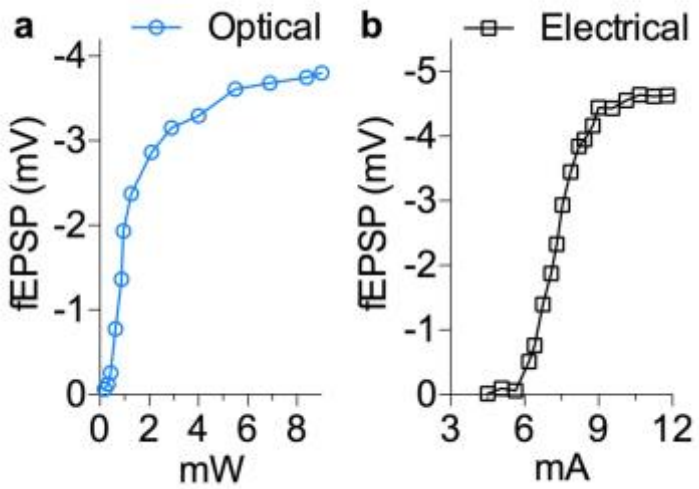

Fig. 2.7.6 Representative i/o curves. (a) Growth of fEPSP amplitude in response to an increase in optical power; (b) growth of fEPSP amplitude in response to an increase in electrical stimulus current.

Baselines were run for a minimum of 30 min before application of any vehicle/drug. Unless otherwise stated LTD was induced with an LFS protocol consisting of 900 pulses at 1 Hz and the stimulation intensity

increased to 95% maximum amplitude for both stimulation modalities. fEPSPs were usually recorded for at least 2 h after the last LFS before a final end-run i/o curve was measured. Background EEG in the hippocampus was monitored (LabChart, AD instruments) throughout the experiment.

2.8 Imaging and eYFP-ChR2 expression

Upon completion of an experiment, the rat was perfused with 4% paraformaldehyde (Sigma) and the brain was stored at 4°C for 24-48 h, after which the brain was transferred to a solution of 30% glucose in 1xPBS w/v for long-term storage at 4°C. For imaging, the brain was mounted longitudinally and submerged in a bath of 4°C phosphate buffered saline (PBS) in a 752M Vibroslice (Campden Instruments). For fluorescence imaging, 200µm coronal slices were suspended in a solution of 4′,6-diamidine-2′-phenylindole dihydrochloride (DAPI; Thermo Scientific, USA) at a concentration of 1µg/ml for 15 min before being wet-mounted on a microscope slide and allowed to dry. Hard set Vectashield (Vector Labs Inc., USA) was added for slice preservation and imaging. Images were acquired on an Olympus BX51 upright microscope, and a Leica SP8 gated stimulated emission depletion (STED) confocal microscope.

We saw robust ChR2 expression in the dorsal hippocampus bilaterally as detected by the presence of fluorescing green eYFP visible in confocal images (Fig. 2.8.1). At higher magnification, it was possible to identify the layers of stratification in detail (Fig. 2.8.2 and 2.8.3). As a

control, saline was injected in the same location, instead of the AAV preparation. As expected, no eYFP fluorescence was detected (Fig. 2.8.3). Ipsilateral Contralateral

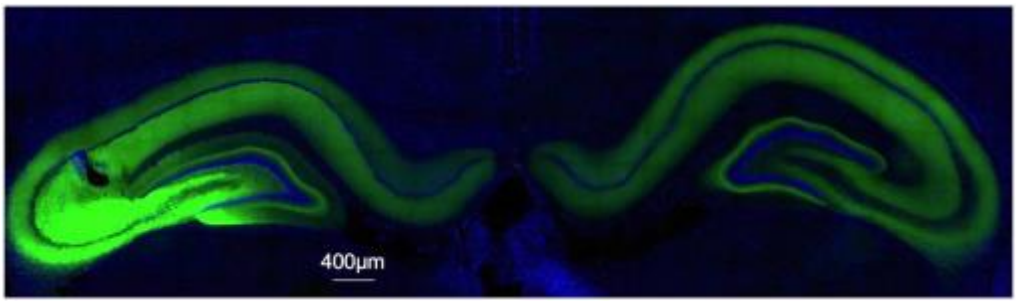

Fig. 2.8.1 Confocal image showing representative bilateral expression profile of green ChR2-EYFP and blue DAPI nuclear stain in the dorsal hippocampus.

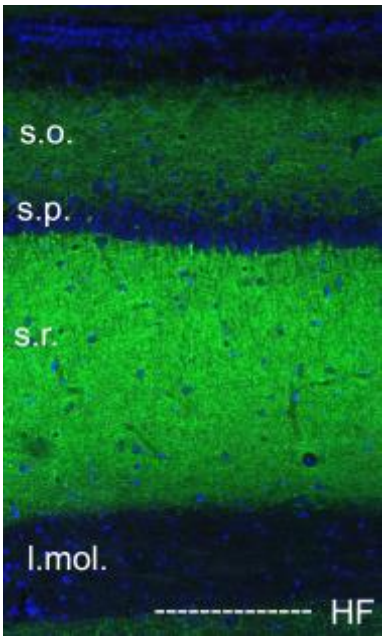

Fig. 2.8.2 High magnification confocal images showing expression of eYFP and DAPI through layers of area CA1 in the dorsal hippocampus ipsilateral to the side of virus injection. s.o.: stratum oriens; s.p.: stratum pyramidale; s.r.: stratum radiatum; l.mol.: stratum lacunosum moleculare; HF: hippocampal fissure.

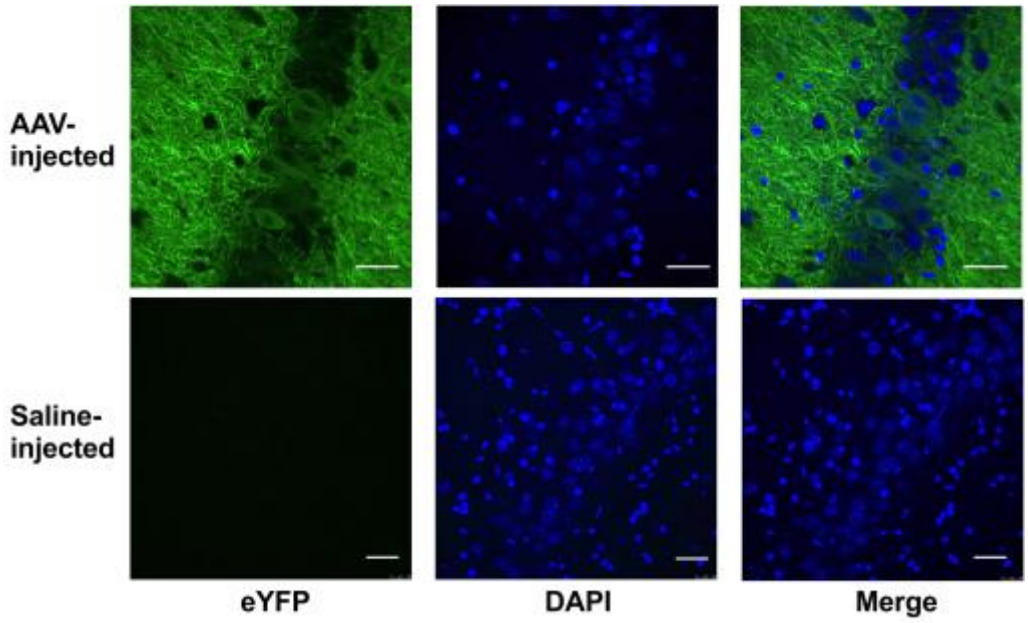

Fig. 2.8.3 High magnification of area CA3 pyramidal cell body layer with DAPI (blue) staining nuclear material and eYFP (green) fluorescence. No eYFP expression was detected in saline, as opposed to AAV, -injected animals. Calibration bar = 20μm.

In order to determine the relative level of expression of ChR2 between the ipsilateral and contralateral-to-injection hemispheres, as well as between the CA3 and CA1 areas of the hippocampus in each hemisphere, a standard oval-shaped area (320 x 220 pixels/ 160 x 110μm, width x height) within the image (software ImageJ, NIH, USA) was used to measure the relative eYFP fluorescence across images acquired using the Olympus BX51 upright microscope, where exposure settings were identical across both hemispheres (Fig. 2.8.4). For each image, a background measurement was taken as well as an integrated density reading for the area of interest. The following equation was used to generate a corrected total cell fluorescence (CTCF) score:

CTCF = Integrated Density – (Area of selected cell X Mean fluorescence of background readings)

The ipsilateral area CA1 had a markedly reduced relative eYFP fluorescence (Ipsi CA1: 0.62 ± 0.11 x 10^6, n = 8, P < 0.05 compared with ipsi CA3: 2.41 ± 0.27 x 10^6, n = 8; paired t-test). Interestingly, the contralateral area CA3 had a higher relative fluorescence than area CA1 on either side (Contra CA3: 1.47 ± 0.35 x 10^6, n = 8; Contra CA1: 0.46 ± 0.10 x 10^6, n = 8, both P < 0.05 compared with ipsi CA3; One-way ANOVA-Šidak).

a b

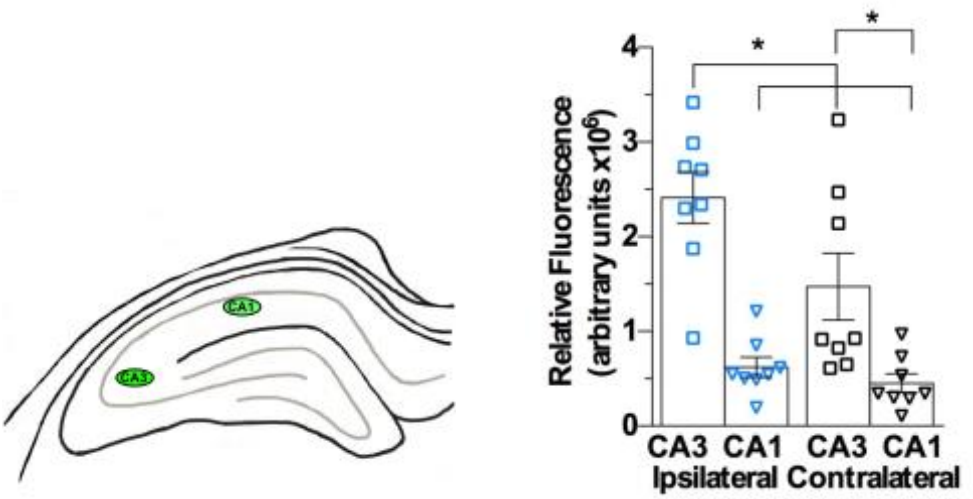

Fig. 2.8.4 Regional eYFP fluorescence. (a) Schema of the oval shaped area used to determine relative fluorescence. (b) Bar chart of relative fluorescence measured near the optrode location in the CA3, and the recording electrode location in the CA1 areas ipsilateral and contralateral to the hemisphere of virus injection. One-way ANOVA-Šidak. *P < 0.05. Calibration bars: vertical, 1mV; horizontal, 10ms.

For light microscopy, 80µm coronal slices were mounted on gelatine-coated (Sigma, 5% w/v in deionised H_2O) pre-cleaned slides (Thermo Sci. Polysine slides). Once slices had dried, they were treated with 96% ethanol to de-fat the tissue. The slides were further washed in 70% ethanol before being rinsed in clean water and exposed to a cresyl violet solution (Sigma). After 5 min, the slides were washed in water and a sequence of 70% and 96% ethanol. A mixture of xylene (Sigma) and ethanol was used before immersion in pure xylene. Once removed from xylene, the slides were coated with a distyrene plasticizer and xylene (DPX, VWR, Belgium) synthetic resin mounting media, cover-slipped and allowed to dry/ harden overnight. The following day, bright field images were acquired (Fig. 2.8.5) and compared with confocal images (Fig. 2.8.6) of the same brain (every alternate slice, in sequence, was saved for confocal imaging instead of Nissl). Cell counts were performed multiple times, and an average was taken. The average Nissl cell count (175 ± 5.9/mm, n = 6) was comparable to the DAPI stain cell body count (185 ± 9.5/mm, n = 6), and the DAPI count was significantly greater than the number of cell bodies clearly positive for eYFP (51 ± 7/mm, n = 6), ($P < 0.05$ compared between groups; unpaired t-test), (Fig. 2.9.3).

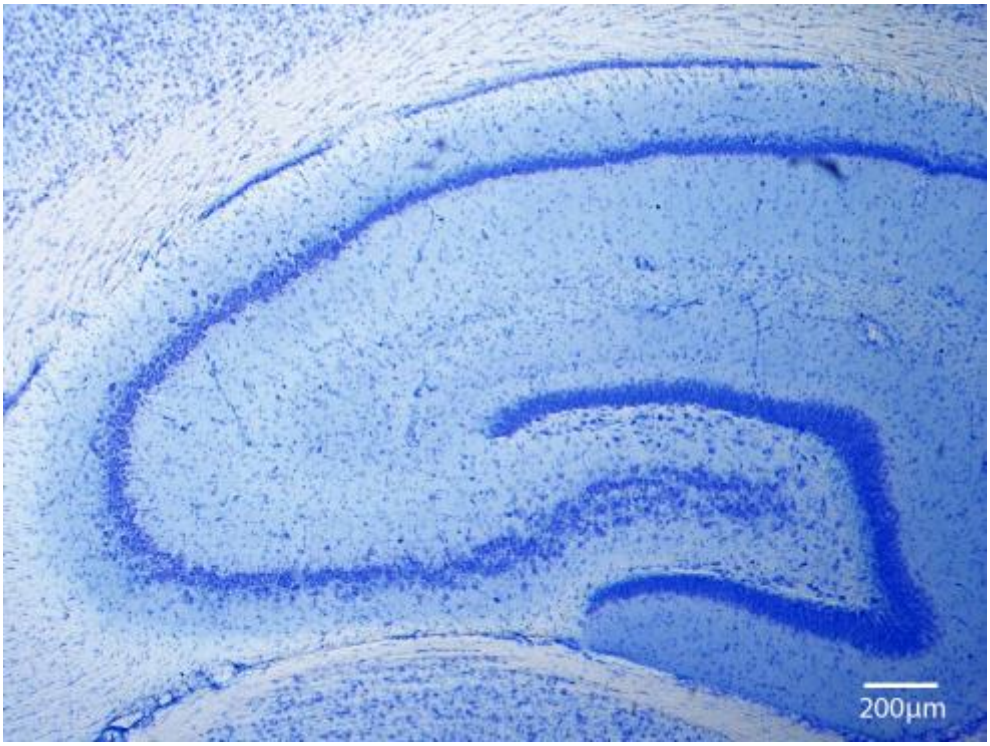

Fig. 2.8.5 Sample image of a transverse hippocampal slice taken with a bright-field microscope illustrating the Nissl stain.

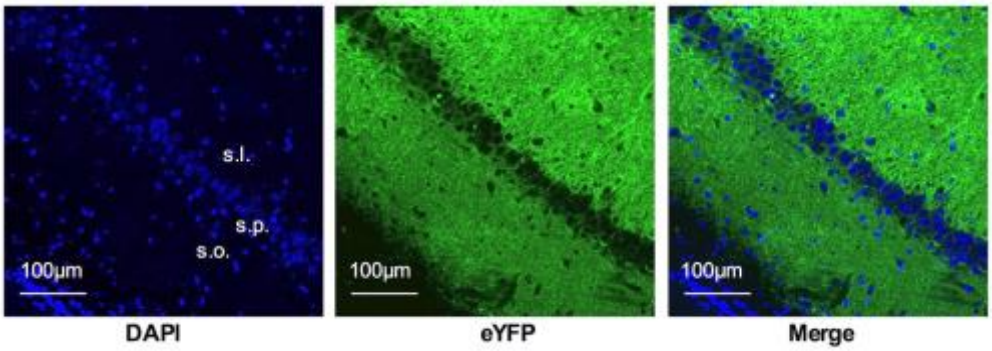

Fig. 2.8.6 Representative confocal images of area CA3 pyramidal cell body layer with DAPI (blue) staining indicating nuclear material and eYFP (green) fluorescence indicating ChR2 expression.

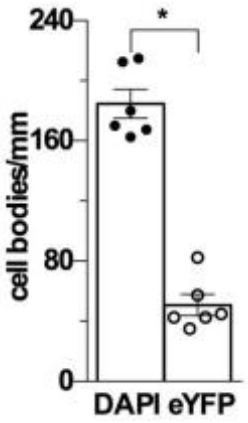

Fig. 2.8.7 Bar chart showing cell count data (number of cell bodies / mm pyramidal cell body layer) showing that eYFP fluorescence, and hence ChR2 expression, was relatively diffuse compared with total DAPI staining of cell bodies in the CA3 area near the site of virus injection. *P < 0.05. Unpaired t-test.

2.9 Compounds

CPP (Abcam), MTEP hydrochloride (Abcam), (+)-MK 801 maleate (dizocilpine), and its less active (-) enantiomer (Tocris), D-AP5 and L-AP5 (Tocris), donepezil hydrochloride (Tocris), emetine dihydrochloride hydrate (Sigma) were prepared in ultra-clean water and diluted into 1 ml saline for injection; 1 ml saline was used as vehicle control. Ro 25-6981 hydrochloride hydrate (Sigma) was dissolved in DMSO before being diluted in saline; a 1ml 10% v/v solution DMSO in saline was used as vehicle control. VU 0360172 (Tocris) was dissolved in 10% Tween-80 (polyethylene sorbitan monooleate, Sigma) in saline; 10% Tween-80 diluted in saline was used as vehicle control. LY 341495 (Abcam), was dissolved in 1.2 molar equivalent sodium hydroxide (NaOH, Sigma) and

diluted in saline; 1ml saline was used for vehicle control. Scopolamine hydrobromide (Sigma) was diluted in saline.

The dose of CPP was chosen based on previous publications including our finding that 10 mg/kg, i.p., completely blocked high-frequency stimulation induced LTP (Doyle et al., 1996). In the case of MTEP, we started with a dose of 3 mg/kg, which we found completely blocked Aβ-facilitated LTD (Hu et al., 2014). MTEP is known to achieve > 90% receptor occupancy after i.p. injection with either 3 or 6 mg/kg (Busse et al., 2004). MK-801 has been reported to achieve maximal specific binding in the rat forebrain at a dose of approximately 3 mg/kg, i.p. (Fernandes et al., 2015) but this dose is unsuited to *in vivo* electrophysiology experiments (Abraham and Mason, 1988). We chose a systemic dose of either 0.5 or 1.0 mg/kg, both of which should produce >50% occupancy, based on the radioligand binding studies of (Fernandes et al., 2015). A dose of 1.0 mg/kg, i.p., but not 0.5 mg/kg, has been reported to prevent the induction of LTP in the dentate gyrus (Abraham and Mason, 1988). The dose of 60 nmol for i.c.v. injection of MK-801 is based on previous research (Yoshiyama and de Groat, 2005). (-)-MK-801 is approximately one-seventh as potent as its active enantiomer MK-801 at NMDA receptors (Wong et al., 1986). The initial dose of D-AP5 was chosen on the basis of previous reports including our previous finding that LTP is blocked by 100 nmol after i.c.v. injection (Hu et al., 2008). D-AP5's stereoisomer L-AP5 is known to be at least 30-fold less potent as an NMDAR antagonist than D-AP5 (Watkins and Evans, 1981).

Aβ-derived diffusible ligands (ADDLs) were used to study the effects of synaptotoxic Aβ aggregates. They were prepared using synthetic Aβ1-42 which was synthesised and purified by the ERI Amyloid laboratory Oxford, CT, USA. As described previously, the solution contained oligomers including protofibrils (Nicoll et al., 2013; Hu et al., 2014). Briefly, a 1 mM solution of Aβ1-42 was prepared in hexafluoroisopropanol and incubated at 37 °C for 1 h, briefly vortexed every 10 min. The hexafluoroisopropanol was evaporated using a speedvac and the dried peptide film stored overnight with desiccant at −20 °C. A peptide solution of 22.5 mg/ml was then prepared in anhydrous dimethylsulfoxide (DMSO) and subsequently diluted 1:50 in Hams F-12 media. After incubation at 4°C for ~14 h the solution was centrifuged at 16,000 x g for 10 min. The supernatant was recovered and absorbance at 275 nm recorded. Aliquots of ADDLs were frozen on dry ice and stored at −80°C until administered at a dose of 1.2 nmol suspended in 10µl.

2.10 Data analysis

The strength of synaptic transmission is expressed as a percentage of the mean ± SEM % fEPSP amplitude during the 30 min baseline just before application of LFS or vehicle/ drug injection. Similar results were obtained when the fEPSP slope was analysed. When the optical fEPSP amplitude maximum was less than 0.5mV, the optical data were not used due to the high variability. Similarly, if the baseline changed more than 10% during the 30 min before LFS the run was terminated, and a new i/o curve and baseline was generated. Control

experiments were interleaved randomly throughout. For time-line graphical representation, fEPSP amplitudes were grouped into 5-min epochs; for statistical analysis, fEPSP amplitudes were grouped into 10-min epochs. Unless otherwise stated, the magnitude of LTD was measured over the last 10 min of the first hour after LFS and compared with the last 10 min prior to LFS. Two-tailed paired Student's *t*-tests (paired *t*) were used to compare pre- and post-LFS data within one group. For two groups with two time-points, a 2-way ANOVA was used, followed by post hoc Šidak multiple comparisons. To compare between groups or time-points of three or more, a one-way ANOVA, followed by post hoc Šidak multiple comparisons, was used. A value of $P < 0.05$ was considered statistically significant.

III. Results

3.1 Physiological activation of mGlu5 receptors supports the ion channel function of NMDA receptors in the induction of hippocampal LTD *in vivo*

3.1.1 Role of NMDA and mGlu5 receptors in the induction of hippocampal synaptic LTD by low-frequency conditioning stimulation *in vivo*

3.1.2 Absolute requirement for GluN2B-subunit-containing NMDARs during LTD induction by LFS *in vivo*

3.1.3 NMDAR ion channel function is required for the induction of LTD *in vivo*

3.1.4 LFS-evoked endogenous glutamate release activates mGlu5Rs to facilitate the induction of LTD

3.2 Diminished role for cholinergic and mGlu receptor modulation in optogenetically induced hippocampal NMDA receptor-dependent LTD *in vivo*

3.2.1 High-intensity optical low-frequency stimulation induced LTD at CA3-to-CA1 synapses *in vivo*

3.2.2 Input selectivity of optical low-frequency stimulation induced LTD *in vivo*

3.2.3 Role of cholinergic transmission in oLFS induction of LTD *in vivo*

3.2.4 NMDAR-dependence of synaptic LTD induced by optical stimulation *in vivo*

3.2.5 Role of mGlu receptors in the induction of hippocampal synaptic LTD by optical conditioning stimulation *in vivo*

3.2.6 Protein synthesis-dependence of oLFS-induced LTD *in vivo*

3.3 GluN2B NMDAR-dependence and lateralisation of Alzheimer's disease Aβ-facilitated LTD

3.3.1 Alzheimer's disease Aβ -facilitated LTD induced by electrical LFS is GluN2B dependent, but not lateralised

3.3.2 Alzheimer's disease Aβ-facilitated LTD induced by optical LFS is lateralised

3.1 Physiological activation of mGlu5 receptors supports the ion channel function of NMDA receptors in the induction of hippocampal LTD *in vivo*

3.1.1 Role of NMDA and mGlu5 receptors in the induction of hippocampal synaptic LTD by low-frequency conditioning stimulation *in vivo*

Because we had previously found that the induction of LTD by LFS, consisting of 900 high-intensity pulses at 1 Hz, was not blocked by standard systemic doses of either NMDAR or mGlu5R antagonists when applied alone (Hu, N.W. et al., 2014), our hypothesis states that both types of receptor may need to be blocked simultaneously. Intriguingly, even though neither of these treatments, when applied alone, affected LTD, the combination completely prevented the induction of synaptic LTD by LFS. Thus, consistent with our previous finding (Hu, N.W. et al., 2014), using a dose (10 mg/kg, i.p.) of the competitive NMDAR antagonist CPP known to completely inhibit synaptic LTP in the CA1 area (Doyle et al., 1996), the application of LFS after injection of CPP induced robust and stable synaptic LTD similar in magnitude to that induced in control, vehicle-injected rats (CPP: 64.4 ± 10%, mean ± SEM fEPSP amplitude expressed as a % of the pre-LFS baseline, n = 10; controls: 66.2 ± 7.1%, n = 10; $P < 0.05$ both compared with respective pre-eLFS baselines, $P > 0.05$ between groups; 2-way ANOVA with Šidak post-hoc analysis), (Fig. 3.1.1.1 a,b). Again, confirming our previous report (Hu, N.W. et al., 2014), application of LFS in MTEP-treated rats induced robust and stable LTD

of electrically evoked field excitatory postsynaptic potentials (fEPSPs). Initially, we tested the standard dose of MTEP (3 mg/kg, i.p., n = 5) which is known to non-competitively block mGlu5Rs, with a rat hippocampal receptor occupancy of >90% (Busse et al., 2004). When this dose proved ineffective we doubled the dose (n = 4) with similar results, so we pooled the data for the two doses (MTEP: 75.0 ± 3.8%, n = 9; controls: 64.3 ± 7.7%, n = 9; $P < 0.05$ both compared with baselines, $P > 0.05$ between groups), (Fig. 3.1.1.1 c,d). Significantly, combined systemic injection of these antagonists completely abrogated electrical induction of synaptic LTD (CPP+MTEP: 96.7 ± 4.9%, n = 8, $P > 0.05$ compared with pre-eLFS baseline; controls: 60.6 ± 3.8%, n = 9, $P < 0.05$ compared with baseline and between groups), (Fig. 3.1.1.1 e,f).

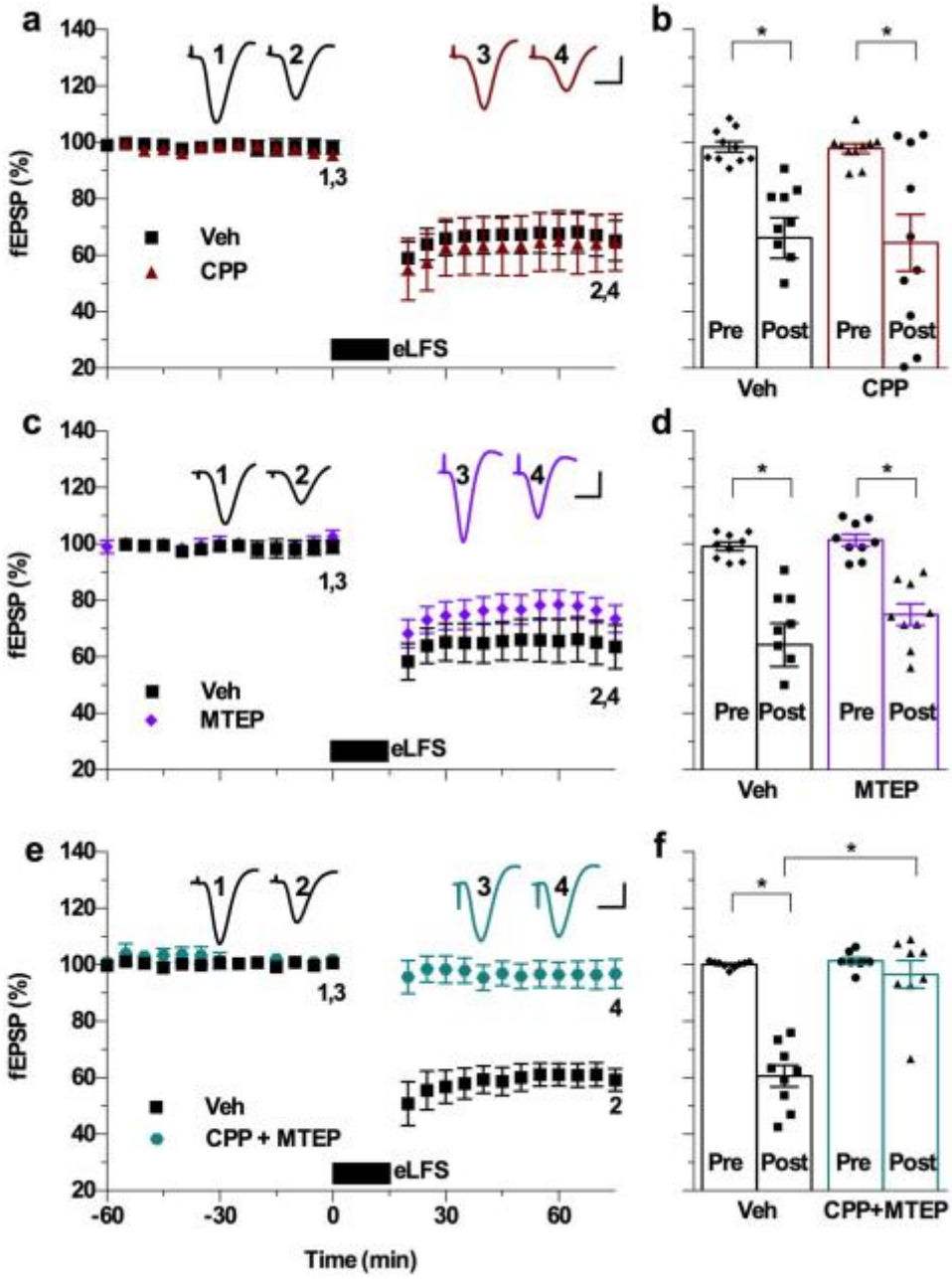

Fig. 3.1.1.1 Combined systemic injection of antagonists of NMDA and mGlu5 receptors prevents the induction of hippocampal synaptic LTD by electrical low-frequency conditioning stimulation *in vivo*. (a) The competitive NMDAR antagonist CPP (10 mg/kg, i.p.), injected 2.25 h prior to eLFS, had no significant effect on LTD. (b) Summary of the mean EPSP amplitude data in (a) before (pre) and 1 h after (post) application of eLFS. (b) Summary of the mean EPSP amplitude data in (a). (c) Injection of the mGlu5R negative allosteric modulator MTEP (3 or 6

mg/kg, i.p. 1 h pre-LFS) alone did not significantly alter the induction of LTD by eLFS 1 h later. (d) Summary of the mean EPSP amplitude data in (c). (e) Combined administration of CPP (10 mg/kg, i.p., 2.25 h pre-eLFS) with MTEP (3 mg/kg, i.p., 1 h pre-eLFS), blocked induction of LTD. (f) Summary of the mean EPSP amplitude data in (e). 2-way ANOVA, with Šidak post-hoc analysis. *P < 0.05. Calibration bars: vertical, 1mV; horizontal, 10ms.

These findings indicate that LFS increases glutamate concentration sufficiently to activate mGlu5Rs, which are found outside, especially on the edge of, the synapse (Lujan et al., 1997). Co-activation of mGlu5Rs with NMDARs located in this vicinity is known to strongly enhance the function of the NMDARs (Doherty et al., 1997; Kotecha et al., 2003; Mannaioni et al., 2001). Therefore, we hypothesised that Group II mGluRs might also co-activate with NMDARs for LTD induction, given that they are also are located perisynaptically (Tamaru et al., 2001), can enhance NMDA-evoked currents (Trepanier et al., 2013; Rosenberg et al., 2016) and have been implicated in the induction/maintenance of LTD (Manahan-Vaughan, 1997; Li et al., 2002; Santschi et al., 2006). However, unlike mGlu5Rs, they do not appear to have a role during LTD induction by LFS *in vivo*. Thus, the high potency selective mGlu2/3R antagonist LY341495 (3 mg/kg, i.p.) failed to significantly affect the magnitude of electrically-induced LTD when administered alone (LY341495; 74.8 ± 5.4%, n = 11; controls: 68.2 ± 2.9%, n = 10; P < 0.05 both compared with baselines, P > 0.05 between groups; 2-way ANOVA with Šidak post-hoc analysis), (Fig. 3.1.1.2 a,b), or when co-administered

with CPP (CPP+LY341495: 60.9 ± 4.7%, mean ± SEM % pre-oLFS baseline at 1 h, n = 4; controls: 63.1 ± 1.8%, n = 6, P < 0.05 compared to respective baselines and P > 0.05 between groups), (Fig. 3.1.1.2 c,d).

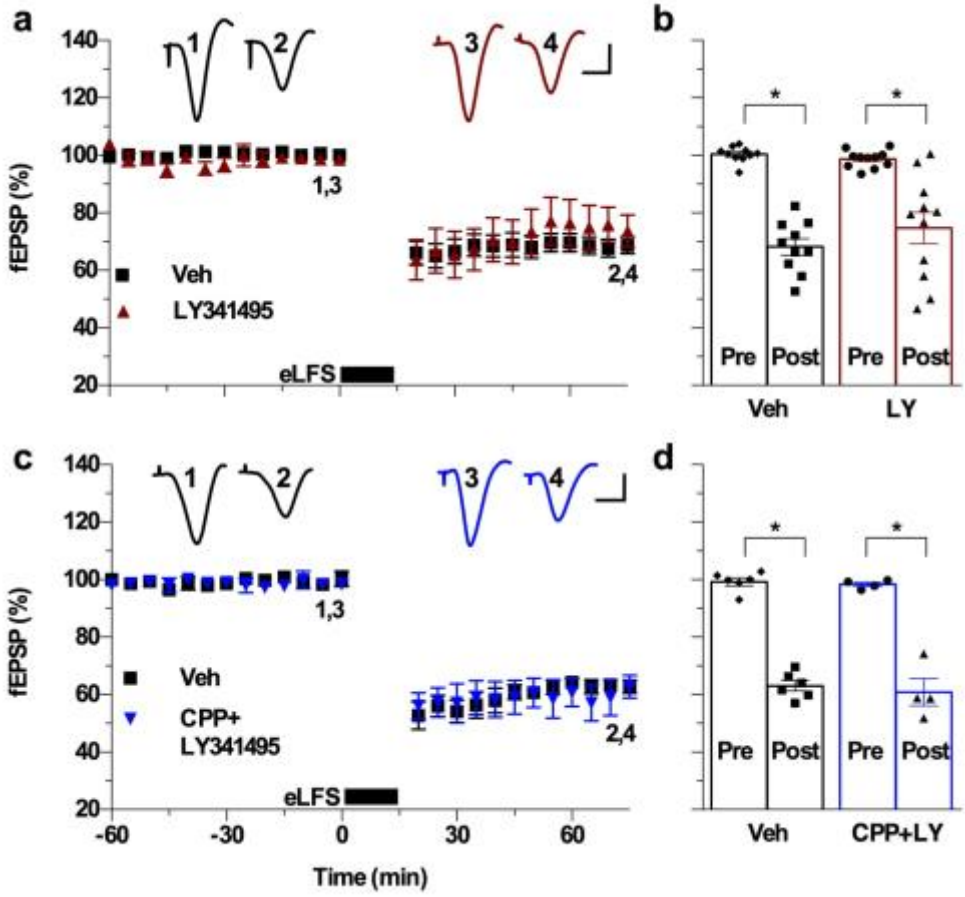

Fig. 3.1.1.2 Group II mGluR antagonism alone or in combination with NMDAR blockade fails to inhibit electrically-induced synaptic LTD *in vivo*. (a) The potent and selective group II mGluR antagonist LY341495 (3 mg/kg, i.p. 1 h pre-LFS) did not affect the induction of LTD. (b) Summary of the mean EPSP amplitude data in (a) before (pre) and 1 h after (post) application of eLFS. (c) Intraperitoneal administration of CPP (10 mg/kg, 2.25 h pre-eLFS) combined with LY341495 (3 mg/kg, 1 h pre eLFS), also had no effect on LTD. (d) Summary of the mean EPSP amplitude data in (c). 2-way ANOVA, with Šidak post-hoc analysis. *P < 0.05. Calibration bars: vertical, 1mV; horizontal, 10ms.

Whereas group II mGluRs enhance GluN2A subunit-containing NMDAR function (Trepanier et al., 2013), mGlu5R enhancement is achieved at least partly by promoting the phosphorylation of GluN2B subunits with consequent increased membrane stabilisation of NMDARs (Sarantis et al., 2015). Therefore, we hypothesised that a non-competitive GluN2B-selective antagonist, the negative allosteric modulator Ro 25-6981, may ameliorate LTD induction in either the presence or absence of MTEP. Consistent with the CPP results, whereas Ro 25-6981 (12 mg/kg, i.p., a dose likely to achieve ~60% NMDA receptor occupancy; Fernandes et al., 2015) alone failed to significantly alter LTD (Ro 25-6981: 63.1 ± 4.6%, n = 5; controls: 64.3 ± 4.2%, n = 6; $P < 0.05$ both compared with baselines, $P > 0.05$ between groups; 2-way ANOVA, with Šidak post-hoc analysis), (Fig. 3.1.1.2 a,b) the same dose of Ro 25-6981 given together with MTEP, greatly reduced the magnitude of electrically induced LTD (Ro 25-6981 + MTEP: 91.7 ± 2.1%, n = 6; controls: 64.2 ± 1.4%, n = 7; $P < 0.05$ compared with respective baselines and between groups), (Fig. 3.1.1.3 c,d).

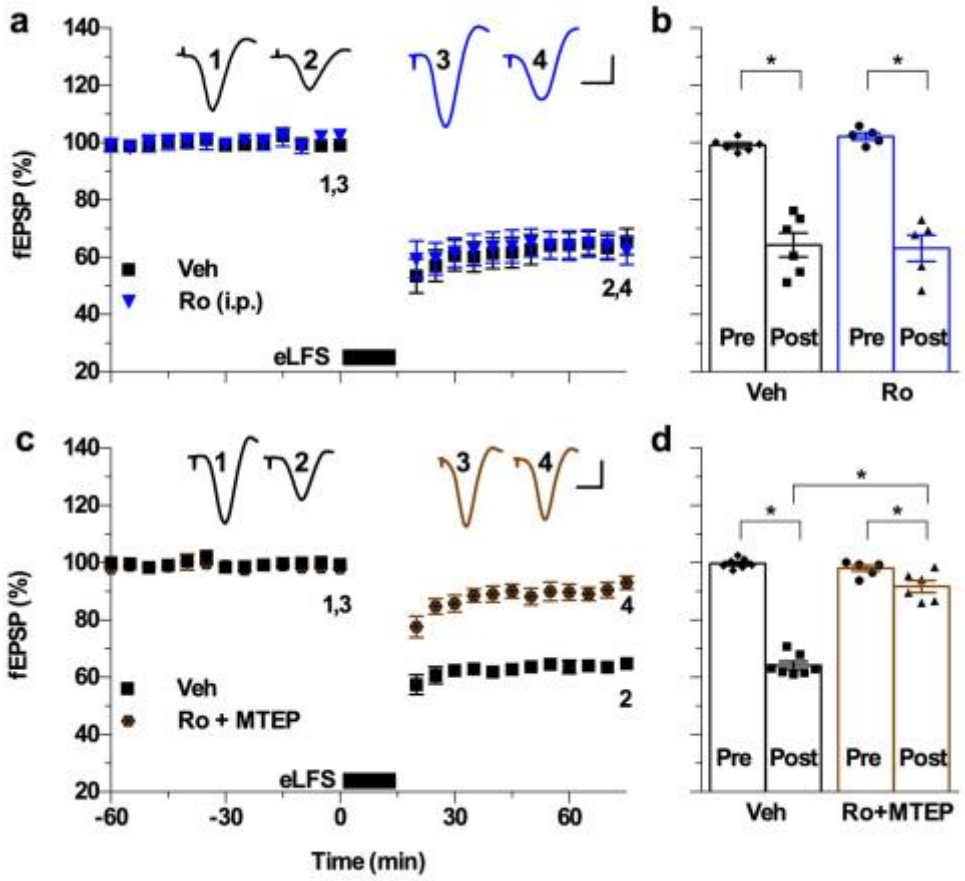

Fig. 3.1.1.3 GluN2B-subunit-selective antagonist, systemically administered with a mGlu5R antagonist, prevents eLFS induction of LTD. (a) The non-competitive GluN2B subtype selective NMDAR antagonist Ro 25-6981 (12 mg/kg, i.p., 1 h pre-eLFS) alone had no effect on LTD induction. (b) Summary of the mean EPSP amplitude data in (a) before (pre) and 1 h after (post) application of eLFS. (c) In contrast, a combination of Ro 25-6981 (12 mg/kg, i.p. 1 h pre-LFS) with MTEP (3 mg/kg i.p 1 h pre-LFS) strongly attenuated ltd. (d) Summary of the mean EPSP amplitude data in (c). 2-way ANOVA, with Šidak post-hoc analysis. *P < 0.05. Calibration bars: vertical, 1mV; horizontal, 10ms.

These findings are consistent with the supposition that the non-synaptic interaction between mGlu5 and GluN2B subunit-containing

NMDA receptors facilitates the induction of NMDAR-dependent LTD. However, an alternative potential explanation of these data is that the activation of either mGlu5Rs or NMDARs by LFS can independently mediate the induction of LTD *in vivo.*

3.1.2 Absolute requirement for GluN2B-subunit-containing NMDARs during LTD induction by LFS *in vivo*

If, as proposed, endogenously released glutamate during LFS activates mGlu5Rs to increase the number of functional NMDARs available for LTD induction, then the dose of NMDAR antagonist required to block LTD should be greater when administered alone, relative to when co-administered with a mGlu5R antagonist. In order to assess this hypothesis, we injected relatively high doses of NMDAR antagonists locally near the hippocampus, via the Intracerebroventricular (i.c.v.) route, thereby minimising the likelihood of significant systemic toxicity. We started by testing the effect of i.c.v. injection of the competitive antagonist D-AP5. Whereas a dose (100 nmol i.c.v. 15 min pre-LFS) that inhibits LTP induction (Hu et al., 2008) was without significant effect, double this dose partially attenuated the magnitude of LTD (Fig. 3.1.2 a,b). As an additional control we tested the same dose (200 nmol) of L-AP5, the D-AP5 stereoisomer that is relatively inactive at NMDARs (Watkins and Evans, 1981), and found that it failed to affect LTD, consistent with a crucial role for NMDARs in LFS induction of LTD (100 nmol D-AP5: 63.1 ± 5.4%, n = 4; controls: 53.0 ± 2.8%, n = 6; $P < 0.05$ compared with respective baselines and $P > 0.05$ between groups; 200

nmol D-AP5: 73.2± 3.9%, n = 5; P < 0.05 compared with baseline, vehicle controls or L-AP5, the NMDAR low-affinity stereoisomer of D-AP5, 51.8 ± 2.6%, n = 4; One-way ANOVA, Holm-Šidak of 1 h post-LFS, and paired t-tests), (Fig. 3.1.2 a,b).

Moreover, given the known importance of GluN2B subunit-containing NMDARs in mediating facilitatory effects of mGlu5R co-activation (Sarantis et al., 2015), i.c.v. treatment with a relatively high dose (2 nmol i.c.v. 15 min pre-LFS) of the very selective Ro 25-6981 greatly diminished the magnitude of LTD induced by LFS, compared with vehicle-treated animals (Ro 25-6981: 90.0 ± 4.5%, n = 4, P > 0.05 compared with baseline; controls: 54.4 ± 4.0%, n = 6, P < 0.05 compared with baseline, 2-way ANOVA, with Šidak post-hoc analysis), (Fig. 3.1.2 c,d).

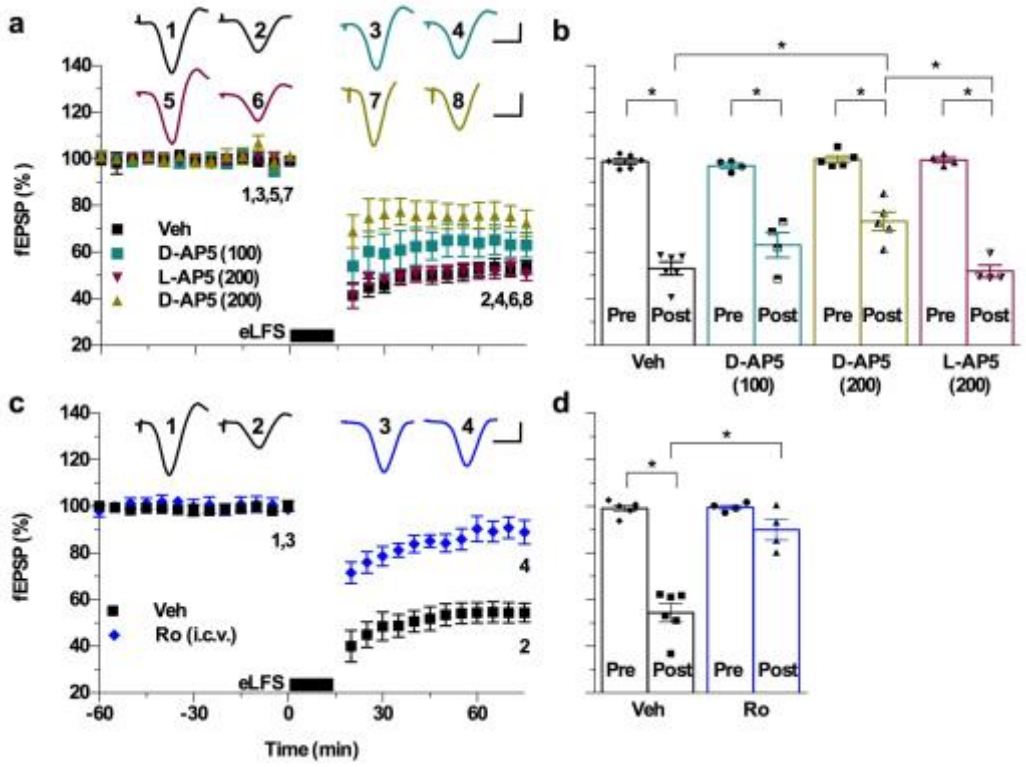

Fig. 3.1.2 High doses of locally-injected NMDAR antagonists prevent LTD induction by eLFS *in vivo*. (a) Intracerebroventricular administration of 200 nmol, but not 100 nmol, of the competitive antagonist D-AP5, 15 min before eLFS attenuated LTD, which was also unaffected by the stereoisomer L-AP5 at 200nmol. (b) Summary of the mean EPSP amplitude data in (a) before (pre) and 1 h after (post) application of eLFS. (c) Furthermore, i.c.v. application of the non-competitive Ro 25-6981 (2 nmol 15 min pre-LFS) strongly inhibited LTD. (d) Summary of the mean EPSP amplitude data in (c). One-way ANOVA, Holm-Šidak, 2-way ANOVA, with Šidak post-hoc and paired t-tests. *P < 0.05. Calibration bars: vertical, 1mV; horizontal, 10ms.

We did not test the effect of high local dose of MTEP on LTD induction because systemic administration of the doses employed in the previous section (see above) achieve very high receptor occupancy (Busse et al., 2004).

3.1.3 NMDAR ion channel function is required for the induction of LTD *in vivo*

In the light of the controversy over the requirement for ion flux through the NMDAR channel in LFS induction of synaptic LTD *in vitro* (Babiec et al., 2014; Gray et al., 2016; Nabavi et al., 2013), next we examined the effect of the use-dependent NMDAR channel blocker MK-801 *in vivo*. Given the results mentioned previously, we tested the hypothesis that potentially local application of an antagonist of the ion flux function of the NMDAR channel may be required to ameliorate LTD. Systemic treatment with a relatively low dose of MK-801 (0.5 mg/kg, i.p., 1 h pre-LFS) had no significant effect on the induction of LTD by LFS (i.p. MK-801: 53.2 ± 5.7%, n = 5; i.p. controls: 65.6 ± 7.6%, n = 6; $P < 0.05$ both compared with baselines, $P > 0.05$ between groups, 2-way ANOVA, with Šidak post-hoc analysis), (Fig. 3.1.3 a,b). In order to reduce the likelihood of significant systemic toxicity with higher doses, we then tested the effects of local injection of MK-801 near the hippocampus. We found that MK-801 (60 nmol, i.c.v. 15 min pre-LFS) prevented LTD induction by electrical stimulation in a stereoselective manner. Consistent with a need for the ion channel function of the NMDARs in the induction of LTD, only the NMDAR-selective (+)-enantiomer (MK-801) reduced the magnitude of LTD whereas the control (-)-enantiomer (60 nmol) appeared inactive (i.c.v. MK-801: 89.5 ± 1.3%, n = 5; i.c.v. (-)-MK-801: 53.2 ± 4.7%, n = 4, $P < 0.05$ compared with respective baselines and between groups), (Fig. 3.1.3c,d).

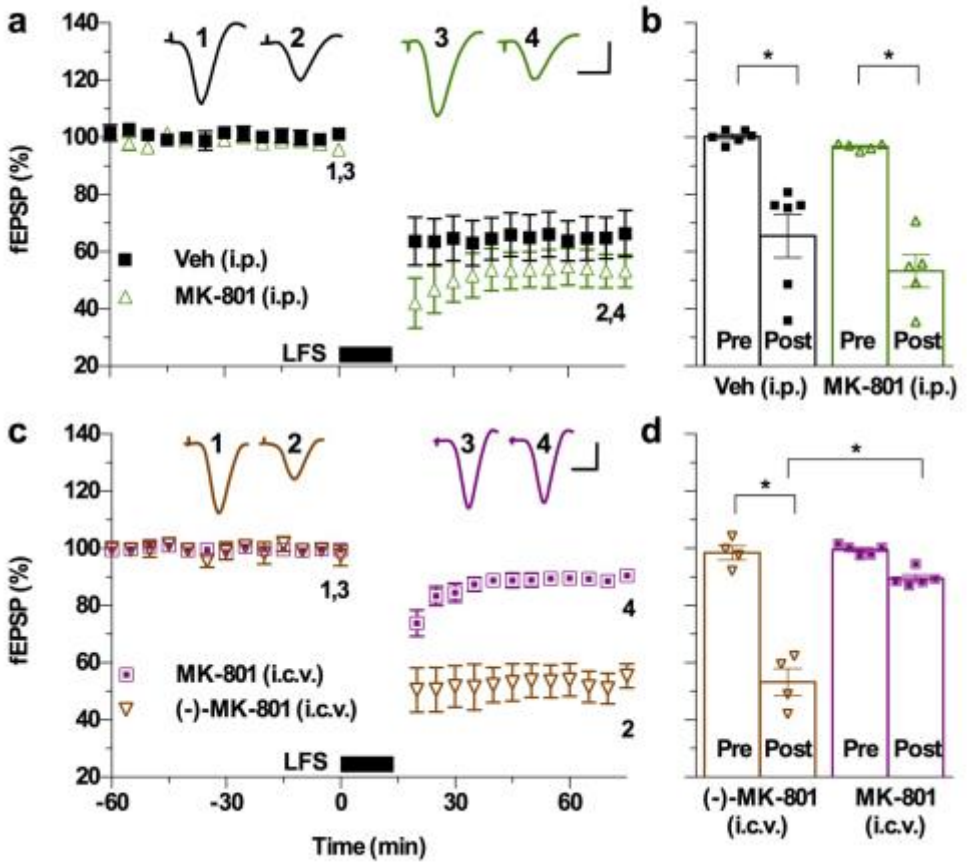

Fig. 3.1.3 Necessity for NMDAR ion channel function in the induction of LTD *in vivo*. (a) The use-dependent NMDAR ion channel blocker MK-801, in keeping with the relatively low potency of the other NMDAR antagonists, failed to significantly affect LTD. (b) Summary of the mean EPSP amplitude data in (a) before (pre) and 1 h after (post) application of eLFS. (c) Importantly, a high dose of locally-injected MK-801 (60 nmol, i.c.v. 15 min pre-LFS), in comparison with the control (-) stereoisomer, strongly inhibited LTD induction *in vivo*. (d) Summary of the mean EPSP amplitude data in (c). 2-way ANOVA, with Šidak post-hoc analysis. *P < 0.05. Calibration bars: vertical, 1mV; horizontal, 10ms.

These data provide strong evidence that the induction of synaptic LTD *in vivo* requires ion flux via NMDARs.

3.1.4 LFS-evoked endogenous glutamate release activates mGlu5Rs to facilitate the induction of LTD

The findings described above support the proposal that mGlu5R co-activation by LFS stabilises GluN2B NMDARs in the plasma membrane to enhance LTD induction. Therefore, we hypothesise that pharmacologically boosting endogenous glutamate activation of mGlu5Rs may facilitate the induction of LTD. We predicted that a positive allosteric modulator of these receptors should lower the threshold for LTD, enabling its induction by weak LFS. Therefore, we examined the effect of the mGlu5R positive allosteric modulator VU 0360172 (15 mg/kg, s.c. 1 h pre-LFS) on the ability of a peri-threshold induction protocol (300 high-intensity pulses at 1 Hz, LFS-300) to induce LTD. VU 0360172 facilitated the induction of robust LTD by the peri-threshold electrical LFS-300 (control: 91.5 ± 2.5%, n=10; $P > 0.05$ compared to baseline; VU 0360172: 62.4 ± 3.8%, n=6, $P < 0.05$ compared with baseline and between groups, 2-way ANOVA, with Šidak post-hoc analysis), (Fig. 3.1.4 a,b).

These data indicate that the relatively low potency of competitive and non-competitive NMDAR antagonists in blocking LTD induction by LFS is likely caused by additional activation of mGlu5Rs that stabilise the membrane localisation of NMDARs. To further test this hypothesis, we assessed the ability of the non-competitive GluN2B antagonist Ro 25-6981 to prevent LTD induced by weak LFS in the presence of the mGlu5R positive allosteric modulator. Whereas the induction of LTD by

LFS-300 in the presence of VU 0360172 was not blocked by a standard systemic dose (12 mg/kg, i.p. 1 h pre-LFS) of Ro 25-6981, local high-dose (2 nmol, i.c.v. 15 min pre-LFS) injection of this antagonist completely blocked this form of LTD (i.c.v. Ro 25-6981: 97.8 ± 3.8%, n=4, $P > 0.05$ compared with baseline, paired t-test; i.p. Ro 25-6981: 51.3 ± 4.2%, n=4, $P < 0.05$ compared with baseline, paired t-test), (Fig. 3.1.4 c,d).

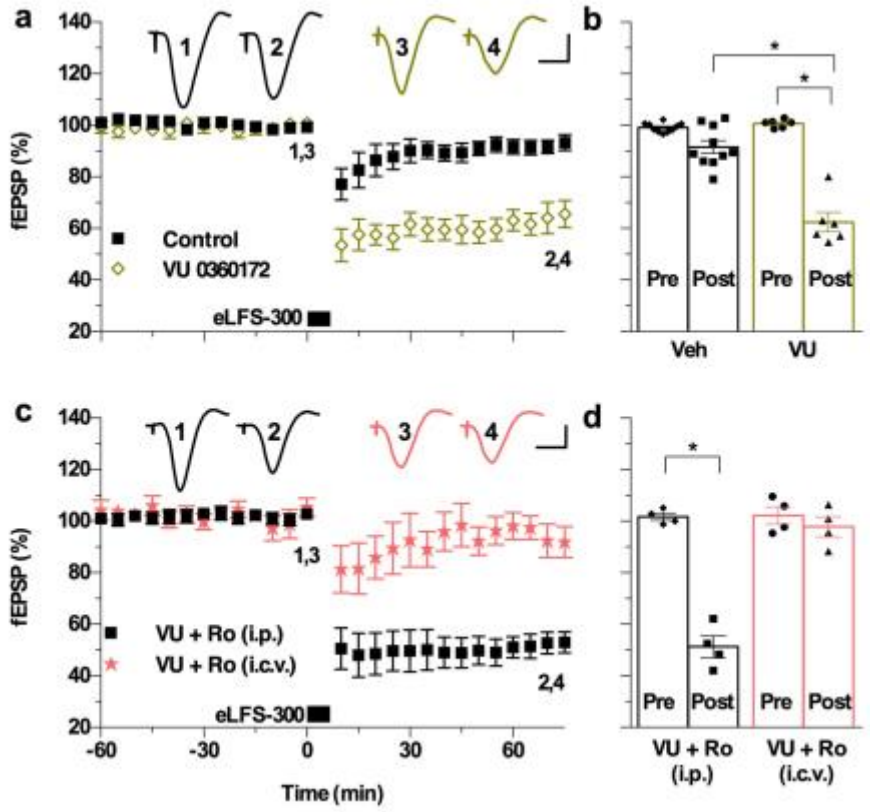

Fig. 3.1.4 Endogenous glutamate release evoked by LFS activates mGlu5Rs to facilitate the induction of LTD *in vivo.* (a) The mGlu5R positive allosteric modulator VU 0360172 (15 mg/kg, s.c. 1 h pre-LFS) facilitated the induction of LTD by a peri-threshold electrical LFS-300 conditioning protocol (300 high-intensity pulses at 1Hz) relative to vehicle controls. (b) Summary of the mean EPSP amplitude data in (a) before (pre) and 1 h after (post) application of eLFS. (c) Local injection of a relatively high dose (2 nmol, i.c.v. 15 min pre-LFS) of the GluN2B antagonist Ro 25-6981 prevented LTD induction by LFS-300 in the presence of VU 0360172, whereas systemic treatment (12 mg/kg, i.p. 1 h pre-LFS) did not. (d) Summary of the mean EPSP amplitude data in (c). 2-way ANOVA, with Šidak post-hoc analysis and paired t-tests. *P < 0.05. Calibration bars: vertical, 1mV; horizontal, 10ms.

The observed positive allosteric mGlu5R modulator-mediated facilitation of LTD induction and the requirement for high-dose local GluN2B antagonist to block this facilitated LTD provide very strong complimentary support for the proposed involvement of mGlu5-NMDA receptor co-activation by LFS.

3.2 Diminished role for cholinergic and mGlu receptor modulation in optogenetically induced, hippocampal NMDA receptor-dependent LTD *in vivo*

The study of LTD in the adult rodent hippocampus has proven challenging both *in vitro* (Ho et al., 2004) and particularly *in vivo* (Errington, 1995; Staubli, 1997). Despite these difficulties, the standard electrical LFS (eLFS, consisting of a set of 900 pulses at 1 Hz) protocol has been reported to induce robust NMDAR-dependent LTD in anaesthetised or freely behaving adult rats, albeit often strongly regulated by exposure to critical behavioural conditions, including stress (Xu, 1997; Kemp, 2004; Fox, 2006; Wong, 2007; Ge, 2010). The requirement for high-intensity pulses, as previously mentioned (Hu, N.W. et al., 2014), was putatively attributed to a need to activate cholinergic fibres during the eLFS (Caruana et al., 2011). Consistent with this idea, the LTD was strongly inhibited by muscarinic acetylcholine receptor (AChR) antagonists and facilitated by blocking ACh breakdown using an anticholinesterase agent. Furthermore, although primarily NMDAR-dependent, mGlu5R activation had a strong positive modulatory effect on LTD induction, supporting a facilitatory interaction between mGlu5R and

NMDAR, most likely at peri-synaptic sites (Lujan et al., 1997; Darnell et al., 2013; Hu et al., 2014).

Most previous research has employed electrical stimulation, which usually activates pathways *en masse* and relatively indiscriminately, both to record synaptic transmission and induce LTD. Unlike standard electrical field stimulation, selective expression of channelrhodopsin in excitatory neurons not only avoids direct activation of cholinergic fibres but also allows more diffuse synaptic activation of specific glutamatergic pathways, more closely mimicking natural spatial patterns, which generally are relatively sparse as occurs during much of normal hippocampal function (Ramirez et el., 2013). As a result, we hypothesised that by using optical stimulation to diffusely activate excitatory neurons, we should be able greatly reduce the likelihood of peri/extra-synaptic glutamate receptor activation (Arnth-Jensen et al., 2002; Scimemi et al., 2004).

The use of optogenetics also opens up the opportunity to address the possibility that LTD, like LTP (Kohl et al., 2011; Shipton et al., 2014), is lateralised. The induction of LTP was found to be asymmetric by selective stimulation of left and right CA3 inputs to CA1 in the stratum radiatum of adult mice *in vitro*; conditioning stimulation of Schaffer collateral or commissural inputs from left, compared with right, hippocampal CA3 pyramidal neurons preferentially triggers LTP at apical dendrites on CA1 pyramidal neurons (Kohl et al., 2011; Shipton et al., 2014). Intriguingly, LTD is preferentially induced in slices from adult mice that congenitally

symmetrically express the type of apical synapse that right CA3 neurons form with CA1 (Kawahara, 2013), raising the prospect that, in wild-type animals, LTD may be preferentially induced at CA1 synapses formed by right CA3 pyramidal neurons.

3.2.1 High-intensity optical low-frequency stimulation induced LTD at CA3-to-CA1 synapses *in vivo.*

With the optical fibre positioned over area CA3, optically evoked transmission at CA3-to-CA1 synapses was recorded in the stratum radiatum in the CA1 area. Responses in the optical pathway were stable for more than 3 h as indicated by the continuous monitoring of the response to test pulse stimulation and comparing the input-output relationship of stimulation intensity to fEPSP amplitude at the start and end of the recording period (Fig. 3.2.1.2). The ability to induce LTD of optically evoked synaptic responses was assessed using a variety of low-frequency (1Hz) protocols. Application of 900 optical pulses at an intensity that evoked 50% maximum fEPSPs (oLFS-50% max) only induced a transient depression of synaptic transmission that quickly reverted to pre-conditioning levels (97.7 ± 4.7% at 40 min post- oLFS-50% max, n = 6; $P > 0.05$ compared with baseline; paired t-test), (Fig. 3.2.1.1 a,c). In contrast, a tetanus consisting of 900 pulses delivered at 75% maximum intensity (oLFS-75% max) triggered an LTD that slowly reversed towards pre-LFS baseline (88.6 ± 1.3% at 40 min, n = 4; $P < 0.05$ compared with baseline), (Fig. 3.2.1.1 b,d).

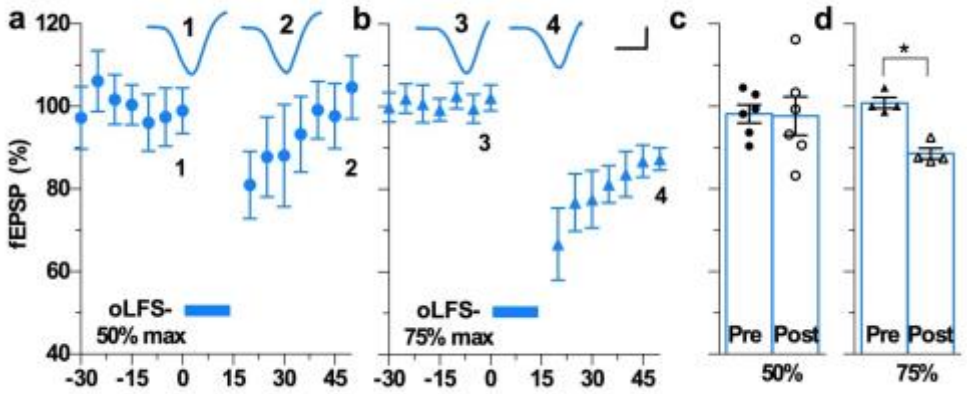

Fig. 3.2.1.1 The ability to induce LTD of optically evoked synaptic responses was assessed using a variety of low-frequency (1Hz) protocols. (a) Optical low-frequency conditioning stimulation consisting of 900 high-intensity pulses at 1 Hz (oLFS), when applied at the test pulse intensity (oLFS-50% max), triggered a short-term depression of optically evoked fEPSPs. Values are expressed as mean ± SEM % baseline EPSP amplitude. (b) Summary of the mean fEPSP amplitude data in (a) before (Pre) and 40 min after (Post) application of oLFS-50% max. (c) Increasing the intensity of the pulses during oLFS to evoke EPSPs that were 75% of the maximum (oLFS-75% max) enabled the induction of a small LTD. (d) Summary of the mean fEPSP amplitude data in (c). Insets show typical fEPSP traces at the times indicated before (Pre) and 40 min after (Post) application of oLFS. Paired t-tests. *P < 0.05. Calibration bars: vertical, 1mV; horizontal, 10ms.

In order to induce robust LTD a stronger 900 pulse 1 Hz protocol needed to be applied. Such LFS, at an intensity that evoked fEPSPs that were approximately 95% of the maximum (oLFS-95% max), triggered a large LTD of optically evoked test fEPSPs that remained stable for at least 3 h (Fig. 3.2.1.2 a) and an associated shift of the input-output curve

to the right (Fig. 3.2.1.2 b). This sequence was repeated in a different animal with just an electrical LFS, at an intensity that evoked fEPSPs that were approximately 95% of the maximum (eLFS-95% max); this triggered a large LTD of electrically evoked test fEPSPs that also remained stable for at least 3 h (Fig. 3.2.1.2 c) and an associated shift of the input-output curve to the right (Fig. 3.2.1.2 d). In both non-tetanised pathways, the input-output curves with not change from the beginning (start) to the end of the experiment (Fig. 3.2.1.2 b,d).

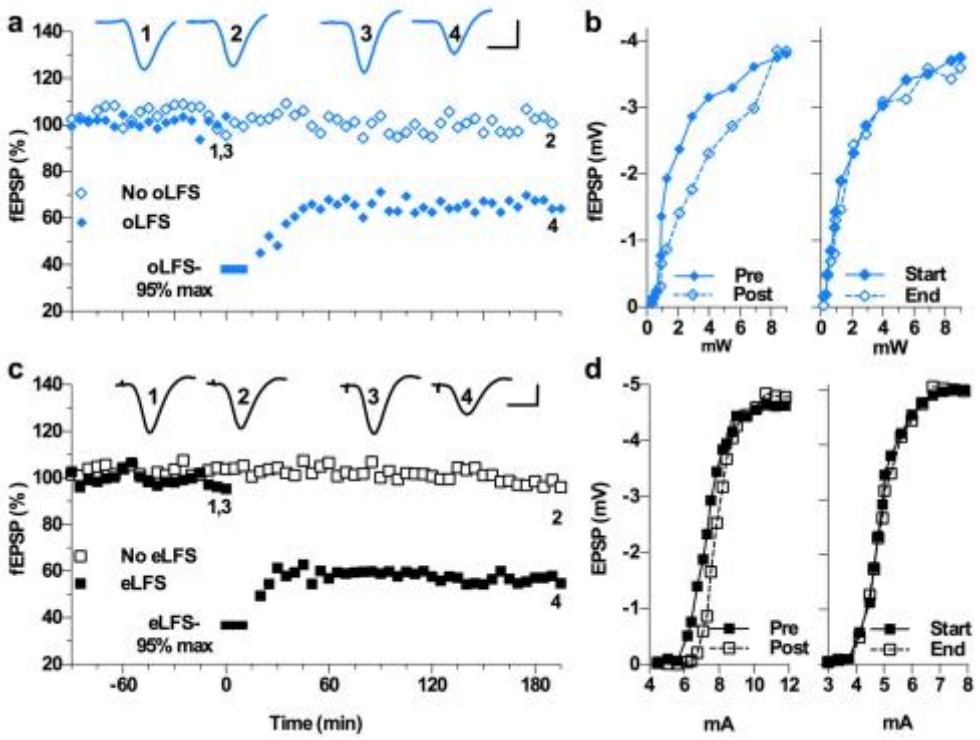

Fig. 3.2.1.2 High-intensity low-frequency stimulation induced robust LTD at CA3-to-CA1 synapses *in vivo*. (a) oLFS (900 high-intensity optical pulses at 1Hz) triggered a persistent depression of optically evoked test fEPSPs (closed diamonds). In contrast, in a control, non-tetanised pathway, the responses were stable over the 4 h recording period (open diamonds). (b) The tetanised pathway showed a shift to the right in the recorded i/o curves from the beginning to the end of the experiment, whereas the non-tetanised pathway did not. (c) Further, in a different animal, eLFS (900 high-intensity electrical pulses at 1Hz) triggered a persistent depression of electrically evoked test fEPSPs (closed boxes). Whereas, in a non-tetanised pathway, the responses were stable over the 4 h recording period (open boxes). (d) The tetanised pathway showed a shift to the right in the recorded i/o curves from the beginning to the end of the experiment, whereas the non-tetanised pathway did not.

Because the induction of LTP at CA3-to-CA1 synapses *in vitro* has been reported to be strongly lateralised (Kohl et al., 2011; Shipton et al., 2014), we hypothesised that we would see lateralisation of optically induced LTD *in vivo,* with more LTD in the right hemisphere, or none in the left. The magnitude of LTD in the left (experimental setup illustrated in Fig. 3.2.1.3 a) and right (Fig. 3.2.1.3 b) hippocampus was not significantly different when both the stimulation and recording electrodes were located in the hippocampus that had been injected with virus (Left: 66.7 ± 3.9%, Right: 67.3 ± 3.1%, values at 3h after oLFS-95% max, n = 7 for each side; $P < 0.05$ compared with baselines, 2-way ANOVA with Šidak post-hoc analysis), (Fig. 3.2.1.3 c,d). Therefore, LTD was induced regardless of which side the virus had been injected.

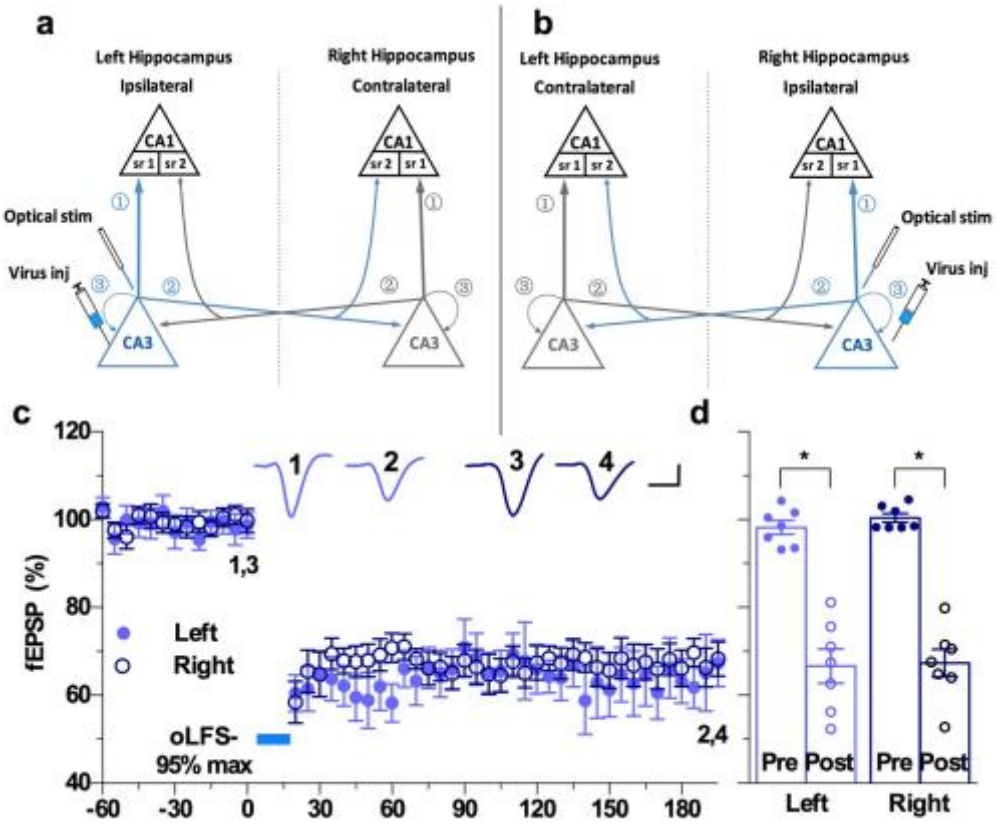

Fig. 3.2.1.3 High-intensity low-frequency LTD at CA3-to-CA1 synapses *in vivo* is not lateralised. (a) Schematic of experimental setup where virus injection and optrode placement were in the left hippocampus. (b) Schematic illustrating the alternative setup where the virus injection and optrode placement were in the right hippocampus. (a) Group averaged time-course data for experiments in which the stimulation and recording electrodes were both in the hippocampus that was injected with virus, in either the left or right hemisphere. (b) Summary of the mean fEPSP amplitude data in (a) before (Pre) and 3 h after (Post) application of oLFS-95% max. 2-way ANOVA with Šidak post-hoc analysis. *P < 0.05. Calibration bars: vertical, 1mV; horizontal, 10ms.

With good expression of eYFP in the hippocampus contralateral to the hemisphere of viral transduction (see Methods 2.8.1), we hypothesised that we should be able to stimulate synaptic EPSPs in the commissural pathway and induce stable LTD. oLFS induced robust LTD in either the left or right hippocampus hemisphere, opposite to the hemisphere of virus injection (experimental setup illustrated in Fig. 3.2.1.4 a,b). Thus, even though baseline fEPSPs were smaller in amplitude (values compared with CA1 fEPSPs evoked and recorded ipsilateral to the side of virus injection in the same animal, and represented in traces in Fig. 3.2.1.4 c), oLFS induced a large LTD (contralateral: 60.3 ± 3.7% at 1 h, n = 4, consisting of 2 for each side; $P < 0.05$ compared with baseline; paired t-test), (Fig. 3.2.1.4 c,d).

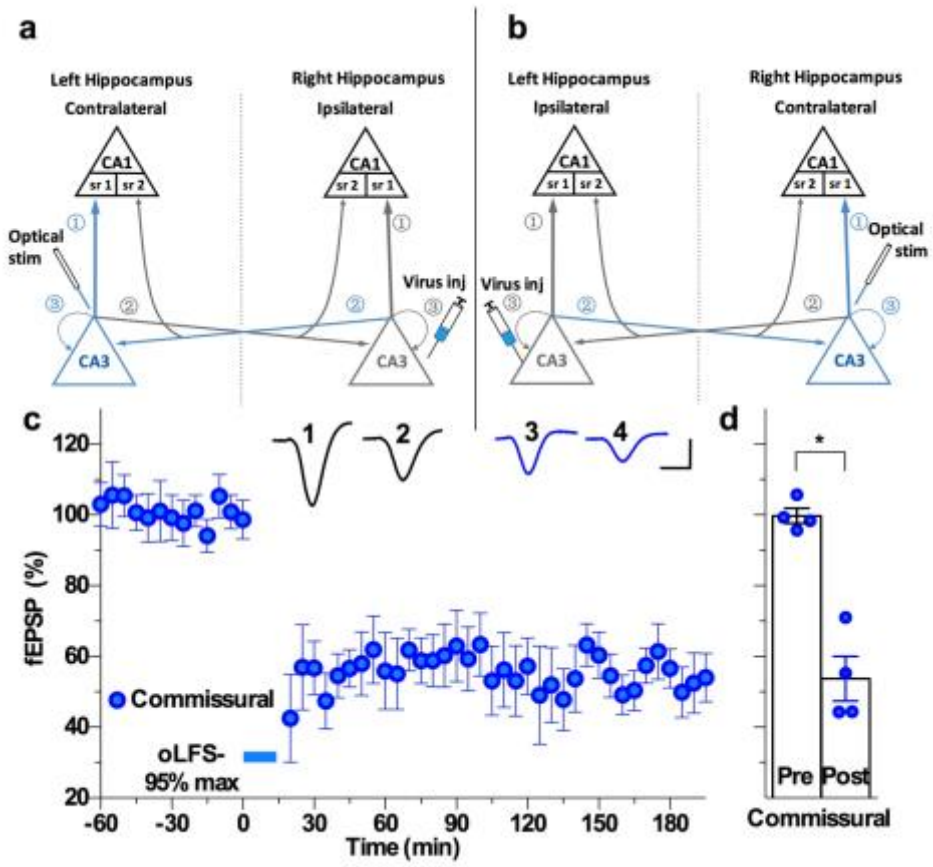

Fig. 3.2.1.4 Robust LTD in either the left or right hippocampus, stimulated and recorded in the hemisphere opposite to the hemisphere of virus injection. (a) Schematic of experimental setup where the optrode and recording electrode were placed in the left-hand side and contralateral to the side of the virus injection in the right hippocampus. (b) Schematic illustrating the alternative setup where the optrode and recording electrode were implanted in the right hippocampus contralateral to the side of the virus injection in the left hippocampus. (c) Time-course data for when the stimulation and recording electrodes were both in the hippocampus contralateral to that which was injected with virus. Representative traces illustrating the optical fEPSP (light blue traces 1 and 2 = left; navy traces 3 and 4= right). (d) Summary of the mean fEPSP amplitude data in (c) before (Pre) and 3 h after (Post) application of oLFS-95% max. Paired t-test. *P < 0.05. Calibration bars: vertical, 1mV; horizontal, 10ms.

3.2.2 Input selectivity of optical low-frequency stimulation induced LTD *in vivo*

We predicted that optically induced synaptic LTD is input-selective and therefore should be independent of electrically induced LTD and vice versa. In order to determine if oLFS-induced LTD in the live animal is input-selective, we tested whether or not the induction of LTD by oLFS affected synaptic responses evoked by electrical stimulation of an independent synaptic pathway between CA3 and CA1 pyramidal neurons (see Methods), and vice versa; the optrode used comprised of the twisted bipolar electrical stimulating electrode glued to the optical fibre stimulator and thus both stimuli were presented in the same general location, but activated different pathways. We applied high-intensity LFS to both pathways separately and continuously monitored, with a single recording electrode in the stratum radiatum in the CA1 area, fEPSPs evoked by alternate optical and electrical test pulses. As predicted, the expression of LTD in one pathway did not appear to affect responses in the other pathway after applying either oLFS or eLFS (Fig. 3.2.2.1 a-d). Thus, LTD induced by a single train of high-intensity oLFS did not affect baseline synaptic responses in the electrical pathway (optical: 71.6 ± 2.2% at 1 h; electrical: 98.8 ± 1.4% at 1 h, n = 10, one-way ANOVA with Šidak post-hoc analysis, compared with respective baseline, paired t-test), (Fig. 3.2.2.1 a,c). Similarly, in a separate group of animals, the induction of LTD by strong eLFS did not alter the baseline of optically evoked fEPSPs (optical: 99.5 ± 1.9% at 1 h; electrical: 70.6 ± 3.3% at 1 h, n = 9, one-way ANOVA, compared with respective baseline, paired t-test), (Fig. 3.2.2.1 b,d).

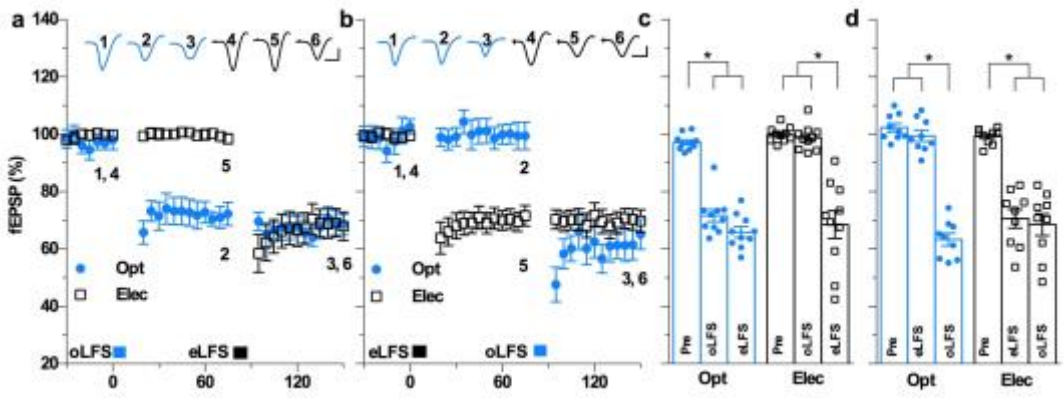

Fig. 3.2.2.1 Pathway independence of oLFS-induced LTD *in vivo*. (a) After 30 min of stable baseline recording from both optical (Opt) and electrical (Elec) pathways in the same animal, application of oLFS induced LTD of optical responses but did not affect the fEPSP in the electrical pathway from CA3 to CA1 pyramidal neurons. Conversely, 1 h after the application of oLFS, eLFS only induced LTD of electrical responses but did not affect the fEPSP in the optical pathway. (b) Similarly, when the conditioning stimulation sequence was reversed, LTD in one pathway did not affect the fEPSP in the other pathway. (c,d) Bar charts summarising the data for before (Pre) and 1 h after each conditioning stimulation in the optical or electrical pathways. The data show both the pathway independence of LTD and the lack of influence of prior eLFS on the ability of oLFS to induce LTD and vice versa. One-way ANOVA with Šidak post-hoc analysis per group. *P < 0.05. Calibration bars: vertical, 1mV; horizontal, 10ms.

Because a single LFS tetanus might not saturate LTD expression, we wondered if repeated LFS of one pathway might influence the expression of LTD in the other pathway (Fig. 3.2.2.2). Repeated application at 1 h

intervals of eLFS (Fig. 3.2.2.2 a,b) or oLFS (Fig. 3.2.2.2 c,d) did not significantly increase the magnitude of LTD (values after 3rd LFS compared with 'first' LTD, for both, respectively; eLFS3: 46.0 ± 5.2%, eLFS1: 52.6 ± 4.8%, n = 4; oLFS3: 56.7 ± 7.3%, oLFS1: 63.7 ± 3.0%, n = 4; $P > 0.05$ in both cases, one-way ANOVA with Šidak post-hoc analysis) or influence its expression in the other pathway (values after 3rd LFS, respectively; optical after eLFS3: 92.9 ± 1.9%, $P > 0.05$ compared with optical baseline 99.8± 3.6%, paired t-test; electrical after oLFS3: 97.5 ± 2.8%, $P > 0.05$ compared with electrical baseline 98.1± 1.3%, paired t-test), indicating that single LFS-900 saturates LTD and confirmed that the expression of LTD in the optical and electrical pathways are truly independent of each other.

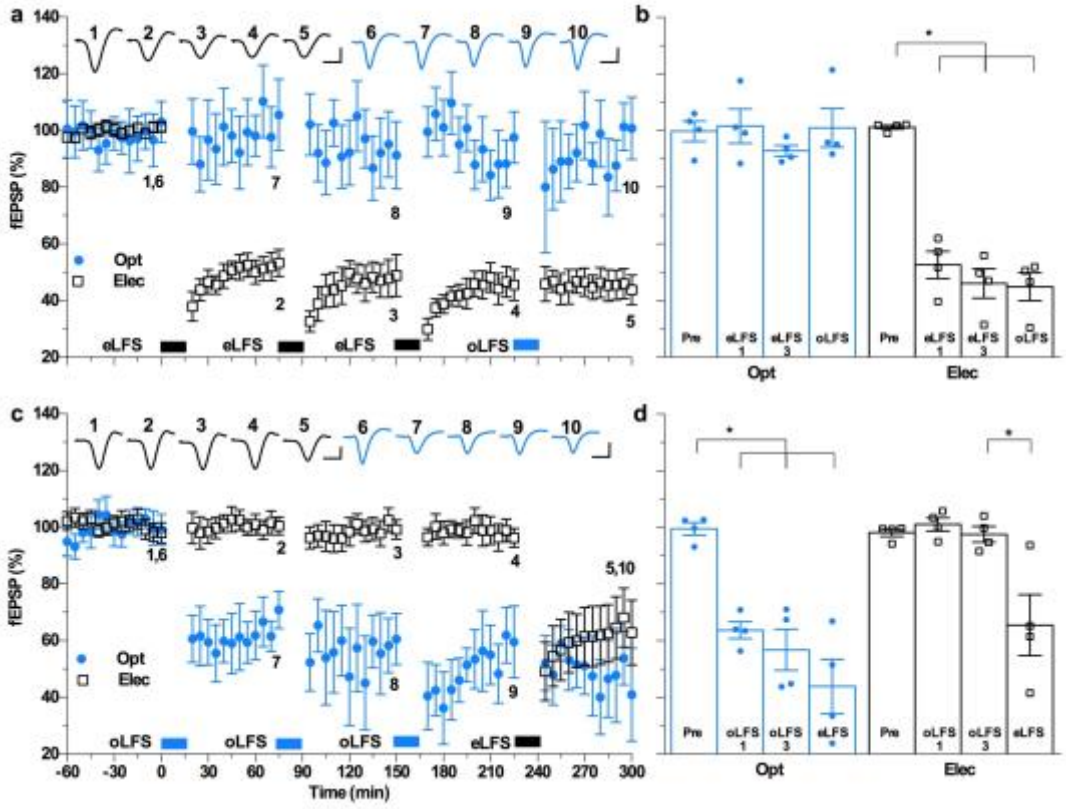

Fig. 3.2.2.2 LTD saturation outlines input selectivity of oLFS-induced LTD *in vivo*. (a) Repeated oLFS failed to affect the electrical pathway responses and the subsequent induction of LTD by eLFS. (c) However, although repeated eLFS did not affect optically evoked fEPSPs, the induction of LTD in the optical pathway by oLFS 1 h after the third electrical tetanus was inhibited. (b,d) Bar charts summarising the data at the times indicated. One-way ANOVA with Šidak post-hoc analysis per group, and selective paired t-tests. *P < 0.05. Calibration bars: vertical, 1mV; horizontal, 10ms.

We also examined if the induction of LTD in one pathway was influenced by the prior induction of LTD in the other pathway. The application of a single (Fig. 3.2.2.1 a) or repeated (Fig. 3.2.2.2 c) oLFS did not significantly affect the subsequent ability to induce LTD with eLFS

(after a single oLFS: 68.5 ± 4.8%, n=10; after three sets of oLFS: 65.5 ± 10.8%, n=4, *P < 0.05; One-way ANOVA with Šidak post-hoc analysis per group, compared with respective baseline, paired t-test). However, even though single eLFS did not significantly affect the subsequent induction of LTD in the optical pathway (Fig. 3.2.2.1 b), three sets of eLFS greatly impeded the subsequent ability to induce LTD with oLFS (after single eLFS: 63.3 ± 2.2%, n=9; after three sets of eLFS: 101.0 ± 6.8%, n=4, *P < 0.05; One-way ANOVA with Šidak post-hoc analysis per group, compared with respective baseline, paired t-test), (Fig. 3.2.2.2 a).

3.2.3 Role of cholinergic transmission in oLFS induction of LTD *in vivo*

Medial septal cholinergic efferent inputs into the CA3 area of the hippocampus synapse onto the pyramidal dendrites and elicit a neuromodulatory role on hippocampal synaptic plasticity (Cobb and Davies, 2005). Recent *in vivo* studies have shown mixed results in implicating this cholinergic input on synaptic plasticity (Huerta and Lisman, 1993; Fernandez de Sevilla et al., 2008) including LTD. From a human disease perspective, currently approved Alzheimer's Disease (AD) drugs are limited to acetylcholinesterase (AChE) inhibitors and memantine (Anand et el., 2014).

Previously we reported that cholinergic transmission, via muscarinic acetylcholine receptors, is required for the induction of robust LTD by the application of high-intensity electrical stimulation in the stratum radiatum

of the CA1 area (Hu et al., 2014). We hypothesised that such strong eLFS activated *en passant* cholinergic fibres to promote LTD. We predicted that oLFS induced LTD should be relatively independent of cholinergic input. We confirmed our previous finding that donepezil, an acetylcholinesterase inhibitor that boosts endogenous acetylcholine (Kryger et al., 1999; Sugimoto et al., 2000), lowered the threshold for the induction of LTD by a peri-threshold conditioning protocol, consisting of 300 high-intensity electrical pulses at 1Hz (eLFS-300), (Fig. 3.2.3.1 e,f). Thus, in control animals eLFS-300 caused little change from baseline (91.5 ± 2.5% at 1 h post- eLFS-300, n = 10; $P > 0.05$ compared with baseline, paired t-test) whereas the same protocol induced robust synaptic LTD in the presence of donepezil (1mg/kg, s.c. 1 h prior to LFS), (64.5 ± 4.9% at 1 h post- eLFS-300, n = 5; $P < 0.05$ compared with baseline, paired t-test, $P < 0.05$ compared with eLFS300 control, 2-way ANOVA with Šidak post-hoc analysis), (Fig. 3.2.3.1 e,f). In contrast, application of 300 high-intensity optical pulses at 1 Hz (oLFS-300) failed to induce LTD in the absence or presence of donepezil (control: 97.6 ± 1.8% at 1 h, n = 11; donepezil: 92.9 ± 8.7% at 1 h, n = 4; $P > 0.05$ compared with baseline or between groups, 2-way ANOVA with Šidak post-hoc analysis), (Fig. 3.2.3.1 a,c). In view of the lack of a facilitatory effect of donepezil on LTD induction by oLFS-300, we decided to determine if it might enhance LTD induced by stronger, yet submaximal conditioning stimulation of the optical pathway (Fig. 3.2.3.1 b,d). Thus, in controls, the application of 600 pulse oLFS induced an initially large depression that slowly reverted towards baseline (oLFS-600; 83.0 ± 2.7%, n = 7; $P < 0.05$ compared with baseline, paired t-test). However,

donepezil also failed to facilitate the induction of LTD by oLFS-600 (86.9 ± 5.1%, n = 4; P > 0.05 compared with baseline, control, 2-way ANOVA).

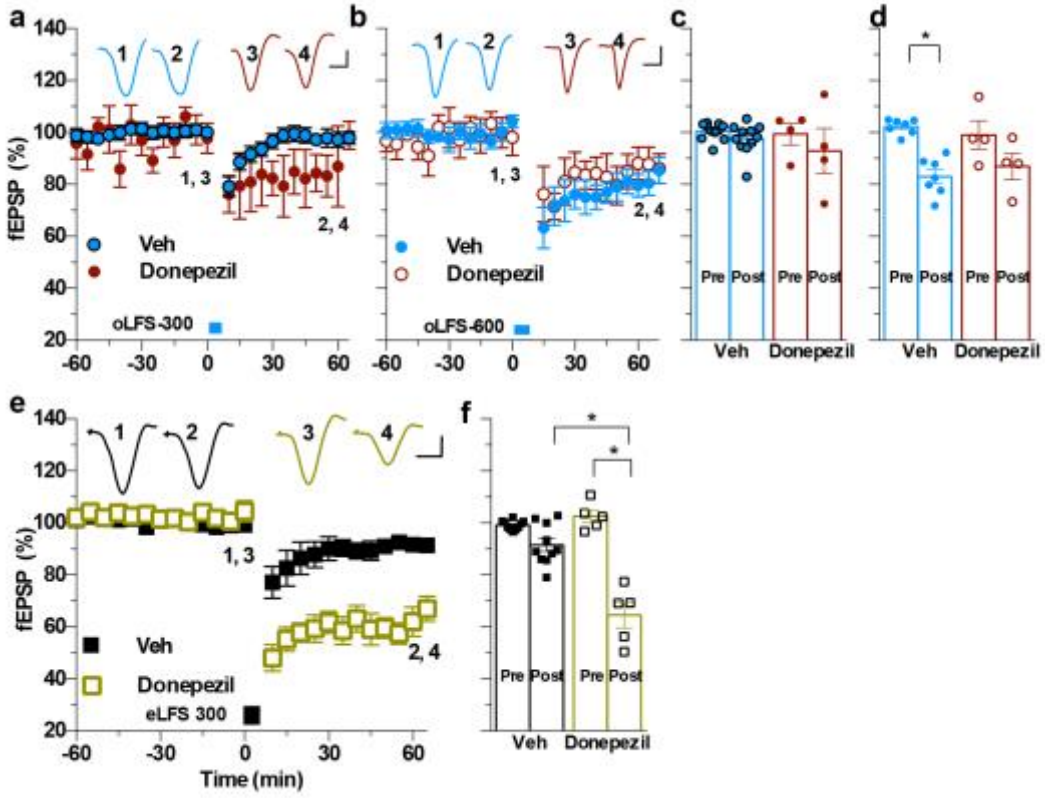

Fig. 3.2.3.1 Effect of the anticholinesterase donepezil (1 mg/kg s.c.) on LTD induction in the optical and electrical pathways. (a) Whereas donepezil facilitated the induction of LTD by eLFS-300 (e,f), it failed to facilitate LTD induction by oLFS-300 (a,c) or oLFS-600 (b,d). Values at 1 h post-LFS are presented in all bar charts. 2-way ANOVA with Šidak post-hoc analysis. *P < 0.05. Calibration bars: vertical, 1mV; horizontal, 10ms.

Next, we assessed if the muscarinic ACh receptor antagonist scopolamine blocked oLFS-induced LTD, since we previously found it to

strongly block LTD 3 h after its induction by high-intensity electrical LFS-900 in the stratum radiatum. Similar to our earlier report, scopolamine (0.2 mg/kg, i.p., 1-2 h pre-LFS) significantly inhibited LTD 3 h after the delivery of eLFS-900 (scopolamine: 90.3 ± 5.2%, n = 5; control: 60.3 ± 5.2%, n = 7, $P < 0.05$ compared with baseline and between groups, 2-way ANOVA with Šidak post-hoc analysis), (Fig. 3.2.3.2 c,d). Conversely, although LTD in the optical pathway appeared to be inhibited in some scopolamine-treated animals, overall there was no significant reduction of LTD magnitude at 3 h post-oLFS (scopolamine: 72.8 ± 7.2%, n = 9; control: 64.5 ± 2.5%, n = 7, $P < 0.05$ compared with baseline, and $P > 0.05$ between groups, 2-way ANOVA), (Fig. 3.2.3.2 a,b). Further, an unpaired t-test comparison of the optical and electrical +180 min data time points from both scopolamine groups show no significant difference ($P > 0.05$). Moreover, the vehicle control data collected for both modalities at +180 mins post-LFS also show no significant difference ($P > 0.05$), utilising an unpaired t-test.

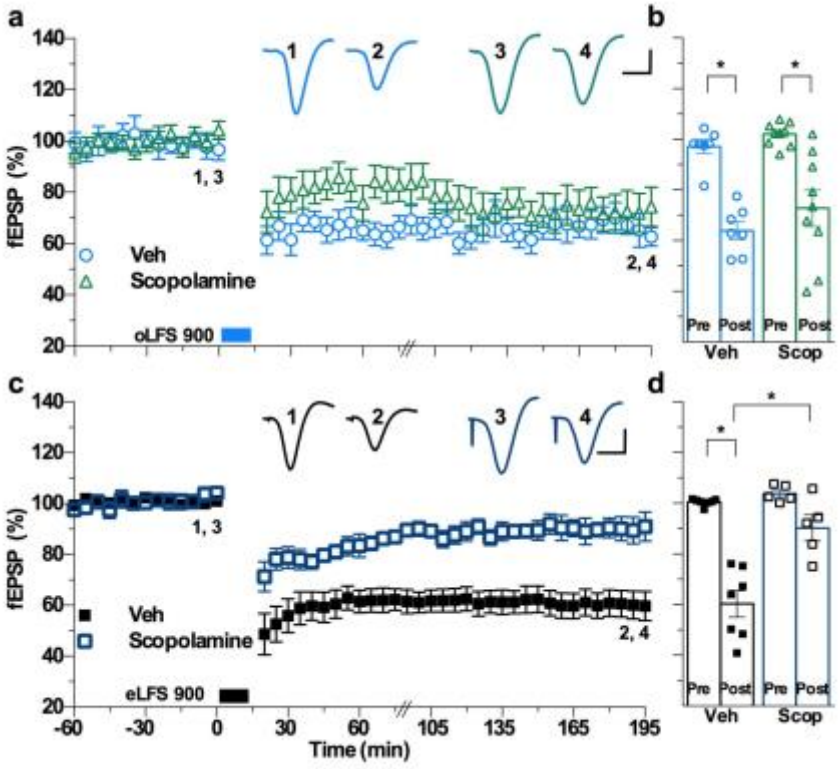

Fig. 3.2.3.2 Cholinergic-independence of oLFS induced LTD *in vivo.* Effect of the muscarinic acetylcholine receptor antagonist scopolamine (0.2 mg/kg, i.p. 1-2 h pre-LFS) on LTD in the optical and electrical pathways. Whereas scopolamine significantly inhibited LTD triggered by eLFS-900 (c,d), it had little effect on LTD induced by oLFS-900 (a,b). Values at 3 h post-LFS are presented in these bar charts. 2-way ANOVA with Šidak post-hoc analysis. *P < 0.05. Calibration bars: vertical, 1mV; horizontal, 10ms.

3.2.4 NMDAR-dependence of synaptic LTD induced by optical stimulation *in vivo*

Previously (Section 3.1.2) we reported that the induction of LTD by eLFS, consisting of 900 high-intensity pulses at 1 Hz, was only blocked by high local intracerebral doses of NMDAR antagonists when given alone, whereas standard systemic doses of NMDAR antagonists were only effective if mGlu5R was simultaneously blocked. We hypothesise that optically induced LTD would require NMDAR function. In order to determine if activation of the NMDAR is needed for the induction of synaptic LTD by oLFS *in vivo*, first, we investigated D-AP5. A dose (100 nmol, i.c.v., 15 min pre-LFS) that failed to prevent LTD induction by eLFS strongly attenuated optically induced LTD (100 nmol D-AP5: 93.2 ± 2.6%, n = 4, P > 0.05 compared with baseline and control; i.c.v. controls: 61.5 ± 2.8%, n = 5, P < 0.05 compared with baseline; 2-way ANOVA with Šidak post-hoc analysis), (Fig. 3.2.4 a,b). Further, a standard systemic dose of the competitive antagonist CPP (10 mg/kg, i.p., 2 h pre-LFS), strongly and significantly attenuated the induction of optically induced LTD (control: 57.4 ± 3.5%, n = 8; CPP: 88.7 ± 2.5%, n = 5; P < 0.05 compared with baseline and between groups, 2-way ANOVA), (Fig. 3.2.4 c,d). Next, we studied the non-competitive GluN2B subunit-selective negative allosteric modulator Ro 25-6981. Ro 25-6981 (6 mg/kg, i.p. 1 h pre-LFS) also strongly blocked the induction of LTD induction by oLFS (control: 68.1 ± 2.3%, n = 5, P < 0.05 compared with baseline; 6 mg/kg Ro 25-6981: 99.0 ± 5.7%, n = 5, P > 0.05 compared with baseline, P < 0.05 compared between groups, 2-way ANOVA), (Fig. 3.2.4 e,f).

In the light of the controversy over the requirement for ion flux through the NMDAR channel in eLFS induction of synaptic LTD *in vitro* (Babiec, 2014; Gray, 2016; Nabavi, 2013), we also examined the effect of the use-dependent NMDAR channel blocker MK-801. A relatively low dose of MK-801 (0.5 mg/kg, i.p., 1 h pre-LFS) strongly blocked the induction of LTD by oLFS (MK-801: 89.2 ± 1.7%, n = 5; control: 67.9 ± 2.3%, n = 6; $P < 0.05$ compared with baseline and between groups, 2-way ANOVA), (Fig. 3.2.4 g,h).

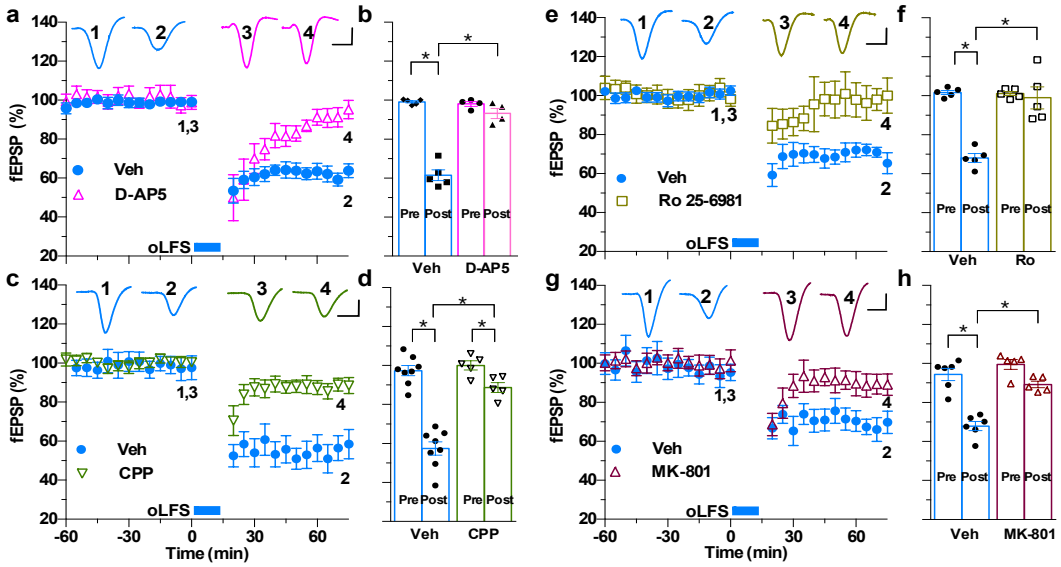

Fig. 3.2.4 NMDAR-dependence of the induction of synaptic LTD by oLFS *in vivo*. (a) Whereas application of oLFS induced robust and stable synaptic LTD in vehicle-pre-treated controls, the same oLFS protocol only induced a decremental LTD in animals pre-injected with a dose of D-AP5 (100 nmol, i.c.v., 15 min pre-LFS) that failed to significantly affect eLFS-induced LTD, 2-way ANOVA with Šidak post-hoc analysis. *P < 0.05. (b) Summary of the mean EPSP amplitude data in (a) before (pre) and 1 h after (post) application of eLFS. (c) Moreover, in animals treated systemically with the competitive NMDAR antagonist CPP (10 mg/kg, i.p., 2.25 h pre-oLFS) a strong inhibition relative to vehicle-treated animals was seen. (d) Summary of the mean EPSP amplitude data in (c). (e) Similarly, systemic administration of the non-competitive GluN2B subtype selective NMDAR antagonist Ro 25-6981 (6 mg/kg, i.p.,1 h pre-LFS) abrogated optically-induced LTD. (f) Summary of the mean EPSP amplitude data in (e). (g) Further, the use-dependent NMDAR ion channel blocker MK-801 (0.5 mg/kg, i.p., 1 h pre-LFS) potently and strongly inhibited optically-induced LTD. (h) Summary of 1 h data in (g). Calibration bars: vertical, 1mV; horizontal, 10ms.

Summarising these results, the induction of synaptic LTD by optical stimulation of glutamatergic fibres *in vivo* was blocked by relatively low doses of NMDAR antagonists that act at either the orthosteric glutamate binding site (CPP), the negative allosteric site on the GluN2B subunit (Ro 25-6981) or the NMDAR ion channel (MK-801).

3.2.5 Role of mGlu receptors in the induction of hippocampal synaptic LTD by optical conditioning stimulation *in vivo*

We tested the hypothesis that optically induced LTD is independent of mGlu5R activation. The mGlu5 receptor negative allosteric modulator MTEP alone did not affect the induction of LTD by oLFS. Thus, in MTEP (3 mg/kg, i.p., 1 h pre-LFS) pre-treated animals, application of oLFS induced robust and stable LTD of optically evoked fEPSPs (MTEP: 68.3 ± 6.7%, n = 5; controls: 68.3 ± 2.4%, n=7, $P < 0.05$ compared with respective pre-oLFS baselines; $P > 0.05$ between groups; 2-way ANOVA with Šidak post-hoc analysis), (Fig. 3.2.5 a,b).

Nevertheless, we wondered if pharmacologically boosting endogenous glutamate activation of mGlu5Rs would facilitate the induction of LTD by optical LFS, similar to eLFS-induced LTD. The mGlu5R positive allosteric modulator VU 0360172 (15 mg/kg, s.c., 1 h pre-LFS) failed to enhance the ability of the peri-threshold oLFS-300 protocol (300 high-intensity optical pulses at 1 Hz) to induce LTD. Thus, oLFS-300 induced a short-term depression of synaptic transmission

either in the absence or presence of VU 0360172 (control: 97.6 ± 1.8% at 1 h, n = 11, P > 0.05 compared with baseline; VU 0360172: 95.1 ± 1.4%, n=4, P > 0.05 compared with baseline and between groups, 2-way ANOVA), (Fig. 3.2.5 c,d).

Equally, the highly selective mGlu2/3R antagonist LY341495, at a dose of 3 mg/kg, i.p. 1 h pre-LFS, failed to significantly affect the magnitude of oLFS-induced LTD (Fig. 3.2.5 e,f), similar to our previous finding for eLFS-induced LTD. (LY341495: 72.0 ± 5.4%, n = 9; controls: 69.1 ± 4.0%, n = 7; P < 0.05 both compared with baselines, P > 0.05 compared between groups, 2-way ANOVA).

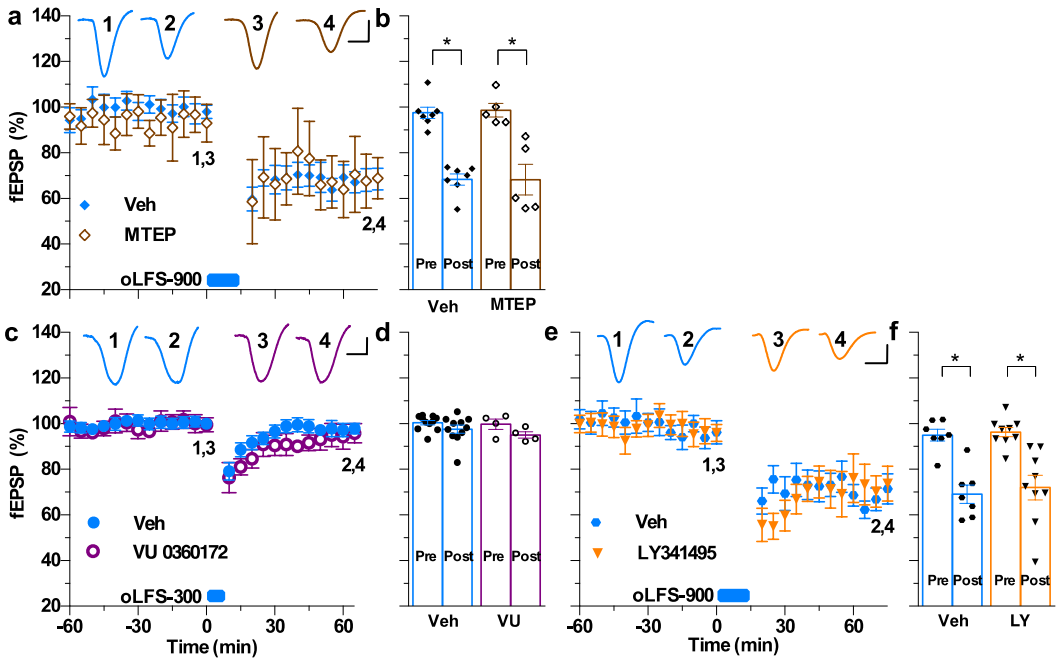

Fig. 3.2.5 mGlu receptor-independence of optically-induced synaptic LTD *in vivo*. (a) Injection of the mGlu5R negative allosteric modulator MTEP (3 mg/kg, i.p., 1 h pre-LFS), did not significantly affect the induction of LTD by oLFS-900. (b) Summary of the mean EPSP amplitude data in (a) before (pre) and 1 h after (post) application of LFS. (c) The mGlu5R positive allosteric modulator VU 0360172 (15 mg/kg, s.c., 1 h pre-LFS) did not facilitate the induction of LTD by a peri-threshold optical LFS conditioning protocol (oLFS-300, 300 high-intensity pulses at 1Hz) relative to vehicle controls. (d) Summary of the mean EPSP amplitude data in (c). (e) Moreover, the group II mGluR antagonist LY341495 (3 mg/kg, i.p., 1 h pre-LFS) did not significantly affect optically induced LTD. (f) Summary of the mean EPSP amplitude data in (e). 2-way ANOVA with Šidak post-hoc analysis. *P < 0.05. Calibration bars: vertical, 1mV; horizontal, 10ms.

3.2.6 Protein synthesis-dependence of oLFS-induced LTD *in vivo*

Protein synthesis has been reported to be necessary for LTD induced by eLFS in area CA1 in rats *in vivo* (Manahan-Vaughan et al., 2000). Here we have described an NMDAR dependent *in vivo* CA3-CA1 hippocampal synaptic LTD inducible with two different stimulus modalities; understanding the sensitivity of this synaptic plasticity to protein synthesis antagonism is paramount to further understanding the underlying molecular mechanisms responsible.

Because the persistence of certain forms of NMDAR-dependent LTD require new proteins to be synthesised we hypothesised that LTD at both pathways would be sensitive to translation inhibition. Therefore, we tested translation inhibitor emetine (240 µg, injected i.c.v. 30 min pre-LFS; Stanton and Sarvey, 1984), which strongly inhibited oLFS-induced LTD (89.2 ± 8.2% at 3 h post-LFS, n = 5, $P > 0.05$ compared with baseline; $P < 0.05$ compared with 62.6± 3.0%, n = 7, in vehicle-treated rats; 2-way ANOVA with Šidak post-hoc analysis), (Fig. 3.2.6 a,b). Further, the same dose abrogated eLFS-induced LTD (91.9 ± 5.9% at 3 h post-LFS, n = 3, $P > 0.05$ compared with baseline; $P < 0.05$ compared with 54.8 ± 3.6%, n = 7, in vehicle-treated rats, 2-way ANOVA), (Fig. 3.2.6 c,d).

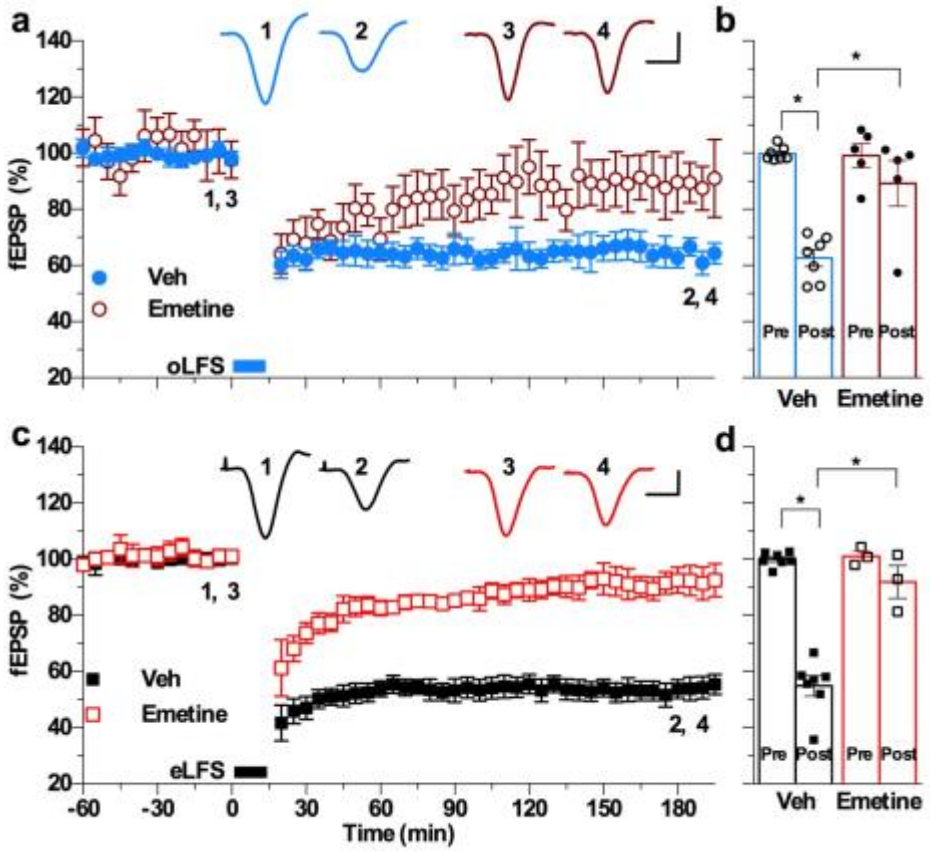

Fig. 3.2.6 Protein synthesis-dependence of LTD *in vivo.* (a) Inhibition of protein synthesis with the translation inhibitor emetine (240 µg, i.c.v.) 30 min prior to high-intensity oLFS-900 strongly inhibited LTD in the optical pathway. (b) Summary of the mean EPSP amplitude data in (a) before (pre) and 3 h after (post) application of oLFS. (c) Further, inhibition of protein synthesis with emetine application prior to eLFS-900 also strongly inhibited LTD in the electrical pathway. (d) Summary of the mean EPSP amplitude data in (c). 2-way ANOVA with Šidak post-hoc analysis. *P < 0.05. Calibration bars: vertical, 1mV; horizontal, 10ms.

3.3 GluN2B NMDAR-dependence and lateralisation of Alzheimer's disease Aβ-facilitated LTD

Synaptic plasticity in the brain is particularly vulnerable to disruption by factors that impair cognition in neurological and psychiatric disease, including Alzheimer's (AD) and related dementias. There is a great scientific and medical need to elucidate the cellular basis of this impairment. Moreover, glutamatergic processes are strongly implicated in causing and mediating the symptoms of AD. A major hallmark symptom of AD is the development of amyloid plaques containing the amyloid-β protein (Aβ). Early studies found that AD-associated Aβ promoted glutamatergic excitotoxicity (Madeira et al., 2015). More recently Aβ was discovered to form soluble oligomers that rapidly and potently disrupt glutamatergic synapses and plasticity mechanisms underlying cognitive function (Hu et al., 2009). Further, as was recently reported, application of synthetic Aβ-derived diffusible ligands (ADDLs) was sufficient in lowering the threshold for LTD induction, allowing a sub-threshold electrical LFS300 to induce strong, stable LTD (Hu et al., 2014). Here we investigated the NMDAR-dependence and lateralisation of the facilitatory effect of Aβ on LTD.

3.3.1 Alzheimer's disease Aβ-facilitated LTD induced by electrical LFS is GluN2B dependent, but not lateralised

Previous work indicated that Aβ-enhanced LTD was NMDAR independent (Hu et al., 2014) since it was not blocked by the GluN2B-selective non-competitive antagonist Ro 25-6981 when systemically injected at standard doses. Given the present results with locally delivered NMDAR agents (Section 3.1.2), we hypothesised that i.c.v. delivery of Ro 25-6981 may abrogate Aβ-facilitated LTD. First, we confirmed that synthetic synaptotoxic aggregates of human Aβ1-42 facilitated the induction of LTD by electrical LFS of the Schaffer collateral/ commissural pathway *in vivo*. Thus, application of the peri-threshold eLFS-300 conditioning protocol 30 min after an i.c.v. injection of Aβ (1.2nmol) induced robust LTD induction (control eLFS-300: 91.5 ± 2.5%, n = 10; Aβ: 64.2 ± 4.5%, n = 10, $P < 0.05$ between all groups, one-way ANOVA, Holm-Šidak of 1 h post-LFS, compared with respective baseline, paired t-test). Importantly, the Aβ enhanced LTD was NMDAR-dependent. A complete ablation of LTD was seen after combined i.c.v. application of Aβ and Ro 25-6981, similar to that previously seen (Hu et al., 2009), where Ro 25-6981 blocked LTP abrogation induced by Aβ. Four animals were administered Ro 25-6981 locally 15 min after Aβ and 15 min before LFS, whereas two animals were given Ro 25-6981 15 min before Aβ and 45 min before LFS; no difference in LTD abrogation was seen therefore the data from all 6 animals were combined (aβ+Ro 25-6981: 88.5 ± 7.1%, n = 6; $P < 0.05$ between all groups, one-way ANOVA, Holm-Šidak of 1 h post-LFS, compared with respective baseline, paired

t-test, and between individual groups, unpaired t-test), (Fig. 3.3.1 a,b). Further, when animals that were tetanised on the left or right hemisphere were compared, there appeared to be no lateralisation of Aβ preferential facilitation of the induction of LTD by eLFS (Aβ-left: 64.5 ± 5.5%, n = 6; Aβ-right: 63.7 ± 8.6%, n = 4), (Fig. 3.3.1 c,d).

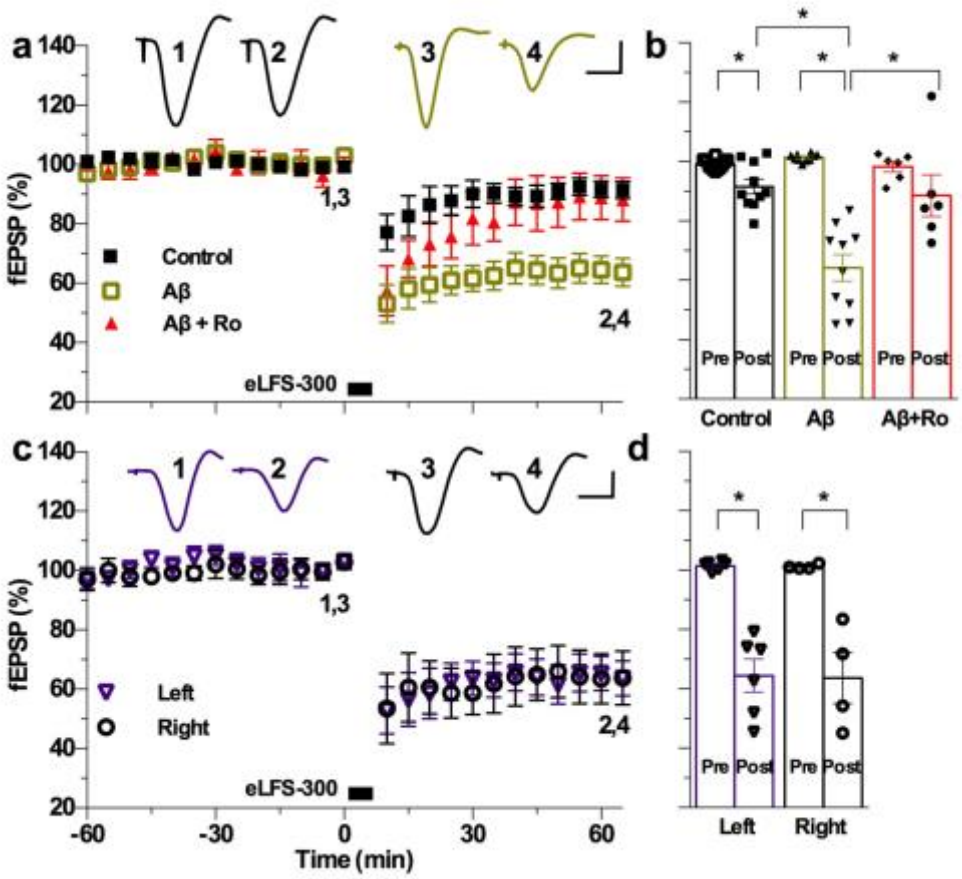

Fig. 3.3.1 Alzheimer's disease Aβ enhanced electrically induced LTD is GluN2B dependent but not lateralised. (a) Application of electrical LFS-300 30 min after the injection of Aβ (1.2nmol, i.c.v.) induced large LTD compared with controls, which was strongly blocked by the GluN2B-selective NMDAR antagonist Ro 25-6981. (b) Summary of the mean EPSP amplitude data in (a) before (pre) and 1 h after (post) application of LFS. One-way ANOVA, Holm-Šidak, post-hoc analysis, and paired t-test. (c) The facilitatory effect of Aβ was not lateralised in Alzheimer's disease Aβ-facilitated LTD. (d) Summary of the mean EPSP amplitude data in (c). 2-way ANOVA with Šidak post-hoc analysis. *P < 0.05. Calibration bars: vertical, 1mV; horizontal, 10ms.

3.3.2 Alzheimer's disease Aβ-facilitated LTD induced by optical LFS is lateralised

Numerous reports indicate that the early cognitive impairment of AD are driven by lateralised hippocampal deficits, but the underlying cellular mechanisms still need to be elucidated. Amyloid-β protein (Aβ) forms synaptotoxic assemblies that disrupt hippocampal synaptic plasticity, and we wondered if such deleterious effects were also lateralised, providing a potential insight into the pathophysiology of early AD. Specifically, we hypothesised that, since Aβ-facilitated LTD is mGlu5R-dependent (Hu et al., 2014) and mGlu5R levels are higher on apical spines of CA1 neurons receiving input from left CA3 pyramidal cells (Shinohara and Hirase, 2009), Aβ would preferentially facilitate at these synapses.

When we administered the same dose of Aβ that facilitated eLFS-induced LTD, the magnitude of LTD induced by oLFS-300 was significantly greater LTD than controls, which were recorded for just 1 h post-LFS (ctrl: 97.6 ± 1.8% at 1 h, n = 11; Aβ: 86.2 ± 3.7%, n = 11, $P < 0.05$ compared with baseline and between groups, 2-way ANOVA with Šidak post-hoc analysis), (Fig. 3.3.2 a,b). Importantly, when we compared animals that had recorded data lasting at least 3 h post-LFS, and were tetanised on the left and right sides, there was clear evidence of lateralisation, such that Aβ preferentially facilitated the induction of LTD by oLFS at Schaffer collaterals in the left hippocampus (Aβ-left: 75.8 ± 5.2% at 3 h post-oLFS; Aβ-right: 98.2 ± 3.6%; n = 5 per group, $P < 0.05$ compared with baseline and between groups, 2-way ANOVA), (Fig. 3.3.2 c,d).

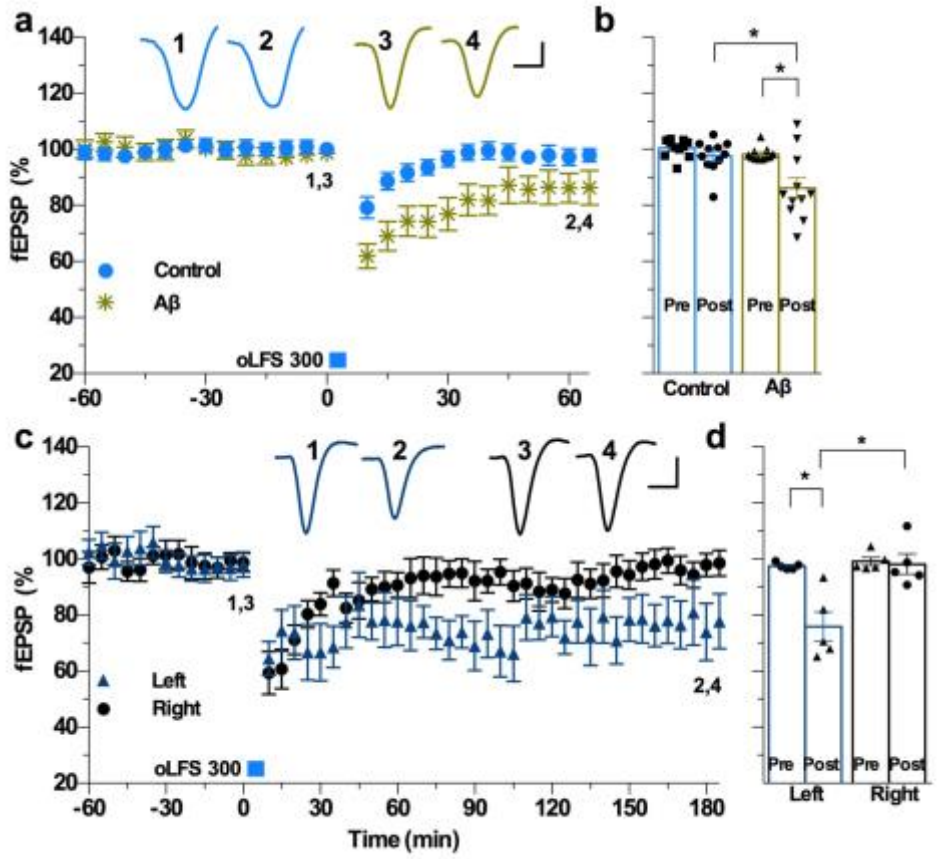

Fig. 3.3.2 Alzheimer's disease Aβ enhances optically induced LTD preferentially at Schaffer collateral input to CA1 in the left hippocampus. (a) Application of optical LFS-300, 30 min after the injection of Aβ (1.2nmol, i.c.v.) induced a significantly larger LTD compared with controls. (b) Summary of the mean EPSP amplitude data in (a) before (pre) and 1 h after (post) application of oLFS. (c) Remarkably, the facilitatory effect of Aβ was lateralised such that oLFS induced robust synaptic LTD at stratum radiatum Schaffer collaterals in the left, but not right, hippocampus. (d) Summary of the mean EPSP amplitude data in (c) before (pre) and 3 h after (post) application of oLFS. 2-way ANOVA with Šidak post-hoc analysis. *P < 0.05. Calibration bars: vertical, 1mV; horizontal, 10ms.

IV. Discussion

4.1 Induction of hippocampal synaptic LTD by optical low-frequency conditioning stimulation *in vivo*

4.2 The role of cholinergic transmission in oLFS induction of LTD *in vivo*

4.3 The role of NMDA and mGlu5 receptors in the induction of hippocampal synaptic LTD *in vivo*

4.4 Absolute requirement for GluN2B-subunit-containing NMDARs and the ion channel function in the induction of LTD *in vivo*

4.5 The roles of GluN2B-subunit-containing NMDARs and lateralisation in Alzheimer's disease Aβ-facilitated LTD

To increase our understanding of *in vivo* LTD, we examined the requirement for cholinergic, as well as the metabotropic and ionotropic functions of glutamate in LTD induction, in different synaptic pathways, in urethane anaesthetised adult rats. We specifically focused on LTD induction by electrical and optical LFS at CA3-to-CA1 apical synapses in the hippocampus and its modulation by synthetic Alzheimer's disease Aβ protein. Seeing that high-intensity electrical LFS is likely to co-activate both the mGlu5R and NMDARs we wondered if an interaction between these receptors was necessary to enable the induction of LTD. Furthermore, given that peri/extra-synaptic glutamate receptor activation is readily evoked by electrical stimulation (Arnth-Jensen et al., 2002; Scimemi et al., 2004) we utilised the recently developed technology of optogenetics to relatively diffusely express light-activatable channelrhodopsin 2 (ChR2-eYFP) in CA3 pyramidal neurons unilaterally, thereby allowing relatively selective excitation of either Schaffer collateral or commissural fibres, avoiding stimulation of *en passant* cholinergic neurons. Thus, optogenetics allowed us to assess the need for peri/extra-synaptic mGlu5R and muscarinic AChR activation in LTD induction. More diffuse and selective probing of plasticity at these synapses *in vivo* may more closely mimic the pattern that occurs during much of normal hippocampal function (Ramirez et al., 2013).

4.1 Induction of hippocampal synaptic LTD by optical low-frequency conditioning stimulation (oLFS) *in vivo*

Ever since its introduction in hippocampal neurons (Boyden et al., 2005) optogenetics has been widely used to study neurotransmitter systems in a variety of CNS regions including the hippocampus (Kohl et al., 2011; Basu et al., 2016; Jackman et al., 2014; Jackman et al., 2016; Broussard et al., 2016; Wang et al., 2015; Bittner et al., 2015) and with specific attention to learning and memory (Ramirez et al., 2013; Nabavi et al., 2014; Redondo et al., 2014; Liu et al., 2012; Liu et al., 2014; Ryan et al., 2015; Shipton et al., 2014). There is keen interest in utilisation of this system for studies relating to the control of behavioural activity (Danielson et al., 2016; Weber et al., 2015; Kwon et al., 2015; Bukalo et al., 2015; Mamad et al., 2015; Kropff et al., 2015) as well as Alzheimer's disease (Roy et al., 2016; Yamamoto et al., 2015), schizophrenia (Duan et al., 2015), epilepsy (Ladas et al., 2015; Chiang et al., 2014), anxiety and depression (Belzung et al., 2014) and autism (Felix-Ortiz et al., 2014).

In this study, we were able to demonstrate that selective expression of ChR2 by AAV transduction in excitatory CA3 pyramidal neurons, elicited functional synaptic responses at apical dendrites in the *stratum radiatum* of area CA1 in the living rat. Considering the novelty of the optogenetic technique employed here and the complexity of hippocampal synaptic plasticity, it was important to confirm the expression of ChR2 was selective and that optical stimulation evoked

stable synaptic field potentials with a similar time course to electrically evoked responses.

To avoid the direct activation of *en passant* cholinergic fibres, we chose the α-calcium/ calmodulin-dependent kinase II (CaMKII) promoter to restrict expression of our channelrhodopsin to excitatory neurons in the hippocampus. Based on previous studies that used a variety of viral vectors and channelrhodopsins, we chose AAV2 or AAV5 directed expression of the H134R/ E123T ChR2 (Tchumatchenko et al., 2013, Zhang et al., 2006, Lórenz-Fonfría and Heberle, 2014) nonselective cation channel. We observed sufficient expression in CA3 pyramidal neurons in the dorsal hippocampus to allow 0.5-1.0mW of blue (473nm) laser light to activate enough current to optically evoke an EPSP that was temporally and structurally comparable to the electrically evoked EPSP.

We noted that sweep-to-sweep variation of optically evoked fEPSPs was greater than electrically evoked fEPSPs, but the average optically evoked responses remained stable over several hours of recording once the initial maximum fEPSP amplitude was greater than ~1mV. It is likely that the optogenetically elicited train of action potentials in the transduced CA3 pyramidal cell population activated native voltage-gated sodium channels in the Schaffer collateral pathway that propagated as a spike to the axon terminals in the stratum radiatum of the CA1 in the dorsal hippocampus. Thus, optically evoked fEPSPs likely share the same mechanisms of presynaptic (such as exocytotic neurotransmitter vesicle pool dynamics) and postsynaptic plasticity (via receptor activation, internalisation and phosphorylation), as would native

or electrically induced action potential trains with similar strength, rates and timing. Thus, the increased sweep-to-sweep variability of optically evoked responses is likely to be caused by the initial variation in the number of ChR2 channels activated by the light. *In vivo* tissue transmission of the optical stimulus will depend on local factors that are constantly fluctuating, including blood flow.

We found that a high-intensity (evoking 95% but not 75 or 50% of maximum responses) optical low-frequency stimulation of 900 (but not 300 or 600) pulses delivered at 1Hz induced LTD at CA3-to-CA1 synapses that was at or near maximum, suggesting that strong synaptic activation is required for robust hippocampal LTD induction by oLFS. Similar magnitude LTD was induced by oLFS in both hemispheres and appeared largely independent of electrical LFS induction and expression of LTD in nearby synaptic pathways. The lack of any lateralisation of *in vivo* optically induced control LTD contrasts with what has been previously reported with optically induced LTP *in vitro* (Kohl, 2011; Shipton, 2014). An additional application of the optogenetic technique tested here was the ability to stimulate CA3 pyramidal neurons commissural fibres after they had traversed to the hippocampal CA3 area contralateral to the side of viral injection. Even though the fEPSPs were smaller with this experimental protocol than those recorded ipsilateral to the site of transduction/ stimulation, robust LTD was induced regardless of which side the virus had been injected.

4.2 The role of cholinergic transmission in oLFS induction of LTD *in vivo*

It is well accepted that CA1 interneurons receive cholinergic projections from the medial septum-diagonal band of Broca (Dutar et al., 1995). Activation of muscarinic acetylcholine receptors (mAChR) and nicotinic ACh receptors (nAChR), can modulate the excitability of interneurons and/ or suppress GABA release (Pitler and Alger, 1992; Fukudome et al., 2004; Cobb and Davies, 2005; Cea-del Rio et al., 2011), and regulate short and long-term plasticity at excitatory synapses in CA1 pyramidal neurons (Huerta and Lisman, 1993; Fernandez de Sevilla et al., 2008). Indeed, the activation of presynaptic mAChRs transiently inhibits excitatory transmission by reducing glutamate release through inhibition of VGCC at Schaffer collateral terminals (Fernandez de Sevilla et al., 2008). However, the association of cholinergic influence on synaptic plasticity *in vivo* remains to be properly explored (Fernandez de Sevilla et al., 2008; Hu et al., 2014). As a result, the use of cholinergic independent optogenetic expression tools could prove invaluable in studying fundamental neurophysiology and how it is modulated in disease, such as Alzheimer's.

When we revisited our previous work indicating the requirement for cholinergic transmission via mAChRs for the induction of LTD, we confirmed the ablation of electrically induced LTD with the mAChR antagonist scopolamine. In contrast, we found scopolamine had no overall effect on optically induced LTD, 3 hours after stimulation. Further,

when we boosted endogenous acetylcholine with the application of the anticholinesterase donepezil, sub-threshold eLFS was now sufficient to induce robust LTD, confirming our previous finding. However, there was a distinct lack of a facilitatory effect of donepezil on LTD induction by oLFS. Taken together, these findings indicate that electrical field stimulation activated *en passant* cholinergic fibres to promote LTD whereas direct optical stimulation of pure Schaffer collateral inputs was sufficient to induce LTD. It seems unlikely that background cholinergic tone, independent of electrical stimulation, strongly regulates LTD in the anaesthetised rat.

4.3 The role of NMDA and mGlu5 receptors in the induction of hippocampal synaptic LTD *in vivo*

In the case of CA3-to-CA1 synapses in the hippocampus, LTD induction has been divided into NMDAR and mGluR–dependent forms. Therefore, we examined the requirement of glutamate receptor function underlying the induction of LTD at these synapses in the hippocampus *in vivo.* We found that relatively high doses of competitive and non-competitive receptor antagonists were required to reveal the NMDAR-dependence of synaptic LTD induced by field electrical stimulation, which activates synapses *en masse*. In contrast, LTD induced by optical stimulation of excitatory synapses containing ChR2 was readily blocked by standard systemic doses of NMDAR antagonists. Remarkably, although mGlu5R antagonism alone failed to affect either optical or electrical LTD, standard doses of NMDAR antagonists were sufficient to prevent eLFS-induced

LTD only when mGlu5Rs were simultaneously blocked. Complementing these findings, a positive allosteric modulator of mGlu5Rs lowered the threshold for electrically-induced, but not optically-induced, LTD. We also found that the NMDAR ion channel function was necessary in synaptic LTD, as were GluN2B containing NMDARs when inhibiting mGlu5R positive allosteric modulator-facilitated electrically induced LTD.

The induction of LTD by eLFS was inhibited only by relatively high doses of a variety of NMDAR antagonists that act via different mechanisms: (1) bind competitively to the orthosteric glutamate binding site (D-AP5), (2) non-competitively block the GluN2B subunit (negative allosteric modulator Ro 25-6981) or (3) non-competitively block the open ion channel (MK-801). This requirement for high doses of NMDAR antagonists is most unlikely to be solely because eLFS increases glutamate release, since the standard doses of D-AP5, CPP and MK-801 used here, that failed to inhibit electrically induced LTD, completely block the induction of LTP by electrical high-frequency conditioning stimulation that greatly increases glutamate release (Hu et al., 2008, Abraham and Mason, 1988, Hu et al., 2009). Moreover, by definition, non-competitive blockade of NMDARs should be relatively independent of ambient glutamate concentration. The requirement for a relatively high concentration of antagonist to achieve significant block of LTD induction, therefore, is much more likely to be caused by an increase in functional NMDAR numbers. Our finding that blocking mGlu5Rs lowered the dose of NMDAR antagonist required to inhibit LTD by LFS strongly indicates that mGlu5R co-activation boosts functional NMDAR numbers. Indeed,

mGlu5 and NMDA receptors are physically associated as part of an interactome (Darnell and Klann, 2013), and perisynaptic co-activation of these receptors enhances NMDAR-mediated excitability (Doherty et al., 1997, Kotecha et al., 2003, Mannaioni et al., 2001). Further, complementary confirmation of the role of mGlu5Rs in the direct regulation of NMDAR function *in vivo* was the ability of a positive allosteric modulator at mGlu5Rs to lower the threshold for the induction of LTD by eLFS. Importantly, similar to LTD induced by standard LFS, a relatively high-dose NMDAR antagonist also was required to inhibit this pharmacologically potentiated LTD.

The finding of a facilitatory role of mGlu5Rs in NMDAR-dependent LTD induction implies that eLFS causes significant co-activation of mGlu5Rs and NMDARs at non-synaptic sites. Such activation is dependent on the spatial pattern of synaptic activation, with electrical field stimulation, as used in the present experiments, providing highly favourable conditions for glutamate spillover-mediated co-activation of mGlu5 and NMDA receptors; however, this likelihood was greatly diminished in LTD induction by relatively diffuse selective optical stimulation of Schaffer collaterals, given that mGlu5Rs are less likely to be activated. Consistent with this scenario, optical LTD induction was blocked by a standard dose of NMDAR antagonist and was not facilitated by the positive allosteric modulator of mGlu5Rs.

Nearby synapses are highly likely to be co-activated under pathological conditions such as epilepsy and spillover to neighbouring

synapses will be increased when glutamate homeostasis is compromised, such as occurs in psychiatric and neurological illnesses. Indeed, in animal models of AD, mGlu5Rs are engaged to enhance synaptic LTD that is resistant to NMDAR antagonism (Hu et al., 2014, Li et el., 2009). Undoubtedly, hippocampal mGlu5Rs act as sentinels of glutamate spillover and, when activated in concert with GluN2B, trigger a persistent down-regulation of potentially redundant or inappropriate synaptic transmission, thus placing mGlu5R facilitation of LTD in the centre of the synaptic physiology-pathology continuum.

The finding that boosting mGlu5R activation with a selective PAM and boosting mAChR activation with a selective acetylcholinesterase inhibitor lowered the threshold for the induction of LTD by eLFS raises the question of the possible relationship between these two pathways. Both are G-protein-linked 7 transmembrane receptors and are known (Wang and Zhou, 2012; Resend and Adhikari, 2009) to engage similar downstream signalling pathways, including PLC, DAG, PKC and calmodulin, leading to ERK and MAPK activation. Although mGlu5 receptors are tightly linked to GluN2B subunits, less is known regarding mAChR-GluN2B interactions (Dennis et al., 2016; Jiang et al., 2014). On the other hand, although the mAChR antagonist scopolamine inhibited eLFS-induced LTD, we failed to observe any disruption of this form of LTD after injection of the mGlu5R antagonist MTEP.

4.4 Absolute requirement for GluN2B-subunit-containing NMDARs and the ion channel function in the induction of LTD *in vivo*

Recent research (Sarantis et al., 2015) emphasises a key role for GluN2B subunits in mediating mGlu5R enhancement of NMDAR excitability, where co-activation of mGlu5R/ NMDAR activates Src kinases, synergistically leading to GluN2B (Tyr1472) phosphorylation to prevent internalisation, stabilising GluN2B-containing NMDARs in the plasma membrane. Indeed, our data demonstrate that GluN2B subunits are critical for LTD induction by eLFS, consistent with previous *in vivo* (Fox et al., 2006; Wong et al., 2007), and *in vitro* studies (see review by Shipton and Paulsen, 2014), although it is important to consider alternative reporting (Bartlett et al., 2007; Kollen et al., 2008). Here we report a similar requirement for GluN2B in LTD induction by optogenetic activation of synapses using high-intensity optical LFS of ChR2 expressing CA3 neurons. GluN2 subunit expression and localisation changes markedly across development, with a higher ratio of GluN2A:GluN2B, and a shift of GluN2B from synaptic to a predominantly perisynaptic and extrasynaptic location, in adulthood (Yashiro and Philpot, 2008). Small changes in age during development affect the magnitude or even the presence of LTD (Ku et al., 2008), consistent with a critical role for GluN2B in the induction of LTD. Based on our findings with Ro 25-6981, GluN1/GluN2B diheteromers are required for synaptic LTD induction *in vivo* but clearly roles for synaptic GluN1/GluN2A diheteromers or GluN1/GluN2A/GluN2B triheteromeric NMDARs cannot

be excluded (Hansen et al., 2014).

The ability of the open-channel, use-dependent, blocker of NMDARs MK-801 (Harris and Pettit, 2007), to inhibit LTD triggered by high-intensity electrical or optical stimulation indicates that the LTD induction is dependent on ion flux through NMDARs. The widely accepted view that the faster and greater Ca^{2+} influx through NMDARs during high-frequency stimulation protocols leads to LTP while slower and smaller Ca^{2+} influx through NMDARs results in LTD at hippocampal synapses is being challenged (Nabavi et al., 2013; Tigaret et al., 2016). However, in the present study LTD induced by either oLFS or eLFS was blocked, albeit with differential sensitivity by MK-801, supporting the view that Ca^{2+} influx through NMDARs is required for LTD induction *in vivo*. Thus, although our data are consistent with a physical interaction between mGlu5Rs and GluN2B facilitating LTD induction by eLFS, the obligatory involvement of NMDAR ion channel function in triggering LTD *in vivo* emerges as paramount.

4.5 The roles of GluN2B-subunit-containing NMDARs and lateralisation in Alzheimer's disease Aβ-facilitated LTD

Many studies have seen an impairment in memory coinciding with the accumulation of soluble extracellular Aβ protein (McLean et al., 1999). Both synthetic and human-derived Aβ soluble aggregates potently disrupt synaptic plasticity (Shankar and Walsh 2009; Hu et al., 2014). Interestingly here, ADDLs had a strong facilitatory effect on electrically induced LTD whereas it caused a modest enhancement of LTD induction

by subthreshold optical LFS. Further, given the successful ablation of synaptic LTD by local injection of a GluN2B containing NMDAR antagonist, we decided to revisit the role of NMDARs in the ability of ADDLs to enhance electrically induced LTD (Hu et al., 2014). The same dose of locally delivered Ro 25-6981 that prevented eLFS-900 LTD also blocked the Aβ-mediated enhancement, providing further evidence suggesting that GluN2B subunit-containing NMDARs mediate the actions of Aβ oligomers (Li et al., 2009). Thus, potentially GluN2B block may be useful in preventing Aβ from promoting glutamatergic excitotoxicity (Haass and Selkoe, 2007) and possibly blocking Aβ acting as an extracellular scaffold and promoting the inappropriate synaptic mobilisation and activation of mGlu5R (Renner et al., 2010). The new findings support the belief that GluN2B plays a key role in mediating the synaptic plasticity disrupting actions of Aβ (Hu et al., 2009; Um et al., 2012; Kessels et al., 2013).

When we parsed the optical data further, it became apparent that the Aβ-facilitated LTD was lateralised, where Aβ preferentially facilitated the induction of optically induced LTD in the left hippocampus. This provides valuable insight into the pathophysiology of AD indicating that the left CA1 neurons receiving input from left CA3 pyramidal cells may be preferentially targeted by Aβ, due to higher mGlu5R levels (Shinohara and Hirase, 2009). As a result, optogenetics could open up new avenues for AD research allowing us to examine a lateralised LTD that is specifically directed by Aβ.

V. Conclusion

The findings presented here within, indicate that input selective optogenetic LFS of excitatory neurons is sufficient to induce an NMDA receptor-dependent, mGlu receptor-independent synaptic LTD that is also independent of cholinergic drive *in vivo* and dependent on *de novo* protein translation. Moreover, mGlu5Rs were recruited to enhance electrically induced LTD, which was also dependent upon the GluN2B subunit as well as the ion channel function of NMDARs. Alzheimer's disease (AD) Aβ-facilitated LTD was lateralised, providing a potentially unique approach to further study Aβ-mediated synaptotoxic mechanisms.

Optogenetics has the potential to help dissect out the synaptic molecular mechanisms that underlie not only LTD, but LTP, and other types of neural plasticity in the brain. We believe our data ads to the growing body of work helping parse out the different levels of involvement of different synaptic transmembrane neurotransmitter binding proteins and the roles they play individually, and synergistically, in learning and memory. Presented here are novel findings that aid in the understanding of LTD and synaptic plasticity, processes that are believed to underlie information storage mechanisms in learning and memory. Ultimately, we believe this work forces us to rethink our understanding of the fundamental mechanisms of LTD *in vivo*.

VI. Suggestions for further work

Further work is required to fully exploit the potential of the optogenetic approach taken here to help parse out the contribution of synaptic membrane proteins in LTP and LTD. We provide strong evidence that currently used optogenetic protocols are suitable for *in vivo* neuroplasticity investigations; nevertheless, some of their limitations for the study of LTP may be addressed using opsins with faster kinetics, for example.

It would be interesting to see if alternative oLFS induction paradigms induced LTD at these synapses, such as paired-pulse LFS. One might hypothesise that optical PP-LFS may be mGluR-dependent providing us with an exceptional tool to help parse the different glutamate receptor functions in synaptic plasticity. Also, it will be necessary to investigate the possible asymmetry of GluN2B-dependent and independent forms of LTD at Schaffer collaterals at different developmental stages to fully evaluate our findings.

It would also be interesting to study commissurally expressed LTD in more detail to examine potential differences in response to pharmacological challenges, including examining if commissural LTD is NMDAR or mGluR dependent. Broadening the commissural story, it would be intriguing to probe any potential laterality to that form of LTD.

Given our discovery of the requirement for GluN2B containing NMDARs in Alzheimer's disease Aβ-enhanced eLFS-induced LTD, might targeting GluN2B prove to be an effective therapeutic strategy, maybe in combination with ACh-related therapy? Moreover, given this finding, might the asymmetrically biased, optically induced Alzheimer's disease Aβ-enhanced LTD be susceptible to GluN2B-NMDAR antagonism? It would also be interesting to examine if the Alzheimer's disease Aβ-enhanced oLFS LTD is mGlu5R-dependent and mAChR independent, as we previously reported for eLFS LTD (Hu et al., 2014). These studies will potentially openo to a new avenue for understanding circuit-level mechanisms and discover candidate therapeutics in Alzheimer's disease.

The present findings also emphasize the need for future studies to determine the extent of lateralisation of (a) glutamate receptor subtypes, in particular, GluN2B and mGlu5 receptors and (b) spine types, in particular, mushroom-type and thin spines at CA3-to-CA1 synapses in the rat hippocampus. Such knowledge will prove invaluable in the interpretation of both physiological and pathological lateralisation.

VII. References

Abraham, W.C. (2003). “How long will long-term potentiation last?” Philos. Trans. R. Soc. Lond. B Biol. Sci. 358, 735–744

Abraham, W.C., Christie B.R., Logan, B., Lawlor P., Dragunow, M. (1994). “Immediate early gene expression associated with the persistence of heterosynaptic long-term depression in the hippocampus.” Proc Natl Acad Sci USA 91:10049–10053.

Abraham, W.C. and Mason, S.E. (1988). “Effects of the NMDA receptor/channel antagonists CPP and MK801 on hippocampal field potentials and long-term potentiation in anesthetised rats.” Brain Res 462, 40-46.

Ahmed T., Sabanov V., D'Hooge R., Balschun D. (2011). “An N-methyl-D-aspartate-receptor dependent, late-phase long-term depression in middle-aged mice identifies no GluN2-subunit bias.” Neuroscience. Jun 30;185:27-38.

Alzheimer A. (1915). “Der Krieg und die Nerven. Breslau: Verlag von Preuf and Jünger”

Anand R., Gill K.D., Mahdi A.A. (2014). “Therapeutics of Alzheimer's disease: Past, present and future.” Neuropharmacology. Jan;76 Pt A:27-50.

Andersen P. (1960) “Interhippocampal impulses. II. Apical dendritic activation of CA1 neurons.” Acta Physiol Scand 48:178–208.

Anwyl, R. (1999). “Metabotropic glutamate receptors: electrophysiological properties and role in plasticity.” Brain Res. Brain Res. Rev. 29, 83–120.

Arnth-Jensen, N., Jabaudon, D. and Scanziani, M. (2002). “Cooperation between independent hippocampal synapses is controlled by glutamate uptake.” Nat Neurosci 5, 325-331.

Babiec W.E., Guglietta R., Jami S.A., Morishita W., Malenka R.C., O'Dell T.J. (2014). “Ionotropic NMDA receptor signalling is required for the induction of long-term depression in the mouse hippocampal CA1 region.” J Neurosci. Apr 9;34(15):5285-90.

Balschun D., Zuschratter W., Wetzel W. (2005). “Allosteric enhancement of metabotropic glutamate receptor 5 function promotes spatial memory.” Neuroscience. Oct 27;142(3):691-702.

Bartlett, T.E., Bannister N.J., Collett V.J., Dargan S.L., Massey P.V., Bortolotto Z.A., Fitzjohn S.M., Bashir Z.I., Collingridge G.L., Lodge D. (2007). “Differential roles of NR2A and NR2B-containing NMDA receptors in LTP and LTD in the CA1 region of two-week old rat hippocampus.” Neuropharmacology 52, 60-70.

Basu J., Zaremba J.D., Cheung S.K., Hitti F.L., Zemelman B.V., Losonczy A., Siegelbaum S.A. (2016). “Gating of hippocampal activity, plasticity, and memory by entorhinal cortex long-range inhibition.” Science. Jan 8;351(6269):aaa5694.

Bear M.F., Malenka R.C. (1994). “Synaptic plasticity: LTP and LTD.” Curr Opin Neurobiol. Jun;4(3):389-99.

Belzung C., Turiault M., Griebel G. (2014). “Optogenetics to study the circuits of fear- and depression-like behaviors: a critical analysis.” Pharmacol Biochem Behav. Jul;122:144-57.

Benarroch E.E. (2011). “NMDA receptors: recent insights and clinical correlations.” Neurology. May 17;76(20):1750-7.

Bir S.C., Ambekar S., Kukreja S., Nanda A. (2015). “Julius Caesar Arantius (Giulio Cesare Aranzi, 1530-1589) and the hippocampus of the human brain: history behind the discovery.” J Neurosurg. Apr;122(4):971-5.

Bittner K.C., Grienberger C., Vaidya S.P., Milstein A.D., Macklin J.J., Suh J., Tonegawa S., Magee J.C. (2015). “Conjunctive input processing drives feature selectivity in hippocampal CA1 neurons.” Nat Neurosci. Aug;18(8):1133-42.

Blennow K., deLeon M. J. and Zetterberg H. (2006). “Alzheimer’s disease.” Lancet 368, 387–403.

Bliss T.V., Collingridge G.L. (1993). “A synaptic model of memory: long-term potentiation in the hippocampus.” Nature 361, 31–39.

Bliss T.V., Lomo T. (1973). “Long-lasting potentiation of synaptic transmission in the dentate area of the anaesthetised rabbit following stimulation of the perforant path.” J Physiol. Jul;232(2):331-56.

Bolshakov V., Siegelbaum S. (1994). “Postsynaptic induction and presynaptic expression of hippocampal long-term depression.” Science 264:1148–1151.

Boyden E.S., Zhang F., Bamberg E., Nagel G., Deisseroth K. (2005). “Millisecond-timescale, genetically targeted optical control of neural activity.” Nat Neurosci; Sep;8(9):1263-8

Braak H., Braak E. (1991). “Neuropathological staging of Alzheimer related changes.” Acta Neuropathol (Berl) 82:239–259

Bredt, D.S., and Nicoll, R.A. (2003). “AMPA receptor trafficking at excitatory synapses.” Neuron 40, 361–379.

Broadbent N.J., Squire L.R., Clark R.E. (2004). “Spatial memory, recognition memory, and the hippocampus.” Proc Natl Acad Sci. Oct

5;101(40):14515-20.

Broussard J.I., Yang K., Levine A.T., Tsetsenis T., Jenson D., Cao F., Garcia I., Arenkiel B.R., Zhou F.M., De Biasi M., Dani J.A. (2016). “Dopamine Regulates Aversive Contextual Learning and Associated *In Vivo* Synaptic Plasticity in the Hippocampus.” Cell Rep. Mar 1;14(8):1930-9.

Buchanan K.A., Petrovic M.M., Chamberlain S.E., Marrion N.V., Mellor J.R. (2010). “Facilitation of long-term potentiation by muscarinic M(1) receptors is mediated by inhibition of SK channels.” Neuron. Dec 9;68(5):948-63.

Bukalo O., Pinard C.R., Silverstein S., Brehm C., Hartley N.D., Whittle N., Colacicco G., Busch E., Patel S., Singewald N., Holmes A. (2015). “Prefrontal inputs to the amygdala instruct fear extinction memory formation.” Sci Adv. Jul;1(6).

Busse, C.S., Brodkin J, Tattersall D, Anderson JJ, Warren N, Tehrani L, Bristow LJ, Varney MA, Cosford ND. (2004). “The behavioral profile of the potent and selective mGlu5 receptor antagonist 3-[(2-methyl-1,3-thiazol-4-yl)ethynyl]pyridine (MTEP) in rodent models of anxiety.” Neuropsychopharmacology 29, 1971-1979.

Cajal S.R. (1894). “The croonian lecture: La fine structure des centres nerveux.” Proceedings of the Royal Society of London 55:444–467.

Cajal S.R. (1911). “Histologie du Système Nerveux de l'Homme et des Vertébrés, Vols. 1 and 2.” A. Maloine. Paris.

Capron B., Sindic C., Godaux E., Ris L. (2006). “The characteristics of LTP induced in hippocampal slices are dependent on slice-recovery conditions.” Learn Mem. May-Jun;13(3):271-7.

Carroll R.C., Beattie E.C., von Zastrow M., Malenka R.C. (2001). “Role of AMPA receptor endocytosis in synaptic plasticity.” Nat Rev Neurosci 2: 315–324.

Caruana D.A., Warburton EC, Bashir ZI. (2011). “Induction of activity-dependent LTD requires muscarinic receptor activation in medial prefrontal cortex. J Neurosci. Dec 14;31(50):18464-78.

Cea-del Rio C.A., Lawrence J.J., Erdelyi F., Szabo G., McBain C.J. (2011). “Cholinergic modulation amplifies the intrinsic oscillatory properties of CA1 hippocampal cholecystokinin-positive interneurons.” J Physiol 589 (Part 3):609–627.

Cheung T.H., Cardinal R.N. (2005). “Hippocampal lesions facilitate instrumental learning with delayed reinforcement but induce impulsive choice in rats.” BMC Neurosci. May 13;6:36.

Chiang C.C., Ladas T.P., Gonzalez-Reyes L.E., Durand D.M. (2014). “Seizure suppression by high-frequency optogenetic stimulation using in

vitro and i*n vivo* animal models of epilepsy." Brain Stimul. Nov-Dec;7(6):890-9.

Cobb S.R, Davies C.H. (2005). "Cholinergic modulation of hippocampal cells and circuits." J Physiol 562 (Part 1):81–88.

Cohen S.J., Munchow, A.H., Rios L.M., Zhang, G., Ásgeirsdóttir H.N. and Stackman Jr. R.W. (2013). "The rodent hippocampus is essential for non-spatial object memory." Curr Biol. Sep 9; 23(17): 1685–1690.

Cole B.J., Klewer M., Jones G.H., Stephens D.N. (1993). "Contrasting effects of the competitive NMDA antagonist CPP and the non-competitive NMDA antagonist MK 801 on performance of an operant delayed matching to position task in rats." Psychopharmacology (Berl). 111(4):465-71.

Collingridge G.L., Isaac J.T., Wang Y.T. (2004). "Receptor trafficking and synaptic plasticity." Nat Rev Neurosci 5: 952–962.

Collingridge G.L., Peineau, S., Howland, J.G. and Wang, Y.T. (2010). "Long-term depression in the CNS." Nat Rev Neurosci 11, 459-473.

Conn P.J., Lindsley C.W., Jones C. (2008). "Activation of metabotropic glutamate receptors as a novel approach for the treatment of schizophrenia." Trends Pharmacol. Sci. 30:25–31

Connor S.A., Wang Y.T. (2016). “A Place at the Table: LTD as a Mediator of Memory Genesis.” Neuroscientist. Aug;22(4):359-71.

Convit A., De L.M., Tarshish C., De S.S., Tsui W., Rusinek H., George A. (1997). “Specific hippocampal volume reductions in individuals at risk for Alzheimer’s disease.” Neurobiol Aging 18:131–138.

Corkin S. (2002). “What's new with the amnesic patient H.M.?” Nat Rev Neurosci. Feb;3(2):153-60.

Cummings J.A., Mulkey R.M., Nicoll R.A., Malenka R.C. (1996). “Ca^{2+} signalling requirements for long-term depression in the hippocampus.” Neuron. 16:825–833.

Curtis D.R., Phillis J.W., Watkins J.C. (1960). “The chemical excitation of spinal neurones by certain acidic amino acids.” J. Physiol.150:656–682.

Curtis D.R., Phillis J.W., Watkins J.C. (1961). “Actions of amino acids on the isolated hemisected spinal cord of the toad.” Br. J. Pharmacol.16:262–283.

Curtis D.R., Watkins J.C. (1960). “The excitation and depression of spinal neurones by structurally related amino acids.” J. Neurochem.6:117–141.

Curtis D.R., Watkins J.C. (1965). “The pharmacology of amino acids related to gamma-aminobutyric acid.” Pharm. Rev.17:347–391.

Danielson N.B., Kaifosh P., Zaremba J.D., Lovett-Barron M., Tsai J., Denny C.A., Balough E.M., Goldberg A.R., Drew L.J., Hen R., Losonczy A., Kheirbek M.A. (2016). “Distinct Contribution of Adult-Born Hippocampal Granule Cells to Context Encoding.” Neuron. Apr 6;90(1):101-12.

Darnell, J.C. and Klann, E. (2013). “The translation of translational control by FMRP: therapeutic targets for FXS.” Nat Neurosci 16, 1530-1536.

Davies J., Francis A.A., Jones A.W., Watkins J.C. (1981). “2-Amino-5-phosphonovalerate (2APV), a potent and selective antagonist of amino acid-induced and synaptic excitation.” Neurosci Lett. 21:77–81.

Dayan P., Willshaw D.J. (1991). “Optimising synaptic learning rules in linear associative memories.” Biol Cybern. 65(4):253-65.

Deng W, Aimone JB, Gage FH. (2010). “New neurons and new memories: how does adult hippocampal neurogenesis affect learning and memory?” Nat Rev Neurosci. May;11(5):339-50

Dennis S.H., Pasqui F., Colvin E.M., Sanger H., Mogg A.J., Felder C.C., Broad L.M., Fitzjohn S.M., Isaac J.T., Mellor J.R. (2016). “Activation of Muscarinic M1 Acetylcholine Receptors Induces Long-Term Potentiation in the Hippocampus.” Cereb Cortex. Jan;26(1):414-26.

Doherty, A.J., Palmer, M.J., Henley, J.M., Collingridge, G.L. and Jane, D.E. (1997). “(RS)-2-chloro-5-hydroxyphenylglycine (CHPG) activates mGlu5, but not mGlu1, receptors expressed in CHO cells and potentiates NMDA responses in the hippocampus.” Neuropharmacology 36, 265-267.

Doralp S., Leung L.S. (2008). “Cholinergic modulation of hippocampal CA1 basal-dendritic long-term potentiation. ”Neurobiol Learn Mem. Sep;90(2):382-8.

Douglas R.M., Goddard G.V. (1975) “Long-term potentiation of the perforant path-granule cell synapse in the rat hippocampus.” Brain Res. Mar 21;86(2):205-15.

Doyère V., Errington M.L., Laroche S., Bliss T.V.P. (1996). “Low-frequency trains of paired stimuli induce long-term depression in area CA1 but not in dentate gyrus of the intact rat.” Hippocampus 6:52–57.

Doyle, C., Holscher, C., Rowan, M.J. and Anwyl, R. (1996). “The selective neuronal NO synthase inhibitor 7-nitro-indazole blocks both long-term potentiation and depotentiation of field EPSPs in rat hippocampal CA1 *in vivo*.” J Neurosci 16, 418-424.

Duan A.R., Varela C., Zhang Y., Shen Y., Xiong L., Wilson M.A., Lisman J. (2015). “Delta frequency optogenetic stimulation of the thalamic nucleus reuniens is sufficient to produce working memory deficits:

relevance to schizophrenia.” Biol Psychiatry. Jun 15;77(12):1098-107.

Dudek S.M., Bear M.F. (1992). “Homosynaptic long-term depression in area CA1 of hippocampus and effects of N-methyl-D-aspartate receptor blockade.” Proc Natl Acad Sci. May 15;89(10):4363-7.

Dunwiddie T., Lynch G. (1978). “Long-term potentiation and depression of synaptic responses in the rat hippocampus: localization and frequency dependency.” J Physiol (Lond) 276:353–367.

Dutar P., Bassant M.H., Senut M.C., Lamour Y. (1995). “The septohippocampal pathway: Structure and function of a central cholinergic system.” Physiol Rev 75:393–427.

Elias G.M., Nicoll R.A. (2007). “Synaptic trafficking of glutamate receptors by MAGUK scaffolding proteins.” Trends Cell Biol. Jul;17(7):343-52.

Enoch M.A., Rosser A.A., Zhou Z., Mash D.C., Yuan Q., Goldman D. (2014). “Expression of glutamatergic genes in healthy humans across 16 brain regions; altered expression in the hippocampus after chronic exposure to alcohol or cocaine.” Genes Brain Behav. Nov;13(8):758-68.

Erreger K., Dravid S.M., Banke T.G., Wyllie D.J., Traynelis S.F. (2005). “Subunit-specific gating controls rat NR1/NR2A and NR1/NR2B NMDA channel kinetics and synaptic signalling profiles.” J. Phys. 563, 345–358.

Errington M.L., Bliss T.V., Richter-Levin G., Yenk K., Doyère V., Laroche S. (1995) “Stimulation at 1-5 Hz does not produce long-term depression or depotentiation in the hippocampus of the adult rat *in vivo*. J Neurophysiol. Oct;74(4):1793-9.

Felix-Ortiz A.C., Tye K.M. (2014). “Amygdala inputs to the ventral hippocampus bidirectionally modulate social behavior.” J Neurosci. Jan 8;34(2):586-95.

Fernandes, A., Wojcik T., Baireddy P., Pieschl R., Newton A., Tian Y., Hong Y., Bristow L., Li Y.W. (2015). “Inhibition of *in vivo* [(3)H]MK-801 binding by NMDA receptor open channel blockers and GluN2B antagonists in rats and mice.” Eur J Pharmacol 766, 1-8.

Fernandez de Sevilla D., Nunez A., Borde M., Malinow R., Buno W. (2008). “Cholinergic-mediated IP3-receptor activation induces long-lasting synaptic enhancement in CA1 pyramidal neurons.” J Neurosci 28:1469–1478.

Fioravante D. and Regehr W.G. (2011). “Short-term forms of presynaptic plasticity.” Curr Opin Neurobiol. Apr; 21(2): 269–274.

Fischer G., Mutel V., Trube G., Malherbe P., Kew J.N., Mohacsi E., Heitz M.P., Kemp J.A. (1997). “Ro 25-6981, a highly potent and selective blocker of N-methyl-D-aspartate receptors containing the NR2B subunit. Characterization in vitro.” J Pharmacol Exp Ther. Dec;283(3):1285-92.

Fisher A. (2008). “Cholinergic treatments with emphasis on m1 muscarinic agonists as potential disease-modifying agents for Alzheimer’s disease.” Neurotherapeutics 5, 433–442.

Fonnum F. (1984). “Glutamate: a neurotransmitter in mammalian brain.” J Neurochem. Jan;42(1):1-11.

Fox C.J., Russell K.I., Wang Y.T., Christie B.R. (2006). “Contribution of NR2A and NR2B NMDA subunits to bidirectional synaptic plasticity in the hippocampus *in vivo*.” Hippocampus. 16(11):907-15.

Frank R.A., Komiyama N.H., Ryan T.J., Zhu F., O'Dell T.J., Grant S.G. (2016). “NMDA receptors are selectively partitioned into complexes and supercomplexes during synapse maturation.” Nat Comm. Apr 27;7:11264

Fukudome Y., Ohno-Shosaku T., Matsui M., Omori Y., Fukaya M., Tsubokawa H., Taketo M.M., Watanabe M., Manabe T., Kano M. (2004). “Two distinct classes of muscarinic action on hippocampal inhibitory synapses: M2-mediated direct suppression and M1/M3-mediated indirect suppression through endocannabinoid signalling.” Eur J Neurosci 19:2682–2692.

Ganguly K., Poo M.M. (2013). “Activity-dependent neural plasticity from bench to bedside.” Neuron. Oct 30;80(3):729-41.

Ge Y., Dong Z., Bagot R.C., Howland J.G., Phillips A.G., Wong T.P., Wang Y.T. (2010) “Hippocampal long-term depression is required for the consolidation of spatial memory.” Proc Natl Acad Sci. Sep 21;107(38):16697-702.

Granger A.J., Nicoll R.A. (2014). “LTD expression is independent of glutamate receptor subtype.” Front Synaptic Neurosci. Jul 8;6:15.

Granger A.J., Shi Y., Lu W., Cerpas M., Nicoll R.A. (2013). “LTP requires a reserve pool of glutamate receptors independent of subunit type.” Nature. Jan 24;493(7433):495-500

Graves A.R., Moore S.J., Bloss E.B., Mensh B.D., Kath W.L., Spruston N. (2012). “Hippocampal Pyramidal Neurons Comprise Two Distinct Cell Types that Are Countermodulated by Metabotropic Receptors.” Neuron. Nov 21;76(4):776-89.

Gil-Sanz C., Delgado-García J.M., Fairén A., Gruart A. (2008). “Involvement of the mGluR1 receptor in hippocampal synaptic plasticity and associative learning in behaving mice.” Cereb Cortex. Jul;18(7):1653-63.

Gray J.A., Shi Y., Usui H., During M.J., Sakimura K., Nicoll R.A. (2011). “Distinct modes of AMPA receptor suppression at developing synapses by GluN2A and GluN2B: single-cell NMDA receptor subunit deletion *in vivo*.” Neuron 71, 1085–1101.

Gray, J.A., Zito, K. and Hell, J.W. (2016). “Non-ionotropic signalling by the NMDA receptor: controversy and opportunity.” F1000Res 5.

Haass C., Selkoe D.J. (2007). “Soluble protein oligomers in neurodegeneration: Lessons from the Alzheimer's amyloid beta-peptide.” Nat Rev Mol Cell Biol. 8:101–112.

Hansen, K.B., Ogden, K.K., Yuan, H. and Traynelis, S.F. (2014). “Distinct functional and pharmacological properties of triheteromeric GluN1/GluN2A/GluN2B NMDA receptors.” Neuron 81, 1084-1096.

Harris, A.Z. and Pettit, D.L. (2007). “Extrasynaptic and synaptic NMDA receptors form stable and uniform pools in rat hippocampal slices.” J Physiol 584, 509-519.

He Y., Kulasiri D., Samarasinghe S. (2014). “Systems biology of synaptic plasticity: a review on N-methyl-D-aspartate receptor mediated biochemical pathways and related mathematical models.” Biosystems. Aug;122:7-18.

Henley J.M. and Wilkinson K.A. (2013). “AMPA receptor trafficking and the mechanisms underlying synaptic plasticity and cognitive aging.” Dialogues Clin Neurosci. Mar; 15(1): 11–27.

Ho O.H., Delgado J.Y., O'Dell T.J. (2004). “Phosphorylation of proteins involved in activity-dependent forms of synaptic plasticity is altered

in hippocampal slices maintained in vitro." J Neurochem. Dec;91(6):1344-57.

Holbro, N., Grunditz, A., and Oertner, T.G. (2009). "Differential distribution of endoplasmic reticulum controls metabotropic signalling and plasticity at hippocampal synapses." Proc. Natl. Acad. Sci. 106, 15055–15060.

Hsia A.Y., Masliah E., McConlogue L., Yu G.Q., Tatsuno G., Hu K., Kholodenko D., Malenka R.C., Nicoll R.A., Mucke L. (1999). "Plaque-independent disruption of neural circuits in Alzheimer's disease mouse models." Proc Natl Acad Sci. Mar 16;96(6):3228-33.

Hu, N.W., Klyubin, I., Anwyl, R. and Rowan, M.J. (2009). "GluN2B subunit-containing NMDA receptor antagonists prevent Abeta-mediated synaptic plasticity disruption *in vivo.*" Proc Natl Acad Sci. 106, 20504-20509.

Hu N.W., Nicoll A.J., Zhang D., Mably A.J., O'Malley T., Purro S.A., Terry C., Collinge J., Walsh D.M., Rowan M.J. (2014). "mGlu5 receptors and cellular prion protein mediate amyloid-β-facilitated synaptic long-term depression *in vivo.*" Nature Communications. Mar 4;5:3374

Hu, N.W., Smith, I.M., Walsh, D.M. and Rowan, M.J. (2008). "Soluble amyloid-beta peptides potently disrupt hippocampal synaptic plasticity in the absence of cerebrovascular dysfunction *in vivo.*" Brain 131, 2414-24.

Huang, C.C., Liang, Y.C., Hsu, K.S. (2001). “Characterization of the mechanism underlying the reversal of long-term potentiation by low frequency stimulation at hippocampal CA1 synapses.” J Biol Chem 276, 48108-48117.

Huber, K.M., Kayser, M.S., and Bear, M.F. (2000). “Role for rapid dendritic protein synthesis in hippocampal mGluR-dependent long-term depression.” Science 288, 1254–1257.

Huber K.M., Roder J.C., Bear M.F. (2001) “Chemical induction of mGluR5- and protein synthesis--dependent long-term depression in hippocampal area CA1.” J Neurophysiol. Jul;86(1):321-5.

Huerta P.T., Lisman J.E. (1993). “Heightened synaptic plasticity of hippocampal CA1 neurons during a cholinergically induced rhythmic state.” Nature 364:723–725.

Hayashi, T. (1952). “A physiological study of epileptic seizures following cortical stimulation in animals and its application to human clinics.” Jpn. J. Physiol. 3:46-64.

Hayashi T. (1954). “Effects of sodium glutamate on the nervous system.” Keio J. Med. 3:192–193.

Homma A., Atarashi H., Kubota N., Nakai K., Takase T. (2016). “Efficacy and Safety of Sustained Release Donepezil High Dose versus Immediate

Release Donepezil Standard Dose in Japanese Patients with Severe Alzheimer's Disease: A Randomized, Double-Blind Trial.” J Alzheimer’s Dis. Mar 11;52(1):345-57.

Hynd M.R., Scott H.L., Dodd P.R. (2004). “Glutamate-mediated excitotoxicity and neurodegeneration in Alzheimer's disease.” Neurochem Int 45:583–595.

Iacobucci G.J. and Popescu G.K. (2017). “NMDA receptors: linking physiological output to biophysical operation.” Nat Rev Neurosci. Mar 17;18(4):236-249.

Iglói K., Doeller C.F., Berthoz A., Rondi-Reig L., Burgess N. (2010). “Lateralized human hippocampal activity predicts navigation based on sequence or place memory.” Proc Natl Acad Sci 107(32):14466–14471

Ivanova E., Pan Z.H. (2009). “Evaluation of the adeno-associated virus mediated long-term expression of channelrhodopsin-2 in the mouse retina.” Mol Vis. Aug 21;15:1680-9.

Jack C.R., Petersen R.C., Xu Y., O’Brien P.C., Smith G.E., Ivnik R.J., Tangalos E.G., Kokmen E. (1998). “Rate of medial temporal lobe atrophy in typical aging and Alzheimer’s disease.” Neurology 51:993–999.

Jackman S.L., Beneduce B.M., Drew I.R., Regehr W.G. (2014). “Achieving high-frequency optical control of synaptic transmission.” J

Neurosci. May 28;34(22):7704-14.

Jackman S.L., Turecek J., Belinsky J.E., Regehr W.G. (2016). “The calcium sensor synaptotagmin 7 is required for synaptic facilitation.” Nature. Jan 7;529(7584):88-91.

Jacquemont S., Curie A., des Portes V., Torrioli M.G., Berry-Kravis E., Hagerman R.J., Ramos F.J., Cornish K., He Y., Paulding C., Neri G., Chen F., Hadjikhani N., Martinet D., Meyer J., Beckmann J.S., Delange K., Brun A., Bussy G., Gasparini F., Hilse T., Floesser A., Branson J., Bilbe G., Johns D., Gomez-Mancilla B. (2011). “Epigenetic modification of the FMR1 gene in fragile X syndrome is associated with differential response to the mGluR5 antagonist AFQ056.” Sci Transl Med. Jan 5;3(64):64ra1

Jessen F., Feyen L., Freymann K., Tepest R., Maier W., Heun R., Schild H.H., Scheef L. (2006). “Volume reduction of the entorhinal cortex in subjective memory impairment.” Neurobiol Aging 27:1751–1756.

Jiang S., Li Y., Zhang C., Zhao Y., Bu G., Xu H., Zhang Y.W. (2014). “M1 muscarinic acetylcholine receptor in Alzheimer's disease.” Neurosci Bull. Apr;30(2):295-307

Jiménez-Sánchez L., Campa L., Auberson Y.P., Adell A. (2014). “The role of GluN2A and GluN2B subunits on the effects of NMDA receptor antagonists in modelling schizophrenia and treating refractory

depression.” Neuropsychopharmacology. Oct;39(11):2673-80.

Jonas P. and Lisman J. (2015). “Structure, function, and plasticity of hippocampal dentate gyrus microcircuits”. Frontiers Media SA.

Kandel E.R. (2001). “The molecular biology of memory storage: a dialogue between genes and synapses.” Science 294 1030–1038 10.1126/science.1067020

Kandel E.R., Dudai Y., Mayford M.R. (2014). “The molecular and systems biology of memory.” Cell 157:163–186.

Kapai N.A., Solntseva E.I., Skrebitskii V.G. (2010). “Donepezil eliminates suppressive effects of β-amyloid peptide (1-42) on long-term potentiation in the hippocampus.” Bull Exp Biol Med. Jul;149(1):33-6.

Kauderer B.S., Kandel ER. (2000). “Capture of a protein synthesis-dependent component of long-term depression.” Proc Natl Acad Sci. Nov 21;97(24):13342-7.

Kawahara A., Kurauchi S., Fukata Y., Martínez-Hernández J., Yagihashi T., Itadani Y., Sho R., Kajiyama T., Shinzato N., Narusuye K., Fukata M., Luján R., Shigemoto R., Ito I. (2013). “Neuronal major histocompatibility complex class I molecules are implicated in the generation of asymmetries in hippocampal circuitry.” J Physiol. Oct 1;591(19):4777-91

Kawakami R., Shinohara Y., Kato Y., Sugiyama H., Shigemoto R., Ito I. (2003). “Asymmetrical allocation of NMDA receptor epsilon2 subunits in hippocampal circuitry.” Science. May 9;300(5621):990-4.

Kemp A., and Manahan-Vaughan D. (2004). “Hippocampal long-term depression and long-term potentiation encode different aspects of novelty acquisition.’ Proc Natl Acad Sci. May 25;101(21):8192-7.

Kemp N., McQueen J., Faulkes S., Bashir Z.I. (2000). “Different forms of LTD in the CA1 region of the hippocampus: role of age and stimulus protocol.” Eur J Neurosci 12:360–366.

Kennedy M.J., Ehlers M.D. (2011). “Mechanisms and function of dendritic exocytosis.” Neuron 69: 856–875.

Kessels H.W., Nabavi S, Malinow R. (2013). “Metabotropic NMDA receptor function is required for β-amyloid-induced synaptic depression.” Proc Natl Acad Sci. Mar 5;110(10):4033-8.

Kim S.H., Kandiah N., Hsu J.L., Suthisisang C., Udommongkol C., Dash A. (2017). “Beyond symptomatic effects: Donepezil's potential for neuroprotection and disease modification in Alzheimer's disease.” Br J Pharmacol. Sep 13.

Kohl M.M., Shipton O.A., Deacon R.M., Rawlins J.N., Deisseroth K., Paulsen O. (2011). “Hemisphere-specific optogenetic stimulation reveals

left-right asymmetry of hippocampal plasticity." Nat Neurosci. Sep 25;14(11):1413-5

Kollen, M., Dutar, P. and Jouvenceau, A. (2008). "The magnitude of hippocampal long-term depression depends on the synaptic location of activated NR2-containing N-methyl-D-aspartate receptors." Neuroscience 154, 1308-1317.

Kotecha, S.A., Jackson M.F., Al-Mahrouki A., Roder J.C., Orser B.A., MacDonald J.F. (2003). "Co-stimulation of mGluR5 and N-methyl-D-aspartate receptors is required for potentiation of excitatory synaptic transmission in hippocampal neurons." J Biol Chem 278, 27742-27749.

Kroker K.S., Moreth J., Kussmaul L., Rast G., Rosenbrock H. (2013). "Restoring long-term potentiation impaired by amyloid-beta oligomers: comparison of an acetylcholinesterase inhibitior and selective neuronal nicotinic receptor agonists." Brain Res Bull. Jul;96:28-38.

Kropff E., Carmichael J.E., Moser M.B., Moser E.I. (2015). "Speed cells in the medial entorhinal cortex." Nature. Jul 23;523(7561):419-24.

Kryger G., Silman I., Sussman J.L. (1999). "Structure of acetylcholinesterase complexed with E2020 (Aricept): implications for the design of new anti-Alzheimer drugs." Structure. Mar 15;7(3):297-307.

Ku, H.Y., Huang, Y.F., Chao, P.H., Huang, C.C. and Hsu, K.S. (2008). “Neonatal isolation delays the developmental decline of long-term depression in the CA1 region of rat hippocampus.” Neuropsychopharmacology 33, 2847-2859.

Kumar A., Singh A., Ekavali. (2015). “A review on Alzheimer's disease pathophysiology and its management: an update.” Pharmacol Rep. Apr;67(2):195-203.

Kuwajima M., Hall R.A., Aiba A., Smith Y. (2004). “Subcellular and subsynaptic localization of group I metabotropic glutamate receptors in the monkey subthalamic nucleus.” J Comp Neurol. Jul 5;474(4):589-602.

Kwon O.B., Lee J.H., Kim H.J., Lee S., Lee S., Jeong M.J., Kim S.J., Jo H.J., Ko B., Chang S., Park S.K., Choi Y.B., Bailey C.H., Kandel E.R., Kim J.H. (2015). “Dopamine Regulation of Amygdala Inhibitory Circuits for Expression of Learned Fear.” Neuron. Oct 21;88(2):378-89.

Ladas T.P., Chiang C.C., Gonzalez-Reyes L.E., Nowak T., Durand D.M. (2015). “Seizure reduction through interneuron-mediated entrainment using low frequency optical stimulation.” Exp Neurol. Jul;269:120-32.

Lamprecht R., LeDoux J. (2004). “Structural plasticity and memory.” Nat Rev Neurosci. Jan;5(1):45-54.

Latif-Hernandez A., Faldini E., Ahmed T., Balschun D. (2016). “Separate Ionotropic and Metabotropic Glutamate Receptor Functions in Depotentiation vs. LTP: A Distinct Role for Group1 mGluR Subtypes and NMDARs.” Front Cell Neurosci. Nov 7;10:252.

LeDoux, J.E. (2012). “Evolution of human emotion: a view through fear.” Prog. Brain Res. 195, 431–442.

Lee H.K., Barbarosie M., Kameyama K., Bear M.F., Huganir R.L. (2000). “Regulation of distinct AMPA receptor regulation sites during bidirectional synaptic plasticity.” Nature 405: 955–959

Leung L.S., Shen B., Rajakumar N., Ma J. (2003). “Cholinergic activity enhances hippocampal long-term potentiation in CA1 during walking in rats.” J Neurosci. Oct 15;23(28):9297-304.

Li N., Lee B., Liu R.J., Banasr M., Dwyer J.M., Iwata M., Li X.Y., Aghajanian G., Duman R.S. (2010). “mTOR-dependent synapse formation underlies the rapid antidepressant effects of NMDA antagonists.” Science 329: 959–964.

Li S., Hong S., Shepardson N.E., Walsh D.M., Shankar G.M., Selkoe D. (2009). “Soluble oligomers of amyloid Beta protein facilitate hippocampal long-term depression by disrupting neuronal glutamate uptake.” Neuron. Jun 25;62(6):788-801.

Li, S.T., Kato K., Tomizawa K., Matsushita M., Moriwaki A., Matsui H., Mikoshiba K. (2002). “Calcineurin plays different roles in group II metabotropic glutamate receptor- and NMDA receptor-dependent long-term depression.” J Neurosci 22, 5034-5041.

Lin, J.Y. (2011). “A User’s Guide to Channelrhodopsin Variants: Features, Limitations and Future Developments.” Exp Physiol. Jan; 96(1): 19–25.

Lin, J.Y., Yang, J., Tsien, R.Y. (2009). “Development and characterization of channelrhodopsin variants for improved optical control of neuronal excitability.” Society for Neuroscience. Chicago

Lisman J. (1989). “A mechanism for the Hebb and the anti-Hebb processes underlying learning and memory.” Proc Natl Acad Sci. Dec;86(23):9574-8.

Liu X., Ramirez S., Pang P.T., Puryear C.B., Govindarajan A., Deisseroth K., Tonegawa S. (2012). “Optogenetic stimulation of a hippocampal engram activates fear memory recall.” Nature. Mar 22;484(7394):381-5.

Liu X., Ramirez S., Redondo R.L., Tonegawa S. (2014). “Identification and Manipulation of Memory Engram Cells.” Cold Spring Harb Symp Quant Biol. 79:59-65.

Long X., Zhang L., Liao W., Jiang C., Qiu B. (2011). “Distinct laterality alterations distinguish mild cognitive impairment and Alzheimer's disease from healthy aging: statistical parametric mapping with high resolution MRI.” Hum Brain Mapp. Dec;34(12):3400-10.

Loonen A.J., Ivanova S.A. (2015). “Circuits regulating pleasure and happiness: the evolution of reward-seeking and misery-fleeing behavioral mechanisms in vertebrates.” Front Neurosci. Oct 23;9:394.

Lórenz-Fonfría V.A., Heberle J. (2014). “Channelrhodopsin unchained: structure and mechanism of a light-gated cation channel.” Biochim Biophys Acta. May;1837(5):626-42.

Lu W., Roche K.W. (2012). “Posttranslational regulation of AMPA receptor trafficking and function.” Curr Opin Neurobiol. Jun;22(3):470-9

Lu W., Shi Y., Jackson A.C., Bjorgan K., During M.J., Sprengel R., Seeburg P.H., Nicoll R.A. (2009). “Subunit composition of synaptic AMPA receptors revealed by a single-cell genetic approach.” Neuron. Apr 30;62(2):254-68

Luchkina N.V., Huupponen J., Clarke V.R., Coleman S.K., Keinänen K., Taira T., Lauri S.E. (2014). “Developmental switch in the kinase dependency of long-term potentiation depends on expression of GluA4 subunit-containing AMPA receptors.” Proc Natl Acad Sci. Mar 18;111(11):4321-6.

Lujan, R., Roberts, J.D., Shigemoto, R., Ohishi, H. Somogyi, P. (1997). “Differential plasma membrane distribution of metabotropic glutamate receptors mGluR1 alpha, mGluR2 and mGluR5, relative to neurotransmitter release sites.” J Chem Neuroanat 13, 219-241.

Lüscher C., Huber K.M. (2010). “Group 1 mGluR-dependent synaptic long-term depression: mechanisms and implications for circuitry and disease.” Neuron 65:445– 459.

Lüscher C., Malenka R.C. (2012). “NMDA receptor-dependent long-term potentiation and long-term depression (LTP/LTD).” Cold Spring Harb Perspect Biol. Jun 1;4(6).

Lüscher C., Xia H., Beattie E.C., Carroll R.C., von Zastrow M., Malenka R.C., Nicoll R.A. (1999). “Role of AMPA receptor cycling in synaptic transmission and plasticity.” Neuron 24: 649–658.

Madeira C., Lourenco M.V., Vargas-Lopes C., Suemoto C.K., Brandão C.O., Reis T., Leite R.E., Laks J., Jacob-Filho W., Pasqualucci C.A., Grinberg L.T., Ferreira S.T., Panizzutti R. (2015). “d-serine levels in Alzheimer's disease: implications for novel biomarker development.” Transl Psychiatry. May 5;5:e561.

Malenka, R.C. and Nicoll, R.A., (1999). “Long-term potentiation - a decade of progress?” Science 285, 1870–1874.

Malinow, R., and Malenka, R.C. (2002). “AMPA receptor trafficking and synaptic plasticity.” Annu. Rev. Neurosci. 25, 103–126.

Mamad O., McNamara H.M., Reilly R.B., Tsanov M. (2015). “Medial septum regulates the hippocampal spatial representation.” Front Behav Neurosci. Jun 30;9:166.

Manahan-Vaughan, D. (1997). “Group 1 and 2 metabotropic glutamate receptors play differential roles in hippocampal long-term depression and long-term potentiation in freely moving rats.” J Neurosci 17, 3303-3311.

Manahan-Vaughan D., Kulla A., Frey J.U. (2000). “Requirement of translation but not transcription for the maintenance of long-term depression in the CA1 region of freely moving rats.” J Neurosci. Nov 15;20(22):8572-6.

Mannaioni, G., Marino, M.J., Valenti, O., Traynelis, S.F. and Conn, P.J. (2001). “Metabotropic glutamate receptors 1 and 5 differentially regulate CA1 pyramidal cell function.” J Neurosci 21, 5925-5934.

Mansour, M., Nagarajan, N., Nehring, R.B., Clements, J.D., and Rosenmund, C. (2001). “Heteromeric AMPA receptors assemble with a preferred subunit stoichiometry and spatial arrangement.” Neuron 32, 841–853.

Mårtensson F. (2007). “Lateralization of language functions in the human brain.” Neurolinguistics.

Martin S.J., Grimwood PD, Morris RG. (2000). “Synaptic plasticity and memory: an evaluation of the hypothesis.” Annu Rev Neurosci. 23:649-711.

Matsuo, N., Reijmers, L., and Mayford, M. (2008). “Spine-type-specific recruitment of newly synthesised AMPA receptors with learning.” Science 319, 1104–1107.

Mayford M., Siegelbaum S.A. and Kandel E.R. (2012). “Synapses and Memory Storage.” Cold Spring Harb Perspect Biol. Jun; 4(6): a005751.

McGaugh J.L. (2000). “Memory–a century of consolidation.” Science 287: 248–251

McLean C.A., Cherny R.A., Fraser F.W., Fuller S.J., Smith M.J., Beyreuther K., Bush A.I., Masters C.L. (1999). “Soluble pool of Abeta amyloid as a determinant of severity of neurodegeneration in Alzheimer's disease.” Ann Neurol. Dec;46(6):860-6.

Medvedev N.I., Popov V.I., Rodriguez Arellano J.J., Dallérac G., Davies H.A., Gabbott P.L., Laroche S., Kraev I.V., Doyère V., Stewart M.G. (2010). “The N-methyl-D-aspartate receptor antagonist CPP alters synapse and spine structure and impairs long-term potentiation and long-

term depression induced morphological plasticity in dentate gyrus of the awake rat." Neuroscience. Feb 17;165(4):1170-81.

Milner B., Taylor L., Sperry R.W. (1968). "Lateralised suppression of dichotically presented digits after commissural section in man." Science. Jul 12;161(3837):184-6.

Moossy J., Zubenko G.S., Martinez A.J., Rao G.R., Kopp U., Hanin I. (1989). "Lateralization of brain morphologic and cholinergic abnormalities in Alzheimer's disease." Arch Neurol. Jun;46(6):639-42.

Motley S.E., Kirwan C.B. (2012). "A parametric investigation of pattern separation processes in the medial temporal lobe." J Neurosci. Sep 19;32(38):13076-85.

Moult, P.R., Gladding, C.M., Sanderson, T.M., Fitzjohn, S.M., Bashir, Z.I., Molnar, E., and Collingridge, G.L. (2006). "Tyrosine phosphatases regulate AMPA receptor trafficking during metabotropic glutamate receptor-mediated long-term depression." J. Neurosci. 26, 2544–2554.

Mucke L., Masliah E., Yu G.Q., Mallory M., Rockenstein E.M., Tatsuno G., Hu K., Kholodenko D., Johnson-Wood K., McConlogue L. (2000). "High-level neuronal expression of abeta 1-42 in wild-type human amyloid protein precursor transgenic mice: synaptotoxicity without plaque formation." J Neurosci. Jun 1;20(11):4050-8.

Mugunthan N, Shanmugasamy K, Anbalagan J, Rajanarayanan S, Meenachi S. (2016). “Effects of Long-term Exposure of 900-1800 MHz Radiation Emitted from 2G Mobile Phone on Mice Hippocampus- A Histomorphometric Study.” J Clin Diagn Res. Aug;10(8):AF01-6.

Mulkey R.M., Malenka R.C. (1992). “Mechanisms underlying induction of homosynaptic long-term depression in area CA1 of the hippocampus.” Neuron. Nov;9(5):967-75.

Mutha P.K., Haaland K.Y., Sainburg R.L. (2012). “The effects of brain lateralization on motor control and adaptation.” J Mot Behav. 44(6):455-69.

Nabavi S., Fox R., Proulx C.D., Lin J.Y., Tsien R.Y., Malinow R. (2014). “Engineering a memory with LTD and LTP.” Nature. Jul 17;511(7509):348-52.

Nabavi, S., Kessels H.W., Alfonso S., Aow J., Fox R., Malinow R. (2013). “Metabotropic NMDA receptor function is required for NMDA receptor-dependent long-term depression.” Proc Natl Acad Sci.110, 4027-4032.

Nagel G., Szellas T., Huhn W., Kateriya S., Adeishvili N., Berthold P., Ollig D., Hegemann P., Bamberg E. (2003). “Channelrhodopsin-2, a directly light-gated cation-selective membrane channel.” Proc Natl Acad Sci. 100:13940–13945.

Nestor P.J., Scheltens P., Hodges J.R. (2004). “Advances in the early detection of Alzheimer’s disease.” Nat Med 10 (Suppl) :S34–S41.

Nicoll R.A., Oliet S.H., Malenka R.C. (1998). “NMDA receptor-dependent and metabotropic glutamate receptor-dependent forms of long-term depression coexist in CA1 hippocampal pyramidal cells. Neurobiol Learn Mem. Jul-Sep;70(1-2):62-72.

Nicoll A.J., Panico S., Freir D.B., Wright D., Terry C., Risse E., Herron C.E., O'Malley T., Wadsworth J.D., Farrow M.A., Walsh D.M., Saibil H.R., Collinge J. (2013). “Amyloid-β nanotubes are associated with prion protein dependent synaptotoxicity.” Nat Commun. 24:2416.

Niswender, C.M., Conn, P.J., (2010). “Metabotropic glutamate receptors: physiology, pharmacology and disease.” Annual Review of Pharmacology and Toxicology. 50,295–322.

Nowak L, Bregestovski P, Ascher P, Herbet A, Prochiantz A. (1984). “Magnesium gates glutamate-activated channels in mouse central neurones.” Nature.; 307(5950): 462–5.

Oliet S.H.R., Malenka R.C., Nicoll R.A. (1997). “Two distinct forms of long-term depression co-exist in CA1 hippocampal pyramidal cells.” Neuron 18:969–982.

O'Riordan K. J., Gerstein H., Hullinger R., Burger C. (2014). “The role of Homer1c in metabotropic glutamate receptor-dependent long-term potentiation.” Hippocampus. Jan;24(1):1-6.

Palmer M.J., Irving A.J., Seabrook G.R., Jane D.E., Collingridge G.L. (1997). “The group I mGlu receptor agonist DHPG induces a novel form of LTD in the CA1 region of the hippocampus.” Neuropharmacology 36:1517–532.

Park P., Volianskis A., Sanderson T.M., Bortolotto Z.A., Jane D.E., Zhuo M., Kaang B.K., Collingridge G.L. (2013). “NMDA receptor-dependent long-term potentiation comprises a family of temporally overlapping forms of synaptic plasticity that are induced by different patterns of stimulation.” Philos Trans R Soc Lond B Biol Sci. Dec 2;369(1633):20130131.

Pelkey K.A., Barksdale E., Craig M.T., Yuan X., Sukumaran M., Vargish G.A., Mitchell R.M., Wyeth M.S., Petralia R.S., Chittajallu R., Karlsson R.M., Cameron H.A., Murata Y., Colonnese M.T., Worley P.F., McBain C.J. (2015). “Pentraxins coordinate excitatory synapse maturation and circuit integration of parvalbumin interneurons.” Neuron. Mar 18;85(6):1257-72.

Penfield W., Milner B. (1958). “Memory deficit produced by bilateral lesions in the hippocampal zone.” AMA Arch Neurol Psychiatry. May;79(5):475-97.

Pennanen C., Kivipelto M., Tuomainen S., Hartikainen P., Hanninen T., Laakso M.P., Hallikainen M., Vanhanen M., Nissinen A., Helkala E.L., Vainio P., Vanninen R., Partanen K., Soininen H. (2004). “Hippocampal and entorhinal cortex in mild cognitive impairment and early AD.” Neurobiol Aging 25:303–310.

Petralia R.S. (2012). “Distribution of extrasynaptic NMDA receptors on neurons.” Scientific World Journal. 267120

Pitler T.A., Alger B.E. (1992). “Cholinergic excitation of GABAergic interneurons in the rat hippocampal slice.” J Physiol 450:127–142.

Porter R.H., Jaeschke G., Spooren W., Ballard T.M., Büttelmann B., Kolczewski S., Peters J.U., Prinssen E., Wichmann J., Vieira E., Mühlemann A., Gatti S., Mutel V., Malherbe P. (2005). “Fenobam: a clinically validated nonbenzodiazepine anxiolytic is a potent, selective, and noncompetitive mGlu5 receptor antagonist with inverse agonist activity.” J Pharmacol Exp Ther. Nov;315(2):711-21

Pöschel B, Manahan-Vaughan D. (2007). “Persistent (>24h) long-term depression in the dentate gyrus of freely moving rats is not dependent on activation of NMDA receptors, L-type voltage-gated calcium channels or protein synthesis.” Neuropharmacology. Jan;52(1):46-54.

Ramirez S., Liu X., Lin P.A., Suh J., Pignatelli M., Redondo R.L., Ryan T.J., Tonegawa S. (2013). “Creating a false memory in the

hippocampus.” Science. Jul 26;341(6144):387-91.

Raymond C. R., Thompson V., Tate W. P. and Abraham W. C. (2000). “Metabotropic glutamate receptors trigger homo- synaptic protein synthesis to prolong LTP.” J. Neurosci. 20, 969–976.

Redondo R.L., Kim J., Arons A.L., Ramirez S., Liu X., Tonegawa S. (2014). “Bidirectional switch of the valence associated with a hippocampal contextual memory engram.” Nature. Sep 18;513(7518):426-30.

Reis H.J., Guatimosim C, Paquet M, Santos M, Ribeiro FM, Kummer A, Schenatto G, Salgado JV, Vieira LB, Teixeira AL, Palotás A. (2009). “Neurotransmitters in the central nervous system and their implication in learning and memory processes.” Curr Med Chem. 16:796–840.

Rempel-Clower N.L., Zola S.M., Squire L.R., Amaral D.G. (1996). “Three cases of enduring memory impairment after bilateral damage limited to the hippocampal formation.” J Neurosci. Aug 15;16(16):5233-55.

Renner M., Lacor P.N., Velasco P.T., Xu J., Contractor A., Klein W.L., Triller A. (2010). “Deleterious effects of amyloid beta oligomers acting as an extracellular scaffold for mGluR5.” Neuron. Jun 10;66(5):739-54

Resende R.R., Adhikari A. (2009). “Cholinergic receptor pathways involved in apoptosis, cell proliferation and neuronal differentiation.” Cell

Commun Signal. Aug 27;7:20.

Richter J.D., Klann E. (2009). “Making synaptic plasticity and memory last: mechanisms of translational regulation.” Genes Dev. Jan 1;23(1):1-11.

Rogers L.J. (2014). “Asymmetry of brain and behavior in animals: Its development, function, and human relevance.” Genesis. Jun;52(6):555-71.

Rondard P., Liu J., Huang S., Malhaire F., Vol C., Pinault A., Labesse G., Pin J.P. (2006). “Coupling of agonist binding to effector domain activation in metabotropic glutamate-like receptors.” J. Biol. Chem. 281(34):24653–61

Rosenberg, N., Gerber, U. and Ster, J. (2016). “Activation of Group II Metabotropic Glutamate Receptors Promotes LTP Induction at Schaffer Collateral-CA1 Pyramidal Cell Synapses by Priming NMDA Receptors.” J Neurosci 36, 11521-11531.

Rosenbrock H., Kramer G., Hobson S., Koros E., Grundl M., Grauert M., Reymann K.G., Schröder U.H. (2010). “Functional interaction of metabotropic glutamate receptor 5 and NMDA-receptor by a metabotropic glutamate receptor 5 positive allosteric modulator.” Eur J Pharmacol. Aug 10;639(1-3):40-6

Roy D.S., Arons A., Mitchell T.I., Pignatelli M., Ryan T.J., Tonegawa S. (2016). “Memory retrieval by activating engram cells in mouse models of early Alzheimer's disease.” Nature. Mar 24;531(7595):508-12.

Ryan T.J., Roy D.S., Pignatelli M., Arons A., Tonegawa S. (2015). “Engram cells retain memory under retrograde amnesia.” Science. May 29;348(6238):1007-13

Sabbagh M., Han S., Kim S., Na H.R., Lee J.H., Kandiah N., Phanthumchinda K., Suthisisang C., Senanarong V., Pai M.C., Narilastri D., Sowani A.M., Ampil E., Dash A. (2016). “Clinical Recommendations for the Use of Donepezil 23 mg in Moderate-to-Severe Alzheimer's Disease in the Asia-Pacific Region.” Dement Geriatr Cogn Dis Extra. Sep 9;6(3):382-395.

Sans N., Vissel B., Petralia R.S., Wang Y.X., Chang K., Royle G.A., Wang C.Y., O'Gorman S., Heinemann S.F., Wenthold R.J. (2003). “Aberrant formation of glutamate receptor complexes in hippocampal neurons of mice lacking the GluR2 AMPA receptor subunit.” J Neurosci. Oct 15;23

Santschi, L.A., Zhang, X.L. and Stanton, P.K. (2006). “Activation of receptors negatively coupled to adenylate cyclase is required for induction of long-term synaptic depression at Schaffer collateral-CA1 synapses.” J Neurobiol 66, 205-219.

Sarantis, K., Tsiamaki, E., Kouvaros, S., Papatheodoropoulos, C. and Angelatou, F. (2015). “Adenosine A(2)A receptors permit mGluR5-evoked tyrosine phosphorylation of NR2B (Tyr1472) in rat hippocampus: a possible key mechanism in NMDA receptor modulation.” J Neurochem 135, 714-726.

Schwartzkroin P.A., Wester K. (1975). “Long-lasting facilitation of a synaptic potential following tetanization in the in vitro hippocampal slice.” Brain Res. May 16;89(1):107-19.

Scimemi, A., Fine, A., Kullmann, D.M. and Rusakov, D.A. (2004). “NR2B-containing receptors mediate cross talk among hippocampal synapses.” J Neurosci 24, 4767-4777.

Scoville W.B., Milner B. (1957). “Loss of recent memory after bilateral hippocampal lesions.” J Neurol Neurosurg Psychiatry. Feb;20(1):11-21.

Seeburg P.H., Burnashev N., Köhr G., Kuner T., Sprengel R., Monyer H. (1995). “The NMDA receptor channel: molecular design of a coincidence detector.” Recent Prog Horm Res. 50:19-34.

Segal M., Auerbach J.M. (1997). “Muscarinic receptors involved in hippocampal plasticity.” Life Sci. 60(13-14):1085-91.

Shankar G.M., Li S, Mehta T.H., Garcia-Munoz A., Shepardson N.E., Smith I., Brett F.M., Farrell M.A., Rowan M.J., Lemere C.A., Regan C.M.,

Walsh D.M., Sabatini B.L., Selkoe D.J. (2008). “Amyloid-beta protein dimers isolated directly from Alzheimer's brains impair synaptic plasticity and memory.” Nat Med. Aug;14(8):837-42.

Shankar G.M., Walsh D.M. (2009). “Alzheimer's disease: synaptic dysfunction and Abeta.” Mol Neurodegener. Nov 23;4:48.

Shi F., Liu B., Zhou Y., Yu C., Jiang T. (2009). “Hippocampal volume and asymmetry in mild cognitive impairment and Alzheimer's disease: Meta-analyses of MRI studies.” Hippocampus. Nov;19(11):1055-64.

Shinohara Y., Hirase H. (2009). “Size and Receptor Density of Glutamatergic Synapses: A Viewpoint from Left-Right Asymmetry of CA3-CA1 Connections.” Front Neuroanat. Jul 1;3:10.

Shinohara Y., Hirase H., Watanabe M., Itakura M., Takahashi M., Shigemoto R. (2008). “Left-right asymmetry of the hippocampal synapses with differential subunit allocation of glutamate receptors.” Proc Natl Acad Sci. Dec 9;105(49):19498-503

Shipton O.A., El-Gaby M., Apergis-Schoute J., Deisseroth K., Bannerman D.M., Paulsen O., Kohl M.M. (2014a). “Left-right dissociation of hippocampal memory processes in mice”. Proc Natl Acad Sci. Oct 21;111(42):15238-43.

Shipton, O.A. Paulsen, O. (2014b). “GluN2A and GluN2B subunit-containing NMDA receptors in hippocampal plasticity.” Philos Trans R Soc Lond B Biol Sci 369, 20130163.

Shouval H.Z., Bear M.F., Cooper L.N. (2002). “A unified model of NMDA receptor-dependent bidirectional synaptic plasticity.” Proc Natl Acad Sci. Aug 6;99(16):10831-6.

Simons J.S. and Spiers H. J. (2003). “Prefrontal and medial temporal lobe interactions in long-term memory.” Nature Reviews Neuroscience 4, 637-648

Slomianka L., Amrein I., Knuesel I., Sørensen J.C., Wolfer D.P. (2011). “Hippocampal pyramidal cells: the reemergence of cortical lamination.” Brain Struct Funct. Nov;216(4):301-17.

Solntseva E.I., Kapai N.A., Popova O.V., Rogozin P.D., Skrebitsky V.G. (2014). “The involvement of sigma1 receptors in donepezil-induced rescue of hippocampal LTP impaired by beta-amyloid peptide.” Brain Res Bull. Jul;106:56-61

Squire L.R. (2009). “The Legacy of Patient H.M. for Neuroscience.” Neuron. Jan 15;61(1):6-9.

Squire L.R., Ojemann J.G., Miezin F.M., Petersen S.E., Videen T.O., Raichle M.E. (1992). “Activation of the hippocampus in normal humans:

a functional anatomical study of memory." Proc Natl Acad Sci. 89(5):1837–1841.

Stanton P.K., Sarvey J.M. (1984). "Blockade of long-term potentiation in rat hippocampal CA1 region by inhibitors of protein synthesis." J Neurosci. Dec;4(12):3080-8.

Staubli, U. and Scafidi, J. (1997). "Studies on long-term depression in area CA1 of the anesthetised and freely moving rat." J Neurosci 17, 4820-4828.

Sugimoto H., Yamanishi Y., Iimura Y., Kawakami Y. (2000). "Donepezil hydrochloride (E2020) and other acetylcholinesterase inhibitors." Curr Med Chem. Mar;7(3):303-39.

Tamaru, Y., Nomura, S., Mizuno, N. Shigemoto, R. (2001). "Distribution of metabotropic glutamate receptor mGluR3 in the mouse CNS: differential location relative to pre- and postsynaptic sites." Neuroscience 106, 481-503.

Tang Y., Nyengaard J.R., De Groot D.M., Gundersen H.J. (2001). "Total regional and global number of synapses in the human brain neocortex. Synapse. Sep 1;41(3):258-73.

Tchumatchenko T., Newman J.P., Fong M.F., Potter S.M. (2013). "Delivery of continuously-varying stimuli using channelrhodopsin-2."

Front Neural Circuits. Dec 6;7:184.

Thompson P.M., Hayashi K.M., de Zubicaray G., Janke A.L., Rose S.E., Semple J., Herman D., Hong M.S., Dittmer S.S., Doddrell D.M., Toga A.W. (2003). “Dynamics of gray matter loss in Alzheimer's disease.” J Neurosci. Feb 1;23(3):994-1005.

Tigaret, C.M., Olivo, V., Sadowski, J.H., Ashby, M.C. and Mellor, J.R. (2016). “Coordinated activation of distinct Ca^{2+} sources and metabotropic glutamate receptors encodes Hebbian synaptic plasticity.” Nat Commun 7, 10289.

Tomek S.E., Lacrosse A.L., Nemirovsky N.E., Olive M.F. (2013). “NMDA Receptor Modulators in the Treatment of Drug Addiction.” Pharmaceuticals (Basel). Feb 6;6(2):251-68.

Tomita S., Stein V., Stocker T.J., Nicoll R.A., Bredt D.S. (2005). “Bidirectional synaptic plasticity regulated by phosphorylation of stargazin-like TARPs.” Neuron 45: 269–277.

Tooby, J., and Cosmides, L. (1992). “The psychological foundations of culture.” In J. H. Barkow, L. Cosmides, and J. Tooby (Eds.), The adapted mind: Evolutionary theory and the generation of culture (pp. 19–136). New York: Oxford Press.

Tovar K.R., McGinley M.J., Westbrook G.L. (2013). “Triheteromeric NMDA receptors at hippocampal synapses.” J. Neurosci. 33, 9150–9160.

Traynelis S.F., Wollmuth L.P., McBain C.J., Menniti F.S., Vance K.M., Ogden K.K., Hansen K.B., Yuan H., Myers S.J., Dingledine R. (2010). “Glutamate receptor ion channels: structure, regulation, and function.” Pharmacol Rev. Sep;62(3):405-96.

Trepanier, C., Lei, G., Xie, Y.F. and MacDonald, J.F. (2013). “Group II metabotropic glutamate receptors modify N-methyl-D-aspartate receptors via Src kinase.” Sci Rep 3, 926.

Um J.W., Nygaard H.B., Heiss J.K., Kostylev M.A., Stagi M., Vortmeyer A., Wisniewski T., Gunther E.C., Strittmatter S.M. (2012). “Alzheimer amyloid-β oligomer bound to postsynaptic prion protein activates Fyn to impair neurons.” Nat Neurosci. Sep;15(9):1227-35.

Vallortigara G., Chiandetti C. and Sovrano V.A. (2010). “Brain asymmetry (animal).” WIREs Cogn Sci 2 146–157

Vann S.D., Nelson A.J. (2015). “The mammillary bodies and memory: more than a hippocampal relay.” Prog Brain Res. 219:163-85.

Vicini S., Wang J.F., Li J.H., Zhu W.J., Wang Y.H., Luo J.H., Wolfe B.B., Grayson D.R. (1998). “Functional and pharmacological differences between recombinant NMDA receptors.” J. Neurophys. 79, 555–566.

Volk, L. J., Pfeiffer, B. E., Gibson, J. R. and Huber, K. M. (2007). “Multiple Gq-coupled receptors converge on a common protein synthesis-dependent long-term depression that is affected in fragile X syndrome mental retardation.” J. Neurosci. 27, 11624–11634.

Wang D.V., Yau H.J., Broker C.J., Tsou J.H., Bonci A., Ikemoto S. (2015). “Mesopontine median raphe regulates hippocampal ripple oscillation and memory consolidation.” Nat Neurosci. May;18(5):728-35.

Wang H., Zhuo M. (2012). “Group I metabotropic glutamate receptor-mediated gene transcription and implications for synaptic plasticity and diseases.” Front Pharmacol. Nov 1;3:189.

Wang L., Swank J.S., Glick I.E., Gado M.H., Miller M.I., Morris J.C., Csernansky J.G. (2003). “Changes in hippocampal volume and shape across time distinguish dementia of the Alzheimer type from healthy aging.” Neuroimage 20:667–682.

Wang, Q., Walsh, D.M., Rowan, M.J., Selkoe, D.J., and Anwyl, R. (2004). “Block of long-term potentiation by naturally secreted and synthetic amyloid beta-peptide in hippocampal slices is mediated via activation of the kinases c-Jun N-terminal kinase, cyclin-dependent kinase 5, and p38 mitogen-activated protein kinase as well as metabotropic glutamate receptor type 5.” J. Neurosci. 24, 3370–3378.

Watkins J.C. and Evans R.H. (1981). “Excitatory amino acid transmitters.” Annu Rev Pharmacol Toxicol 21, 165-204.

Watkins J.C. and Jane D.E. (2006). “The glutamate story.” Br J Pharmacol. Jan;147

Weber F., Chung S., Beier K.T., Xu M., Luo L., Dan Y. (2015). “Control of REM sleep by ventral medulla GABAergic neurons.” Nature. Oct 15;526(7573):435-8.

Wenthold, R.J., Petralia, R.S., Blahos, J., II, and Niedzielski, A.S. (1996). “Evidence for multiple AMPA receptor complexes in hippocampal CA1/CA2 neurons.” J. Neurosci. 16, 1982–1989

Wess J, Eglen RM, Gautam D. (2007). “Muscarinic acetylcholine receptors: mutant mice provide new insights for drug development.” Nat Rev Drug Discov. Sep;6(9):721-33.

Whitlock, J.R., Heynen, A.J., Shuler, M.G., and Bear, M.F. (2006). “Learning induces long-term potentiation in the hippocampus.” Science 313, 1093–1097.

Willard S.S., Koochekpour S. (2013). “Glutamate signalling in benign and malignant disorders: current status, future perspectives, and therapeutic implications.” Int J Biol Sci. 2013 Aug 9;9(7):728-42.

Winder D. G., Mansuy I. M., Osman M., Moallem T. M. and Kandel E. R. (1998). “Genetic and pharmacological evidence for a novel, intermediate phase of long-term potentiation suppressed by calcineurin.” Cell 92, 25–37.

Wixted J.T. and Squire L.R. (2011). “The medial temporal lobe and the attributes of memory.” Trends Cogn Sci. May; 15(5): 210–217.

Wolf H., Grunwald M., Kruggel F., Riedel-Heller S.G., Angerhöfer S., Hojjatoleslami A., Hensel A., Arendt T., Gertz H. (2001). “Hippocampal volume discriminates between normal cognition; questionable and mild dementia in the elderly.” Neurobiol Aging. Mar-Apr;22(2):177-86.

Wong, E.H., Kemp J.A., Priestley T., Knight A.R., Woodruff G.N., Iversen L.L. (1986). “The anticonvulsant MK-801 is a potent N-methyl-D-aspartate antagonist.” Proc Natl Acad Sci. 83, 7104-7108.

Wong, T.P., Howland J.G., Robillard J.M., Ge Y., Yu W., Titterness A.K., Brebner K., Liu L., Weinberg J., Christie B.R., Phillips A.G., Wang Y.T. (2007). “Hippocampal long-term depression mediates acute stress-induced spatial memory retrieval impairment.” Proc Natl Acad Sci. 104, 11471-11476.

Wu H., Williams J., Nathans J. (2014). “Complete morphologies of basal forebrain cholinergic neurons in the mouse.” Elife. May 7;3:e02444.

Xiong W., Kojic L.Z., Zhang L., Prasad S.S., Douglas R., Wang Y., Cynader M.S. (2006). “Anisomycin activates p38 MAP kinase to induce LTD in mouse primary visual cortex.” Brain Res. Apr 26;1085(1):68-76.

Xu, L., Anwyl, R. and Rowan, M.J. (1997). “Behavioural stress facilitates the induction of long-term depression in the hippocampus.” Nature 387, 497-500.

Xu L, Holscher C, Anwyl R., Rowan MJ. (1998). “Glucocorticoid receptor and protein/RNA synthesis-dependent mechanisms underlie the control of synaptic plasticity by stress.” Proc Natl Acad Sci. Mar 17;95(6):3204-8.

Yamamoto K., Tanei Z., Hashimoto T., Wakabayashi T., Okuno H., Naka Y., Yizhar O., Fenno L.E., Fukayama M., Bito H., Cirrito J.R., Holtzman D.M., Deisseroth K., Iwatsubo T. (2015). “Chronic optogenetic activation augments aβ pathology in a mouse model of Alzheimer disease.” Cell Rep. May 12;11(6):859-65.

Yang X.D., Connor J., Faber D. (1994). “Weak excitation and simultaneous inhibition induce long-term depression in hippocampal CA1 neurons.” J Neurophysiol 71:1586–1590.

Yashiro K., Philpot B.D. (2008). “Regulation of NMDA receptor subunit expression and its implications for LTD, LTP, and metaplasticity.” Neuropharmacology 55, 1081–1094.

Yau SY, Li A, So KF. (2015). “Involvement of Adult Hippocampal Neurogenesis in Learning and Forgetting.” Neural Plast. 717958.

Yoshiyama, M. and de Groat, W.C. (2005). “Supraspinal and spinal alpha-amino-3-hydroxy-5-methylisoxazole-4-propionic acid and N-methyl-D-aspartate glutamatergic control of the micturition reflex in the urethane-anesthetised rat.” Neuroscience 132, 1017-1026.

Zhu, J. J., Esteban, J. A., Hayashi, Y. and Malinow, R. (2000). “Postnatal synaptic potentiation: delivery of GluR4‐containing AMPA receptors by spontaneous activity.” Nat. Neurosci. 3, 1098–1106.

Zhang F., Wang L.P., Boyden E.S., Deisseroth K. (2006). “Channelrhodopsin-2 and optical control of excitable cells.” Nat Methods. Oct;3(10):785-92.

Zhang Y., Schuff N., Jahng G.H., Bayne W., Mori S., Schad L., Mueller S., Du A.T., Kramer J.H., Yaffe K., Chui H., Jagust W.J., Miller B.L., Weiner M.W. (2007). “Diffusion tensor imaging of cingulum fibers in mild cognitive impairment and Alzheimer disease.” Neurology 68: 13–19.

Zhang Y.P., Oertner T.G. (2007). “Optical induction of synaptic plasticity using a light-sensitive channel.” Nature Methods; 4:139-41.

Full plasmid sequence from
http://www.everyvector.com/sequences/show_public/110

VII. Appendix

- Table of Drugs used in Thesis

Drug	Mode of application	Dose	Timing	Method of Action	Vehicle
CPP	i.p.	10mg/kg	2h 15 min pre- LFS	Orthosteric competitive NMDAR antagonist	Diluted in water, added to saline for application
MTEP	i.p.	3mg/kg or 6mg/kg	1h pre- LFS	Group I mGlu5R antagonist	Diluted in water, added to saline for application
LY341495	i.p.	3mg/kg	1h pre- LFS	Group II mGluR antagonist	Dissolved in 1.2 molar equivalent NaOH
Ro 25-6981	i.p.	6mg/kg or 12mg/kg	1h pre- LFS	Use-dependent NMDAR antagonist	Diluted in DMSO, added to saline for application, 10% v/v
	i.c.v.	2nmol	15 min pre- LFS		
D-AP5	i.c.v.	100nmol or 200nmol	15 min pre- LFS	Orthosteric competitive NMDAR antagonist	Diluted in water, added to saline for application

Drug	Mode of application	Dose	Timing	Method of Action	Vehicle
L-AP5	i.c.v.	100nmol	15 min pre- LFS	30-fold less active orthosteric competitive NMDAR antagonist	Diluted in water, added to saline for application
VU 0360172	s.c.	15mg/kg	1h pre- LFS	Positive allosteric modulator of group 1 mGlu5R	Dissolved in 10% Tween-80; diluted in saline for application
MK-801 or (-)-MK-801	i.p.	0.5mg/kg or 1.0mg/kg	1h pre- LFS	Non-competitive NMDAR antagonist	Diluted in water, added to saline for application.
	i.c.v.	60nmol	15 min pre- LFS		
Donepezil	s.c.	1mg/kg	1h pre- LFS	Acetylcholinesterase inhibitor	Diluted in water, added to saline for application.

Drug	Mode of application	Dose	Timing	Method of Action	Vehicle
Scopolamine	i.p.	0.2 mg/kg	1-2h pre- LFS	Anticholinergic	Diluted in saline
Emetine	i.c.v.	240 µg	30min pre- LFS	Translation inhibitor	Diluted in water, added to saline for application
Aβ - ADDL	i.c.v.	1.2nmol	30min pre- LFS		Prepared in DMSO and diluted in Hams F-12 media